WOOD MATERIAL BEHAVIOR IN SEVERE ENVIRONMENTS

by

Christopher A. Lenth

Dissertation submitted to the Faculty of the Virginia Polytechnic Institute and State University in partial fulfilment of the requirements for the degree of

DOCTOR OF PHILOSOPHY

in

Wood Science and Forest Products

APPROVED:

Dr. Frederick A. Kamke, chair

Dr. Charles E. Frazier | Dr. Joseph R. Loferski | Dr. Audrey G. Zink-Sharp

Dr. David A. Dillard | Dr. Layne T. Watson

May 1999
Blacksburg, Virginia

ABSTRACT

An improved knowledge of wood material behavior in hot-pressing environments can provide the benefit of an increased understanding of material properties during the manufacture of wood-based composites as well as insight into the development of new processes and products which manipulate the viscoelastic nature of wood. Two specific areas where additional knowledge is needed are: the high temperature equilibrium moisture content (EMC) behavior and the moisture dependent softening behavior.

EMC data was collected and desorption isotherms were generated for mature and juvenile wood of aspen, loblolly pine and yellow-poplar at 50 and 160 °C. High temperature EMC behavior was found to be distinct from that at lower temperatures, and considerable differences between the isotherms for juvenile and mature wood were detected. Substantial thermal degradation was observed during desorption at 160 °C and found to be strongly influenced by relative humidity.

The thermal softening behavior of wood was evaluated using dielectric thermal analysis (DETA) at moisture levels from 0 to 20 percent. Coincident *in situ* relaxations of hemicellulose and amorphous cellulose in the range of 20 to 200 °C were observed and found to exhibit the characteristics of a secondary (glass) transition. The moisture dependence of this transition was characterized, and differences in the observed T_g were detected between juvenile and mature wood. Time-temperature superposition was also shown to be applicable to the wood – water system.

ACKNOWLEDGEMENTS

Funding for this research originated from the United Sates Department of Agriculture Competitive Grants Program. Additional financial support from the Department of Wood Science and Forest Products and the Center for adhesive and Sealant Science at Virginia Polytechnic Institute and State University is also gratefully acknowledged.

The author would like to express sincere gratitude to Dr. Frederick A. Kamke. Without his vision, intelligence, guidance and patience, this effort would certainly not have come to fruition. Appreciation is also extended to Drs. Charles Frazier, Joseph Loferski, Audrey Zink-Sharp, David Dillard and Layne Watson for their valuable input to this work. Gratefulness is put forth for the generous support of the exceptional and too often unsung staff at the Brooks Forest Products Center. I would also like to thank Ms. Elena Kultikova for her involvement in various parts of this project.

Indeed I owe much to my family, for giving me roots and giving me wings; for providing in me the drive and the self confidence necessary to accomplish this task. Finally, I would like to express love and thanks to all my dear and wonderful friends, for helping to make this part of my life which existed around and through this work the most splendid of times.

TABLE OF CONTENTS

LIST OF TABLES

LIST OF FIGURES

List of Figures (continued)

CHAPTER 1. PROJECT DESCRIPTION

INTRODUCTION

The hot-press consolidation process used in the manufacture of wood-based composite products creates an environment which accentuates viscoelastic behavior. This viscoelastic behavior often results in densification from transverse compression of the constituent wood elements. Wood densification can have both permanent and recoverable components, which together have significant influence on the physical and mechanical properties of the composite product. It is known that the local environment of moisture content and temperature during hot-pressing influences densification, density gradient formation and non-recoverable strain. Furthermore, it has been observed that the increased density, and other physical or chemical changes, result in modified wood properties. These changes have considerable implications for improved product performance, yet their nature and the mechanisms responsible for them remain essentially unresolved.

The overall goal of this ongoing research effort is to characterize the viscoelastic behavior of wood as it pertains to conditions found during hot-pressing. This study employed a materials science approach to understanding the process of viscoelastic compression; an initiative which began by quantifying the pertinent characteristics exhibited by the material in processing environments and subsequently studied how those characteristics can be manipulated to maximize material utilization. This is fundamental research that will increase the understanding of material behavior during the manufacture of wood-based composites and provide insight for the development of new and improved products and processes using viscoelastic-thermal-compression (VTC). This research initiative has three sequential and interrelated components. The author maintains these to be the necessary steps for understanding the phenomena involved in viscoelastic compression, and delineating the mechanisms through which this procedure can be harnessed into improved manufacturing technology.

The initial phase of this work involved investigations of the wood-water relationship at conditions relevant to the hot-pressing of wood composites. To date, little information has been documented on the equilibrium moisture content (EMC) behavior of wood subjected to temperature above 100 °C and pressure exceeding atmospheric conditions (101 kPa). This data is essential in understanding the influence of moisture on the viscoelastic behavior of wood. The goals of this portion of the study were to develop technology for collecting sorption isotherm data at high temperatures and pressures, and to investigate the EMC vs. relative humidity behavior of selected

wood species in these severe environments. This work provided the foundation for a fundamental study of the viscoelastic behavior of wood as it pertains to conditions found during hot-pressing.

The second phase of the VTC research effort built upon the knowledge gained in the high-temperature EMC study, an evaluation of the viscoelastic behavior of wood as a function of moisture content. This study investigated the thermal *softening* of the constituent wood polymers and the influence of wood moisture content on viscoelastic behavior. The viscoelastic behavior was probed through observation of the glass transition (T_g) temperature of the *in situ* amorphous component of wood using microdielectric analysis. The results of this work allow for the definition of optimum conditions for the viscoelastic thermal compression of wood.

In the third phase of this study, wood specimens were transversely compressed in a variety of environments relative to the T_g vs. EMC relationship. Physical, mechanical and chemical evaluations of compressed and control specimens were undertaken to expose favorable densification conditions and to help delineate the important mechanisms involved in viscoelastic-thermal-compression. This research is ongoing and will not be further addressed herein. The information collected here will also be implemented into a three dimensional model for the viscoelastic compression of flat pressed wood-based composites. Upon completion of this work, knowledge gained on the VTC process will then be available to fuel more practical investigations; investing this technology into process modifications and product development.

Project Goal

The goal of this research is to characterize the viscoelastic behavior of wood as it pertains to conditions found during hot-pressing. This study will employ a materials science approach to understanding the process of viscoelastic compression. This is fundamental research that will increase the understanding of material behavior during the manufacture of wood-based composites and provide insight for the development of new and improved products and processes using viscoelastic-thermal-compression.

Technical Objectives

1. Characterize the EMC vs. relative humidity behavior of wood in high-temperature environments relevant to hot-pressing.
2. Characterize the glass transition behavior of wood as a function of moisture content at conditions pertinent with wood-based composites manufacture.

RATIONALE AND SIGNIFICANCE

This research has the potential for far-reaching impact on the wood products industry. At issue here is the manipulation of wood density, and perhaps thermal-induced, chemical modifications, to improve properties. The immediate economic gains are admittedly limited. However, the value of this research must be placed in context with a backdrop of the current and expected timber availability in the U.S. In the long term, the results of this work can influence an initiative to re-evaluate timber production for a major segment of the industry, that is, managing forests for high value, wood-based, composite products. In the short-term, these results can provide technical information and incentive for decisions regarding processing modifications for improved product performance.

In recent years, the trend in natural resource policy has been the withdrawal of millions of acres of timber from commercial use. While this has been most pronounced in the Western U.S., indications of decreased harvests in other regions are becoming evident. These land use issues will certainly have an increased impact on timber harvests nationwide as we move into the next century. The long-range outlook is for tighter control on traditional timber supplies, which must reduce the availability of high grade saw logs and peeler logs. While the industry has already begun the shift to structural lumber substitutes and non-veneer structural panels, some of these products require high modulus veneer or other expensive treatments to provide the necessary structural properties. The makeup of the available timber base can not indefinitely supply these needs, even if production levels remain constant. The consumer will demand better performance, yet the quality of the raw material is declining.

This research has been aimed toward demonstrating the feasibility of enhancing wood properties using relatively simple and inexpensive procedures. Previous research has already demonstrated the ability to more than double the bending modulus of wood by judicious viscoelastic transverse compression (Casey, 1987). Preliminary investigations in this area indicate that the tensile strength and stiffness of densified southern pine and yellow-poplar are considerably higher than that of undensified material (Figure 1.1). Much of the gains in strength and stiffness resulting from transverse compression are due to those properties being closely linked to wood density (Armstrong et al., 1984). Such material enhancement could be performed either on-line or off-line during composite manufacture. Unfortunately, we do not understand the intricacies of this process, nor are we aware of the full implications on product performance. If this process could be defined and

harnessed, rapid growth, low density timber could supply a significant segment of the industry. In effect, density, and thus strength and stiffness, would become another manufacturing variable, to be manipulated at will.

The rapid growth of intensively managed trees often leads to a much higher percentage of juvenile wood. The detrimonious effects of juvenile wood on the properties of lumber have been well documented (Barret and Kellog 1986; Bendsten and Senft 1986; Bendsten 1978). However, Pugel et al. (1990a, 1990b) found that while the dimensional stability of wood composite panels made from eight year old southern pine wood was inferior to that of panels made from mature wood, the mechanical properties of both panel types were similar. A pessimist would argue that juvenile wood is the undesirable result of rapid tree growth, and therefore should be unconditionally avoided. It must be accepted that juvenile wood is not a barrier, but an increasingly important facet of our wood resource, one that must be utilized and manipulated to yield useful products. In a practical sense, it may be considered by some that to create robust products through modification of inferior material is not cost effective. Future cost effectiveness will likely be defined by quite a different economic paradigm. Fundamental research can not be dictated by short-term considerations of cost effectiveness. The future of the forest products industry will depend heavily on how well we can utilize this resource, not how we can avoid it.

While converting juvenile wood and low density wood into high performance products may require more involved processing techniques and increased manufacturing time, the extra effort can be considered as a trade-off for a 50 to 75 year decrease in rotation times. The key to success in this endeavor is application of a fundamental materials science approach to product and process development, founded on a solid understanding of material behavior under processing conditions.

CHAPTER 1 FIGURES:

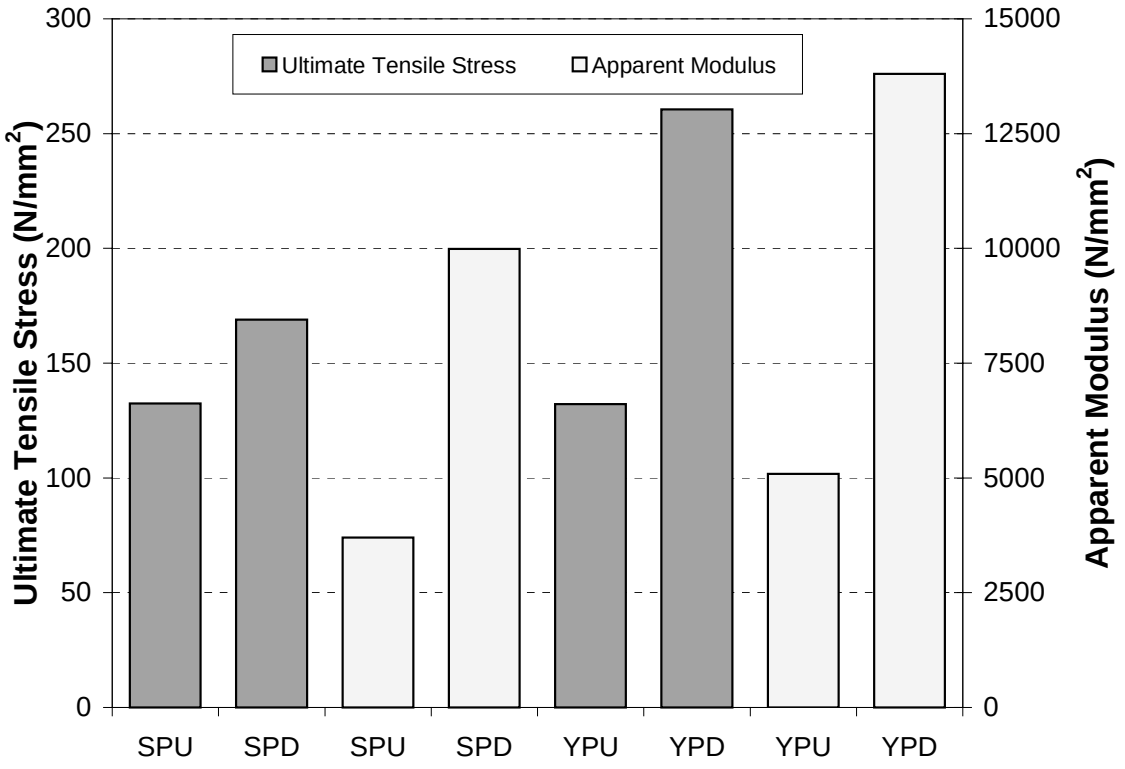

Figure 1.1. Preliminary tensile results for samples of southern pine and yellow-poplar densified to 50 % strain as well as undensified controls. SPU is undensified southern pine, YPD is densified yellow-poplar, etc.

CHAPTER 2. HIGH TEMPERATURE EMC BEHAVIOR OF WOOD

INTRODUCTION

The hot-press consolidation process used in the manufacture of wood-based composites creates an environment that accentuates viscoelastic behavior. This viscoelastic behavior often results in densification from transverse compression of the constituent wood particles. Wood densification can have both permanent and recoverable components, which together have significant influence on the physical and mechanical properties of the composite product. It is known that the local environment of moisture and temperature during hot-pressing influences densification, density gradient formation and non-recoverable strain. Furthermore, it has been observed and documented that the increased density, and other physical or chemical changes, result in modified wood properties. These changes have implications for improved product performance, yet their nature and the mechanisms responsible for them remain essentially unresolved.

This research effort focused on investigations of the wood-water relationship at conditions relevant to the hot-pressing of wood-based composites. Very little information has been documented on the equilibrium moisture content (EMC) behavior of wood in environments of elevated temperature and pressure. This data is essential in understanding the influence of moisture on the viscoelastic behavior of wood. The specific objectives of this study were: to develop apparatus and techniques suitable for collecting sorption isotherm data at high temperatures and pressures, and to characterize the EMC vs. relative humidity behavior of selected wood species in environments relevant to hot-pressing. This work provides the foundation for a fundamental study of the viscoelastic behavior of wood as it pertains to conditions found during hot-pressing.

BACKGROUND

During the hot-pressing of wood-based composites, internal mat temperature has been measured in excess of 150 °C and relative humidity calculated to reach or exceed 75 percent (Humphrey and Bolton, 1989; Kamke and Casey, 1989; Kamke and Wolcott, 1991). Such severe processing conditions are adequate to transcend the glass transition of the viscoelastic wood polymers (Kelley et al., 1987) and have been reported to change the properties of the wood component (Geimer et al., 1985; Price, 1976; Casey, 19887). Casey (1988) found as much as a 30 percent increase in specific dynamic bending modulus for flakes that were tested before and after being consolidated in a

flakeboard panel. Such results suggest that there is much to gain from an improved understanding of wood-water relations in hot-pressing environments and how they bear upon material properties.

The relationship that exists between a wood element and the water vapor in its local environment is likely the single most significant factor affecting its behavior in both manufacture and service. Wood-water relations in ambient to moderate conditions have been well addressed in excellent texts by Skaar (1972, 1988) and Siau (1971, 1984, 1995). The data compiled by U.S. Forest Products Laboratory (1987) for the equilibrium moisture content (EMC) of Sitka spruce as a function of relative humidity, in oscillating desorption at temperatures from 0 to 130 °C, has become the foundation from which nearly all EMC predictions are made. Simpson (1971, 1973, 1980) has evaluated theoretical sorption models using statistical regression analysis and determined that, while several exhibit an excellent fit to the Forest Products Laboratory EMC data, none can accurately predict the heat of sorption of wood. Avramidis (1989) evaluated four empirical moisture sorption models that incorporate temperature as an independent variable in addition to relative humidity. He found that they are as effective in fitting the FPL data as the theoretical sorption models presented by Simpson (1973), and simpler to apply to data representing a range of temperatures. The Hailwood-Horrobin model (Hailwood and Horrobin, 1946) with coefficients determined by Simpson (1973) is probably the most widely used equation for predicting EMC of wood.

Experimental data on the EMC behavior of wood at temperatures above 100°C is not nearly as well represented in the literature. Keylwerth (1949), Grumach (1951) and Kohlman and Malmquist (1952) have collected EMC data in pure steam at temperatures up to 154°C. High temperature EMC values in pressurized, saturated environments have been determined though a variety of methods by Hahn (1966), Strickler (1968), Lutz (1974), Englehardt (1979) and Resch et al. (1988). These studies employ a range of techniques, and while they reported contradictions in both the shape of the EMC vs. relative humidity curve and the existence of adsorption-desorption hysteresis, they all clearly show that the nature of the wood-water relations changed significantly as temperature and pressure increased. With the exception of the study by Lutz (1974), all of these researchers have suggested some influence of wood degradation at high temperatures. Using a gravimetric technique for moisture content determination, Engelhardt (1979) and Resch et al. (1988) attempted to correct for these degradation losses. This phenomena agrees with research on wood stability as reviewed by Hillis (1984), however the

time frame necessary for such degradation to occur makes it more of a concern in the characterization of long term EMC experiments than in the manufacture of wood-based composites.

High-temperature EMC predictions obtained through various methods of extrapolation from low-temperature data have also been presented by Keylwerth (1949), Sturany (1952), Kauman (1956), and Ladell (1957). Rosen (1980) derived psychrometric relationships for superheated steam environments and discussed their influence on the EMC of wood. Simpson and Rosen (1981) provided a review of previous high temperature EMC work and presented a method of extrapolation at atmospheric pressure based on a fit of the Hailwood-Horrobin equation to the Forest Products Laboratory EMC data.

EXPERIMENTAL

Mature log sections of yellow-poplar (*Liriodendron tulipifera*), loblolly pine (*Pinus taeda*) and aspen (*Populus tremuloides*) were obtained and cut into cants. These cants were further separated into juvenile, mature and intermediate portions. Juvenile wood was defined as the wood inside the tenth growth ring and mature wood as that material outside the thirtieth growth ring, as per Kretschmann and Bendsten (1992). The wood material was then end sealed and allowed to air dry at ambient laboratory conditions for approximately 12 months.

Equilibrium moisture content data was collected and used to create desorption isotherms at 50 °C and 160 °C in order to provide information across the range of temperatures found in wood-based composites manufacture. Different gravimetric methods were employed for the 50 °C and 160 °C isotherm experiments. Below 100 °C, experiments can be conducted at atmospheric pressure. Above 100 °C , a pressurized vessel is required to obtain water vapor pressure values in excess of atmospheric pressure.

For the 50 °C desorption, juvenile, mature and intermediate wood specimens of yellow-poplar and loblolly pine were machined to dimensions of approximately 8 cm (tangential) by 5 cm (radial) by 2 cm (longitudinal). Due to the smaller size of the aspen log, aspen specimens were longer in the longitudinal direction, and smaller in the transverse dimensions. Specimens for the 160 °C experiments were created to maximize surface area, and thus speed up the desorption process. Wood strips approximately 5 cm (tangential) by 0.4 cm (radial) by 25 cm (longitudinal) were

separated by 4 mm wooden spacers and bound together using thin chromel wire (Figure 2.1). This configuration comprised one specimen.

At 50 °C, desorption was carried out in a 1 m^3 environment cabinet with recirculating, forced-air flow (Parameter Generation and Control, Inc.). Dry bulb and wet bulb thermocouples were used to monitor temperature and humidity of the environment to within 0.1 °C and 0.5 percent relative humidity.

For the 50 °C the air-dried specimens were first allowed to equilibrate at 50 °C and 95% relative humidity within the chamber. Specimens were then subjected to an initial desorption to 25 percent relative humidity, after which they were again reconditioned to 95% relative humidity. Henceforth, EMC data was collected as the specimens equilibrated in a humidified environment which was reduced in a stepwise fashion in 5% percent increments to 25% relative humidity. The final step was oven-drying the specimens at 103 °C in a convection oven. Specimens were maintained at each relative humidity step until weight loss was less than 0.1% per day, as determined by weighing on a laboratory balance. Weight measurements required the removal of the specimens from the chamber.

A special pressurized sorption apparatus was created to conduct the EMC experiments at 160 °C. A test chamber that could be pressurized was necessary to generate wood EMC conditions near fiber saturation at temperatures above 100 °C (Figure 2.2). This device consisted of a 50 liter stainless steel vessel which could withstand internal pressures in excess of 6 atmospheres. It had computer control of temperature and internal pressure. A computer algorithm compared the current internal conditions with user-defined setpoints. Based on this information, digital outputs were used to energize or de-energize electric resistance heating elements, control the high pressure pump for make-up water, and to open a solenoid valve for venting.

Temperature control was achieved using three electronic resistance heaters mounted on the exterior of the pressure vessel. The primary and secondary heaters were encased in cast aluminum jackets that conformed to the circumference of the cylindrical vessel. Both the primary and secondary heaters were 100 ampere, 220 volt units. The primary heater, surrounding the lower part of the vessel, was run at 100 percent power and the secondary heater, surrounding the upper portion of the vessel was operated at 50 percent power. The tertiary heater was a flat ring shaped unit fixed to the bottom of the cylinder. This heater was rated at 220 volts, 10 amperes and operated at 100 percent power. The primary and tertiary heaters were controlled to maintain a constant setpoint

temperature measured on the external surface of the cylinder. The secondary heater was controlled to maintain a constant sorption specimen temperature that was measured with a type-K thermocouple embedded in a piece of wood adjacent to the sorption specimen. After the initial heat-up sequence, most of the temperature control was accomplished with the secondary heater.

EMC data was collected by monitoring the weight of a wood specimen (Figure 2.1) within the sorption vessel as the total pressure, and thus the relative humidity, of the internal water vapor environment was reduced in a stepwise fashion from saturation to atmospheric pressure. Constant temperature of the specimen was maintained throughout. A paramount concern was protecting the sensitive weighing instrumentation from the corrosive steam environment. To do this, an external weighing apparatus was created to monitor the weight of the specimen while it was suspended inside the chamber (Figure 2.3). This device consisted of a load beam (0 to 227 g. range max, 0 to 10 volt output, 0.25% of full scale combined error) mounted on the outside of the vessel. The load beam was attached to the specimen by means of a chromel wire (0.025 mm diameter), which passed through a small orifice (0.030 mm diameter) in the lid. The small leak inherent to this design served to improve circulation within the vessel, and was compensated for by introducing de-oxygenated, distilled make-up water. The loss of water vapor through the orifice created a natural circulation of water vapor from the bottom of the vessel, past the specimen, and out the top. A stainless steel cylinder served as a shield to protect the specimen from direct heat radiation from the vessel wall. This allowed the specimen temperature to closely match the temperature of the water vapor atmosphere.

Prior to each of the desorption experiments, the load beam was calibrated with brass weights. The influence of temperature and pressure was determined by hanging a brass weight on the weighing mechanism and performing a complete desorption cycle. This was done using weights reflecting the upper (saturated) and lower (dry) limits of weight for the desorption specimens.

The control sequence steps for the high-temperature desorption experiments are shown in Table 2.1. Preliminary experiments were carried out to determine the soak times necessary at each humidity step. The time increments used in the work by Resch et al. (1988) were employed as guidelines and adjusted based on observations with the wood species and specimen geometry used in this study. It was also necessary to determine the amount of wood degradation that took place during each humidity step. Results from the wood degradation tests provided a framework for subsequent correction of EMC data due to loss of wood substance. Specimens for the degradation

tests were assembled, weighed, and hydrated at 95% relative humidity. A matched specimen was used to calculate an approximate oven-dry weight. Specimens were placed in the sorption vessel with three liters of water, and the vessel was sealed and heated to 160 °C. The pressure was increased to the level necessary for the first relative humidity step (95%), and the weight of the specimen was recorded throughout the duration of that step. The chamber was then depressurized and the specimen's weight was recorded, after which the specimen was oven-dried at 103 °C and weighed again. This procedure was repeated for all the relative humidity steps listed in Table 2.1. Due to concerns of wood degradation in the severe environments, specimens were not subjected to an initial adsorption - desorption cycle at 160 °C, as in the 50 °C experiments.

Specimens were assembled from the air-dried wood and then hydrated in an environment of 95% relative humidity at 25 °C before placement in the pressurized sorption apparatus. A small piece of each specimen was oven dried at both at 103 °C and at 160 °C to determine the initial moisture content using a gravimetric technique,. This information was then used to compute the approximate initial oven dry weight. Three liters of liquid water were added before the pre-hydrated specimens were suspended from the weighing mechanism and sealed inside the vessel. The vessel was heated at approximately 2 °C per minute until the isotherm temperature of 160 °C was reached. Once the internal pressure had attained a level corresponding to 95% relative humidity (587 kPa, 85psia at 160 °C), the desorption sequence was initiated. At this time essentially all of the air initially in the vessel had been displaced by water vapor. The isotherm temperature was then maintained as the internal pressure was reduced to atmospheric pressure in seven steps. Figure 2.4 illustrates the targeted environmental conditions for the high-temperature experiments as well as characteristic temperature and relative humidity values recorded during the desorption. Some fluctuation in relative humidity and temperature about the setpoint conditions was evident. The relative humidity is tied closely to temperature through the saturated water vapor pressure, and thus minor fluctuations in temperature, inherent to the heating system employed, resulted in subsequent variations in relative humidity. It was occasionally such that this variation resulted in equilibrium not being achieved at a given step, in which case the control sequence continued to the next step and EMC data at that condition was limited to the remaining replications of that wood type. Specimens were judged to have reached equilibrium when their observed weight was unchanged for five minutes.

Once the desorption experiment was complete and the apparatus had cooled, specimens were removed, weighed, and placed in a convection oven at 160 °C to dry. This oven-dry weight was compared to the initial oven dry weight to determine the amount of wood substance lost during desorption due to hygro-thermal degradation. Together with the results of the wood degradation experiments, this value was used to correct the oven dry weight for subsequent moisture content calculations. The oven dry weight after desorption was also compared to the final measured weight in the sorption vessel at atmospheric pressure to compensate for drift of the load beam over time.

A chemical analysis was carried out on small samples taken from mature wood specimens of all three species both before and after desorption. A standard HPLC carbohydrate analysis with Klason lignin was performed as per the technique of Kaar et al. (1991) on the treated and untreated samples. Ash content was also determined by thermogravimetric analysis (TGA) (700°C, 10°C/min.).

RESULTS AND DISCUSSION

Figure 2.5 shows 50 °C desorption isotherms for yellow-poplar, aspen and loblolly pine. The experimental isotherms exhibit the sigmoid shape commonly reported for wood (Simpson, 1980) and are free from any suspicious anomalies. Each data point represents an average of at least ten specimens: four each of juvenile and mature wood, and two to four of intermediate wood. The solid line indicates predicted EMC using the Hailwood-Horrobin 1-hydrate model.

$$EMC = \frac{1.80}{W}\left[\frac{Kh}{1-Kh} + \frac{K_1 Kh}{1+K_1 Kh}\right] \qquad \textbf{2.1}$$

where W, K and K_1 are temperature dependent parameters and h is the relative vapor pressure.

The Hailwood-Horrobin 1- hydrate model fit to the FPL Sitka spruce (*Picea sitchensis*) data, over the range of 0 to 100 °C, gives the following polynomial equations for the temperature dependent parameters as reported by Siau (1995) based on the work of Simpson (1973).

$K = 4.73 + 0.048\ (T) - 0.0005(T^2)$
$K_1 = 0.706 + 0.0017(T) - 0.000006(T^2)$
$W = 0.223 + 0.0007(T) + 0.000019(T^2)$

The experimental and predicted values agree only up to a relative vapor pressure of about 0.4, after which the data points gradually diverge upwards from the predicted curve, reaching a maximum deviation of 4% EMC at a relative vapor pressure of 0.95. Considering that the predictions are based on data from Sitka spruce, this difference is not remarkable.

Figures 2.6, 2.7 and 2.8 illustrate the EMC and relative vapor pressure relationships between mature and juvenile wood for aspen, loblolly pine and yellow-poplar, respectively. At a given humidity level, EMC for juvenile wood was generally higher than that for mature wood. The largest difference occurred at the highest relative humidity, with a maximum deviation of 1.3% MC for loblolly pine at 95% relative humidity. The Levenberg Marquardt method of nonlinear regression analysis was used to fit the Hailwood-Horrobin 1 - hydrate model to the data from this study, using the values reported by Siau (1995) as starting values for the parameters K, K_1 and W. The "best fit" parameters of the model evaluated at 50 °C are given in Table 2.2. With this method, best fit was qualified as the parameter values yielding the smallest mean square error (MSE). For all nonlinear curve fits, a sensitivity study was performed wherein the starting values of the parameters were varied by +/- one order of magnitude. This was done in order determine if the best fit parameters observed represented merely a local minima in the sum of squares. This sensitivity study exposed no parameter values that yielded a smaller MSE than the original starting values after Siau (1995).

Experiments conducted to evaluate degradation of wood indicated that at 160 °C, weight loss due to thermal degradation was much more severe at high relative humidities than at low relative humidities (Figure 2.9). This behavior can be explained by the drastic increase in thermal degradation of wood that occurs with increasing moisture content. Skaar (1976) reported reaction rates for thermal degradation in wet wood to be as high as ten times those for dry wood. Hillis (1984) also reviewed several studies that corroborate these findings.

To account for wood material lost to thermal degradation, a relationship to distribute the degradation weight loss among the stages of the desorption process was developed. This function preferentially attributed the degradation loss to the higher moisture content portion of the desorption experiments and corrected the observed EMC by adjusting the oven dry weight to reflect the weight of wood substance lost at each step. The degradation loss correction function applied to the wood degradation data is shown in Figure 2.9. Both actual and predicted degradation loss were normalized and displayed as a cumulative distribution function. Note that the loss of wood material is dependent on temperature, moisture content, and time. The results in Figure 2.9 are based on the time needed to achieve equilibrium at each relative humidity step of the desorption experiment. It was assumed that the wood degradation occurring during the heat-up phase of the experiment was negligible. This was justified because the amount of heat-

up time during which both the temperature and the relative humidity were sufficiently high was quite short.

Relationships for EMC and relative vapor pressure at 160 °C for the mature and juvenile wood of aspen, loblolly pine and yellow-poplar, respectively, are shown in Figures 2.10, 2.11 and 2.12. An identical nonlinear regression technique to that described above, including the starting value sensitivity study, was again used to fit the Hailwood-Horrobin 1 - hydrate model to the high temperature desorption data. Once more, no parameter values that yielded a smaller MSE than the original starting values were recorded. The best fit parameters of the model, evaluated at 160 °C are given in Table 2.3. The high temperature desorption isotherms were distinctly lower than their 50 °C counterparts, an expected result of the reduction in both the activity of water and the hygroscopicity of wood with increasing temperature. The initial linear portion and the first inflection point (near 0.1 relative vapor pressure) characteristic of the traditional, sigmoid shaped, isotherm are not visible in the fit curves. This behavior is consistent with the results of Strickler (1968), Engelhardt (1979) and Resch et al. (1988) and appears to reflect the extremely low EMC wood of at relative vapor pressures below 0.15 in high temperature environments. EMC initially increased rather slowly with relative vapor pressure, in a more or less linear fashion, up to a level of around 0.5. At this point, EMC increased at an accelerating rate as saturation was approached. This behavior suggested that some type of change in the material occurred around 50% relative humidity, affecting the sorptive behavior of the wood. Strickler (1968), recorded similar results, including a reversal effect at high relative vapor pressures whereas the EMC increases with increasing temperature, causing the sorption isotherms to cross over those at lower temperatures. He suggested a revised theory of sorption for high temperatures, postulating that this inflection was due to a combination of multi-layer sorption and inordinate swelling of the wood structure due to softening of the glassy wood polymers.

The temperature and humidity conditions at which the EMC increases rapidly are above the reported range for lignin to exceed its glass transition temperature (Kelley, et al. 1987). When a material goes through a glass transition, it is theorized that a corresponding increase in free volume occurs. Free volume is defined as the intermolecular space within a network of polymer molecules (Aklonis and MacKnight, 1983). Above the glass transition, the number of accessible primary sorption sites available in wood increases rapidly, yielding in effect an expanding

monolayer of sorbed water molecules. The data of Hahn (1965) and Englehardt (1979) also support the idea that plasticization of wood influences the slope of the EMC and relative humidity relationship. In addition, the results of Strickler (1968) indicate that as the isotherm temperature is increased from 100 to 170 °C, the point of increasing slope in the EMC curve moves toward lower relative vapor pressures. This appears to reflect the coupling affect between temperature and moisture on the glass transition of polymers. As temperature increases, the moisture level necessary for the onset of the glass transition is reduced (Aklonis and MacKnight, 1983). Researchers have also reported this phenomena on sorbents other than wood. Urquhart and Williams (1924), observed a similar reversal effect at high relative humidities which they attributed to "swelling of the material and consequent exposure of new surface." Jeffries (1960) also noted similar behavior with synthetic polymers at 120 and 150 °C.

At 160 °C, all three species illustrate an apparent difference in EMC behavior between juvenile and mature wood. Curiously, EMCs for juvenile wood were lower than those for mature wood at 160 °C, whereas this hierarchy was reversed at 50 °C. This was likely a result of the chemical differences between the two wood types, which was in some way manifested as a difference in sorptive behavior at high temperatures.

Table 2.4 lists the results of the chemical analyses performed on mature wood samples before and after desorption experiments. However, the observed changes in chemical composition are not significant in light of the accuracy of the technique. In general, mature wood samples tended to lose 2 – 3.5 % of their hemicelluloses during desorption, with southern pine recording the highest losses. As a result of these hemicellulose losses, there was an increase in percent lignin and cellulose content resulting from desorption. Southern pine exhibited the largest increase in total lignin, and the smallest increase in cellulose. Because resources were not available to analyze juvenile wood specimens, these results unfortunately do little to explain the differences in sorptive behavior between mature and juvenile specimens.

When compared to mature wood, juvenile wood has a higher concentration of hemicelluloses and lignin, at the expense of cellulose (Panshin and deZeeuw, 1980). Concerning the three primary components of wood, hemicelluloses are both the most hygroscopic, and the most susceptible to thermal degradation. Lignin is both the least hygroscopic and least susceptible to wood degradation (Fengel and Wegener, 1989; Christensen and Kelsey, 1959). At low temperatures, juvenile wood should thus be slightly more hygroscopic than mature wood,

explaining the higher EMC exhibited by juvenile wood at 50 °C. Juvenile wood at 160 °C would have, due to the relative thermal instability of the hemicellulose, lost its most sorptive component and become less hygroscopic than mature wood.

Based on the sorptive nature of the different wood components, a difference in the amount of wood material lost due to thermal degradation would have helped to explain the temperature effect on the differences in EMC between mature and juvenile wood. However, all specimens exhibited similar degradation losses, ranging from of 8 to 11 % of their oven dry weight. Hsu et al. (1988) treated wood with saturated steam at approximately 200 °C for 4 minutes and found an increase of water soluble compounds of 15% for aspen and 10% for lodgepole pine. There was essentially no change in the cellulose and lignin content.

The measured degradation losses due to the desorption experiments may not reflect the complete nature of the wood decompostion process. It is quite probable that some of the hemicelluloses could have been degraded such that their hygroscopicity was reduced, yet the degradation products still remained within the wood structure. Thus, many of the degradation products would contribute to the non-sorptive weight of the specimen, but not actively participate in adsorbing or desorbing water.

Figures 2.13 and 2.14 display the 160 °C isotherm data from this study along with data collected by others. The technique used by Resch et al. (1988) to collect data for the EMC of yellow-poplar at 160 °C (Figure 2.13) was the most similar. Resch et al. only considered time when correcting for weight lost due to wood degradation. EMC was calculated at each step based on the initial oven-dry weight of the specimens. Whereas EMC values in this study were calculated based on the (corrected) oven-dry weight at each step. When corrected as per the method used herein, the data of Resch et al. appear closer to the EMC results generated in this study for yellow-poplar (juvenile and mature). Results of Hahn (1966) for yellow-poplar tend to agree more closely with the data presented here, while the data of Engelhardt (1979) for Beech tend to fall in between. The EMC data of Strickler (1968) for adsorption of grand fir at 150 and 170 °C is slightly elevated in comparison to the desorption EMC data for loblolly pine (combined mature and juvenile wood) presented in this paper (Figure 2.14). Larger deviations occur above 0.8 relative vapor pressure. The temperature dependent parameters of the Hailwood-Horrobin 1-hydrate model presented by Siau (1995) failed to adequately describe EMC behavior at 160 °C exhibited here and in the literature, and predicted nonsensical values of EMC at temperatures above 155 °C.

CONCLUSIONS

Equilibrium moisture content data in the form of desorption isotherms was collected for mature and juvenile wood of aspen, loblolly pine and yellow-poplar. This data pertains to the understanding of material behavior during the manufacture of wood-based composites.

A high-temperature sorption apparatus was designed to generate the environments necessary to achieve saturation conditions at 160 °C. This apparatus had the instrumentation and control features necessary to create a constant temperature, water vapor environment, and to reduce the humidity level of that environment in a stepwise fashion from saturation to atmospheric conditions. A gravimetric method of MC determination was performed continuously inside the apparatus.

At 50 °C, EMC behavior of the wood species studied deviated only slightly (and only at high humidities) from predictions based on the data derived from Sitka spruce. EMC behavior at 160 °C, however, was distinctly different from the 50 °C data, or any extrapolation from existing low temperature data. Isotherms generated at 160 °C initially exhibited low EMCs before turning sharply upwards above 60% relative humidity. This behavior suggested that a change in the sorptive properties of the wood occurred as temperature and moisture conditions exceeded the glass transition temperature for lignin.

Considerable differences existed between the EMC relationships of juvenile and mature wood. At 50 °C juvenile wood tended to equilibrate at higher EMCs than mature wood. At 160 °C, however, juvenile wood exhibited markedly lower EMCs than mature wood. Substantial thermal degradation of wood was measured during desorption experiments. This degradation was manifested as weight loss and was much more severe at high humidity levels. Reduction in the sorptive behavior as a result of thermal degradation was proposed as a possible explanation for differences in EMC behavior for juvenile and mature wood at 160 °C.

RECCOMMENDATIONS

The collection of additional EMC data at temperatures between 100 and 160 °C would be helpful in further understanding the sorptive behavior of wood in conditions relative to wood-based composites manufacture, and would likely help to shed light on some of the questions raised by this work. An in depth study of thermal degradation of wood as a function of moisture content, with accompanying chemical analysis would assist in delineating contributions to sorption by: the

degraded and lost material, degraded material which is present within the wood structure, and the undegraded wood components. This approach should also help to explain differences in the sorptive behavior of mature and juvenile wood. A review of sorption models to determine if there exists a relationship which can describe the unique high temperature EMC behavior of wood, in terms of structural and sorptive changes resultant from exceeding the glass transition, would also be warranted.

CHAPTER 2 TABLES

Table 2.1. Control sequence for high-temperature desorption experiments.

			Control Setpoints		
Step	Action	Time (min.)	Temp (°C)	Pressure (kPa, psia)	Rel. Hum. (%)
	Heat-up sequence				
1	increase internal temperature	75[a]	160	583.8 (84.7)	94.5
2	wait for pressure to reach saturation	10[a]	160	583.8 (84.7)	94.5
	Desorption sequence				
3	hold at this condition	45	160	583.8 (84.7)	94.5
4	ramp pressure setpoint to next	10	160		
5	hold at this condition	45	160	549.3 (79.7)	88.8
6	ramp pressure setpoint to next	20	160		
7	hold at this condition	45	160	480.4 (69.7)	77.7
8	ramp pressure setpoint to next	20	160		
9	hold at this condition	45	160	411.4 (59.7)	66.6
10	ramp pressure setpoint to next	20	160		
11	hold at this condition	45	160	342.4 (49.7)	55.4
12	ramp pressure setpoint to next	20	160		
13	hold at this condition	45	160	273.5 (39.7)	44.2
14	ramp pressure setpoint to next	20	160		
15	hold at this condition	45	160	204.5 (29.7)	33.01
16	ramp pressure setpoint to next	20	160		
17	hold at this condition	45	160	135.5 (19.7)	21.9
18	ramp pressure setpoint to next	20	160		
19	hold at this condition	45	160	101.0 (14.7)	16.4
	Shutdown sequence				
20	cool to ambient temperature	225	20	101.0 (14.7)	16.4

[a] approximate time

Table 2.2. Parameters of the Hailwood-Horrobin 1-hydrate model evaluated at 50 °C.

Specie	Parameters			Source
	W	K	K_1	
Sitka Spruce	0.306	5.88	0.776	Simpson (1973)
Aspen				
Juvenile	0.330	8.010	0.841	[a]
Mature	0.340	7.334	0.839	
Loblolly pine				
Juvenile	0.278	5.837	0.801	[a]
Mature	0.263	5.171	0.777	
Yellow-poplar				
Juvenile	0.315	6.178	0.832	[a]
Mature	0.295	4.836	0.816	

[a] Fit to the data in this study.

Table 2.3. Parameters of the Hailwood-Horrobin 1-hydrate model evaluated at 160 °C.

Specie	Parameters			Source
	W	K	K_1	
Aspen				
Juvenile	-0.010	-1.012	0.830	[a]
Mature	0.004	-0.990	0.771	
Loblolly pine				
Juvenile	0.016	-0.981	0.664	[a]
Mature	0.004	-.990	0.771	
Yellow-poplar				
Juvenile	0.002	-0.996	0.776	[a]
Mature	0.005	-0.971	0.572	

[a] Fit to the data in this study.

Table 2.4. Chemical composition of mature wood samples of southern pine, aspen and yellow-poplar before and after a desorption experiment at 160°C.

Sample ID[a]	Sugar Composition[b], %						Lignin, %			Ash[d], %
	Cellulose	Non-Cellulose				Total Sugar	Acid[c] Insoluble	Acid Soluble	Total Lignin	
	Glucan	Xylan	Galactan	Arabinan	Mannan					
SPMu	43.94	6.97	2.22	0.00	15.17	68.29	25.55	0.29	25.84	0.03
SPMt	44.43	5.63	1.54	0.00	13.12	64.71	29.41	0.58	29.99	0.58
ASMu	42.95	17.04	0.00	0.00	1.85	61.85	19.24	3.07	22.31	0.43
ASMt	44.40	14.80	0.00	0.00	1.66	60.86	21.59	2.97	24.56	0.13
YPMu	43.91	13.76	0.00	0.00	1.51	59.18	22.06	3.91	25.97	0.41
YPMt	47.58	12.26	0.00	0.00	1.68	61.52	25.35	3.18	28.53	0.02
Sigma Oat Spelts Xylan (control)	11.19	66.66	0.00	6.49	0.00	84.34	2.20	0.57	2.77	3.22

[a] SPMu = untreated southern pine mature wood, ASMt = aspen mature wood after desorption, YPM = yellow-poplar mature wood.

[b] Sugar composition and lignin content determined according to procedure described by Kaar et. al., 1991, *J. Wood Chem. Technol.*, 11(4):447-469

[c] (Klason), also includes extractives in this analysis

[d] Ash content determined by thermogravimetric analysis (TGA @ 700°C, 10°C/min)

Total composition of a sample is not 100 %, due to not measuring uronic acids and acetyl content.

CHAPTER 2 FIGURES

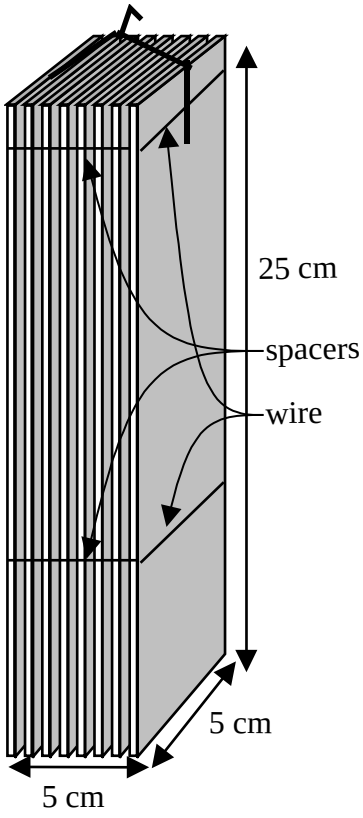

Figure 2.1. Diagram of 160 °C desorption specimen.

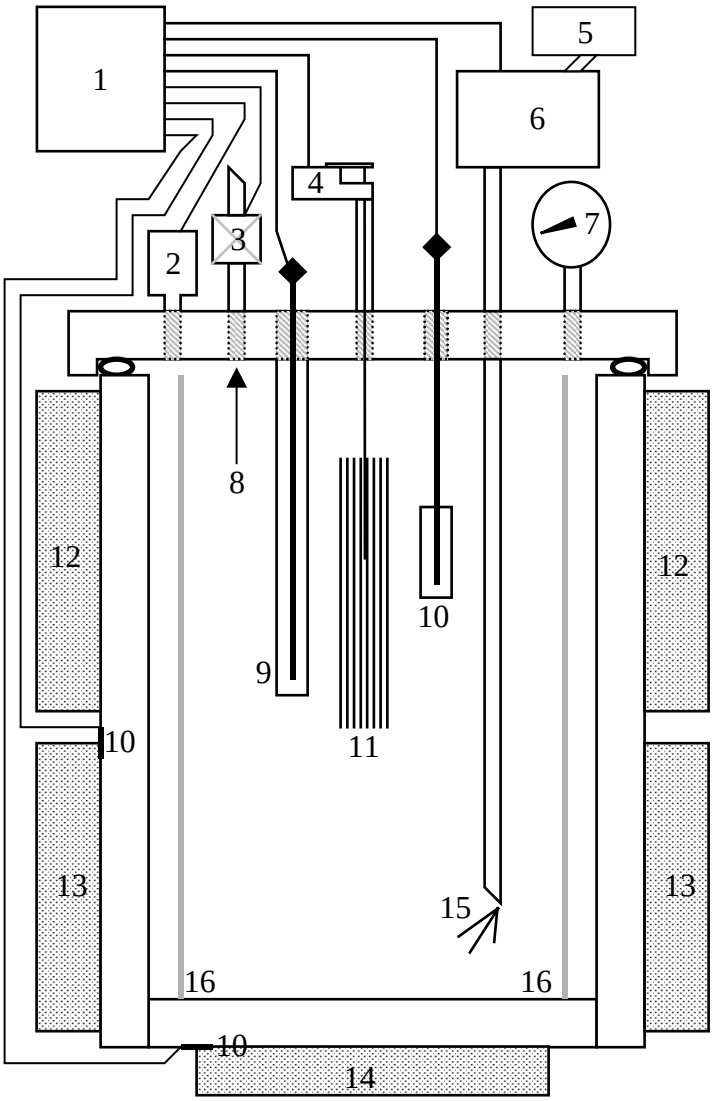

1 - Control and acquisition system
2 - Pressure transducer
3 - Solenoid valve
4 - Load beam
5 - Make-up water reservoir
6 - High pressure water pump
7 - Pressure gauge
8 - Venting port
9 - Thermocouple well
10 - Control thermocouple
11 - Wood sample
12 - Secondary heating element
13 - Primary heating element
14 - Tertiary heating element
15 - Water injection port
16 - Radiation shield

Figure 2.2. Schematic of pressurized sorption apparatus.

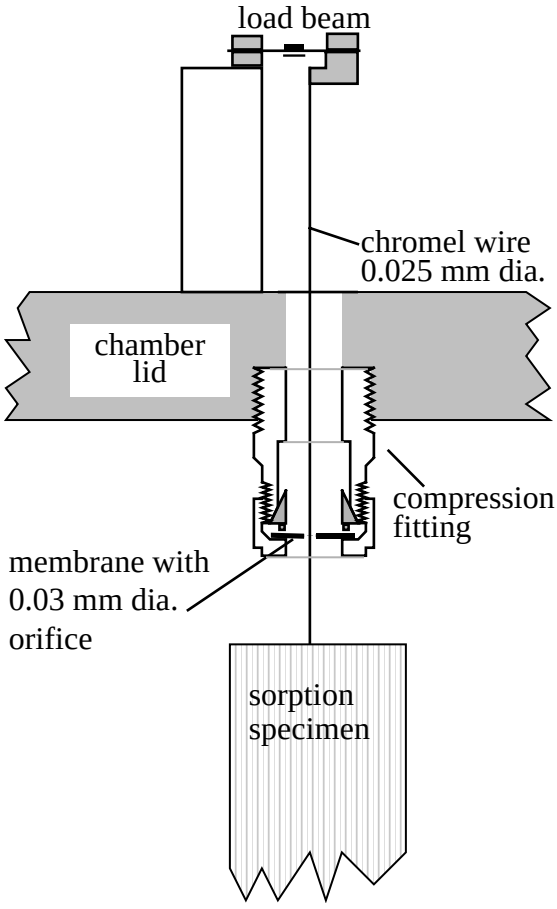

Figure 2.3. Schematic of weighing mechanism for the pressurized sorption apparatus.

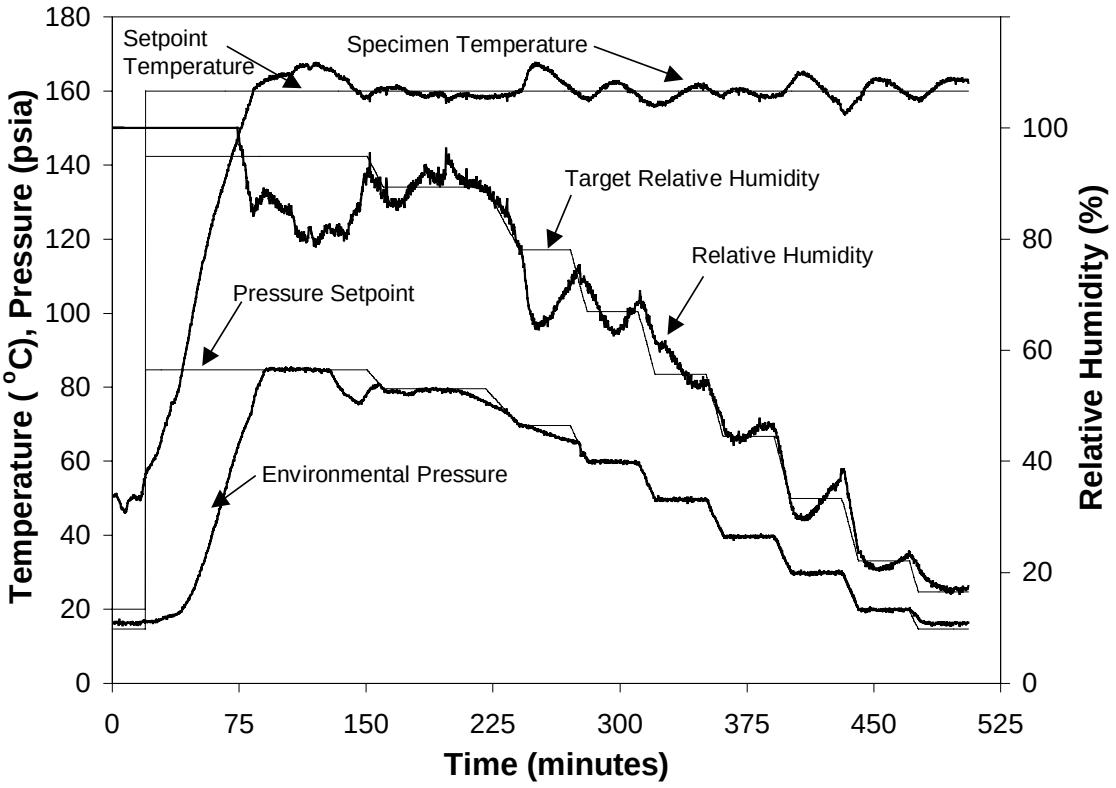

Figure 2.4. Environmental conditions and specimen temperature for a desorption experiment at 160 °C.

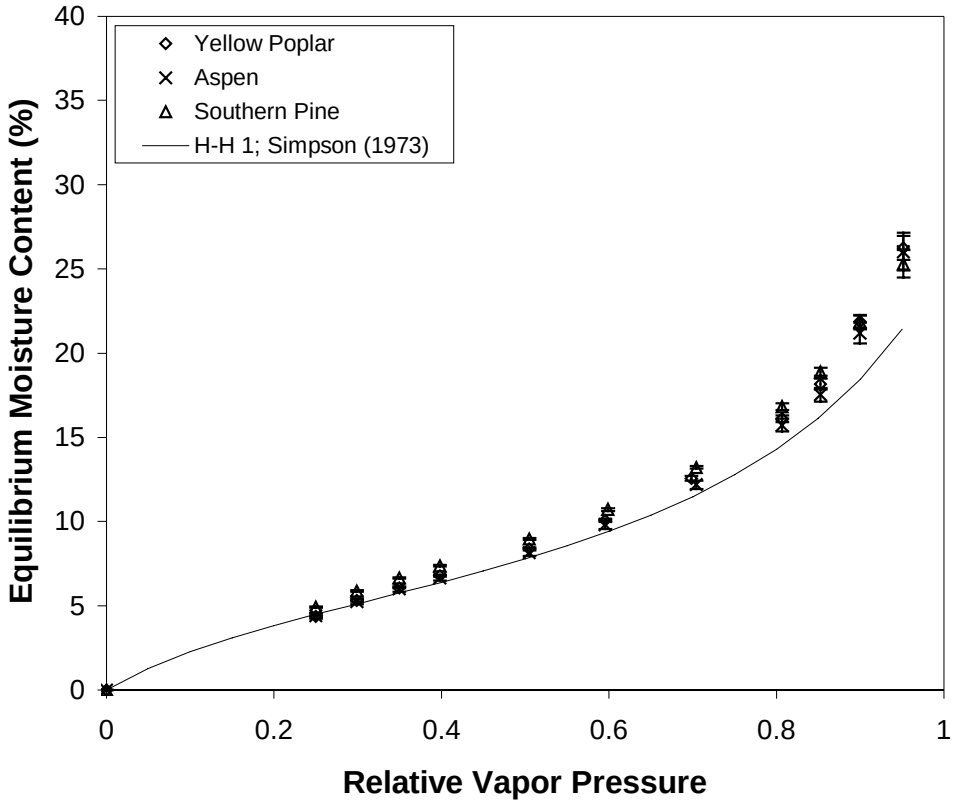

Figure 2.5. Desorption isotherms at 50 °C. Data points represent the average value for each wood type with error bars indicating one standard deviation. Solid line is EMC predicted by the Hailwood-Horrobin 1-hydrate model with parameters after Simpson (1973).

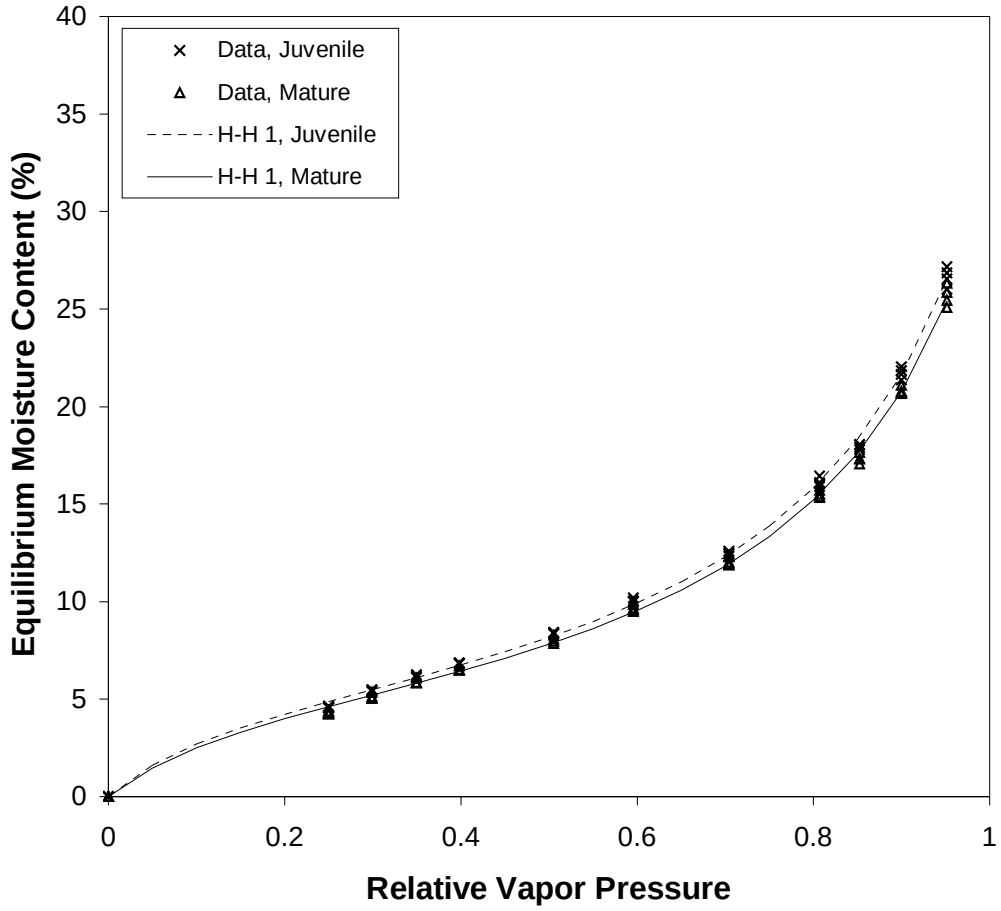

Figure 2.6. Desorption isotherm data for juvenile and mature aspen wood at 50 °C. Lines represent a nonlinear fit to the Hailwood-Horrobin 1-hydrate model.

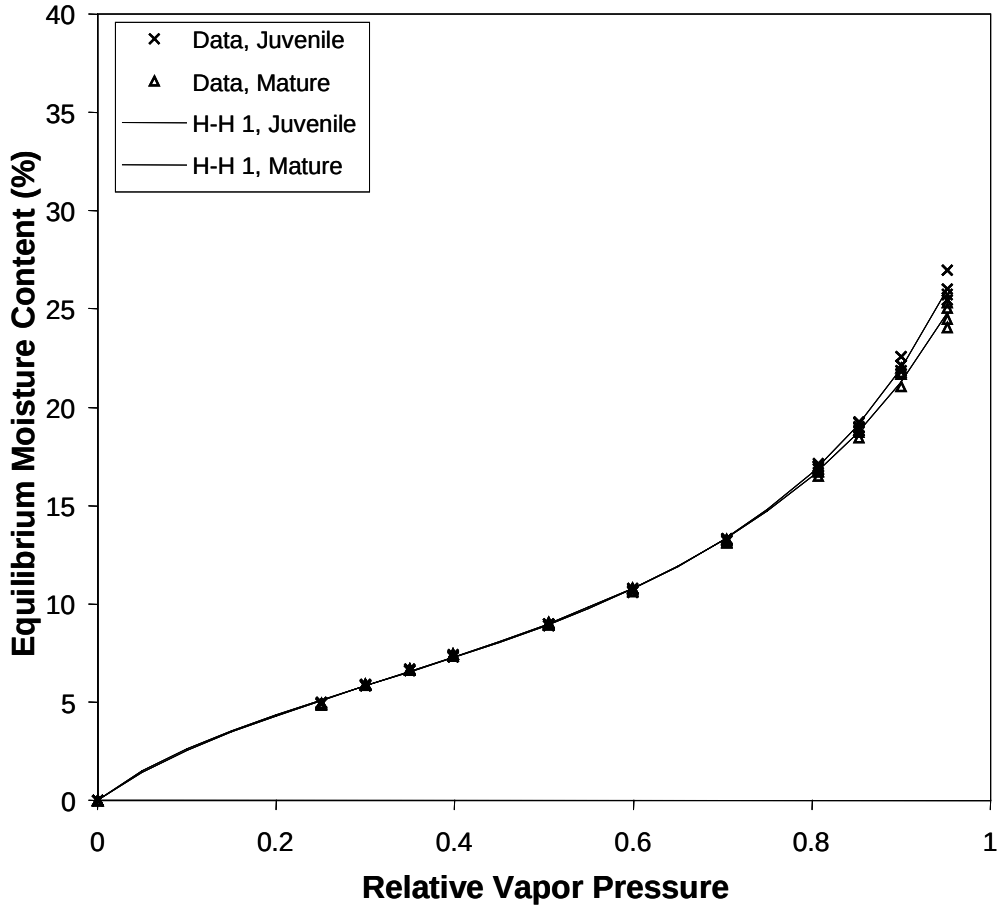

Figure 2.7. Desorption isotherm data for juvenile and mature loblolly pine wood at 50 °C. Lines represent a nonlinear fit to the Hailwood-Horrobin 1-hydrate model.

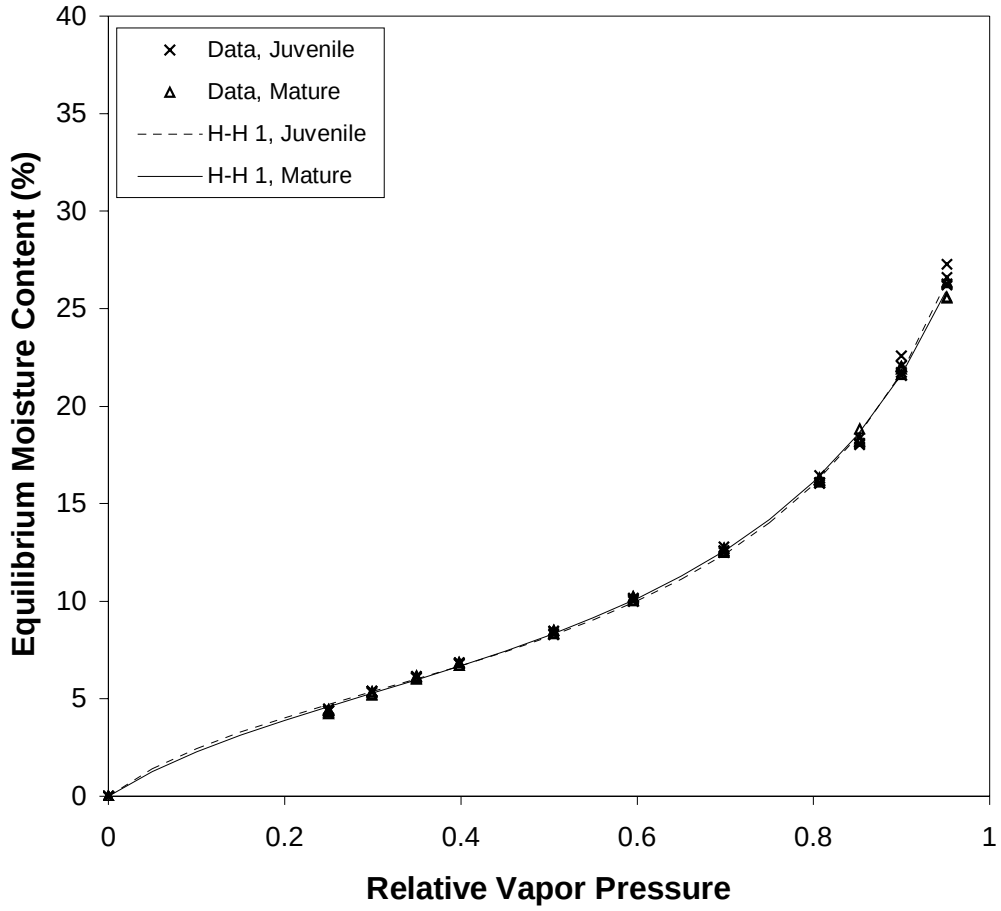

Figure 2.8. Desorption isotherm data for juvenile and mature yellow-poplar wood at 50 °C. Lines represent a nonlinear fit to the Hailwood-Horrobin 1-hydrate model.

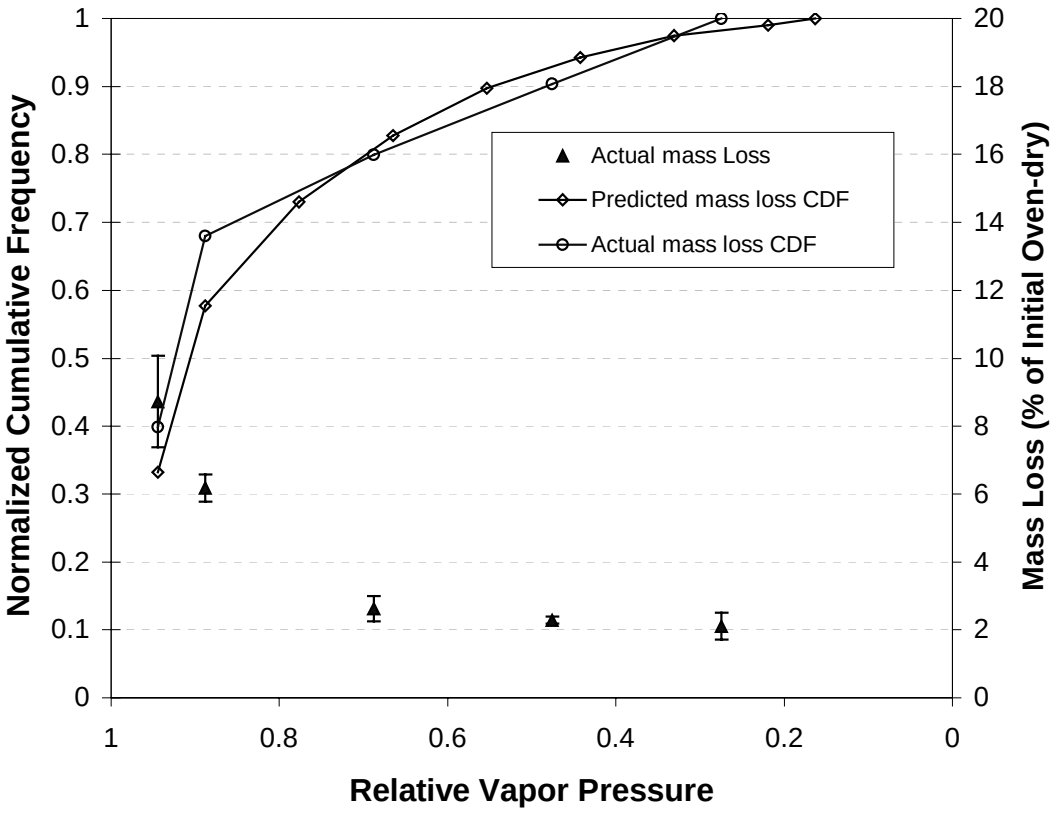

Figure 2.9. Weight loss due to degradation as a function of relative vapor pressure, for desorption of mature yellow-poplar at 160 °C, reflecting the time needed to equilibrate at each step. Lines represent normalized degradation loss in the form of a cumulative distribution function (CDF).

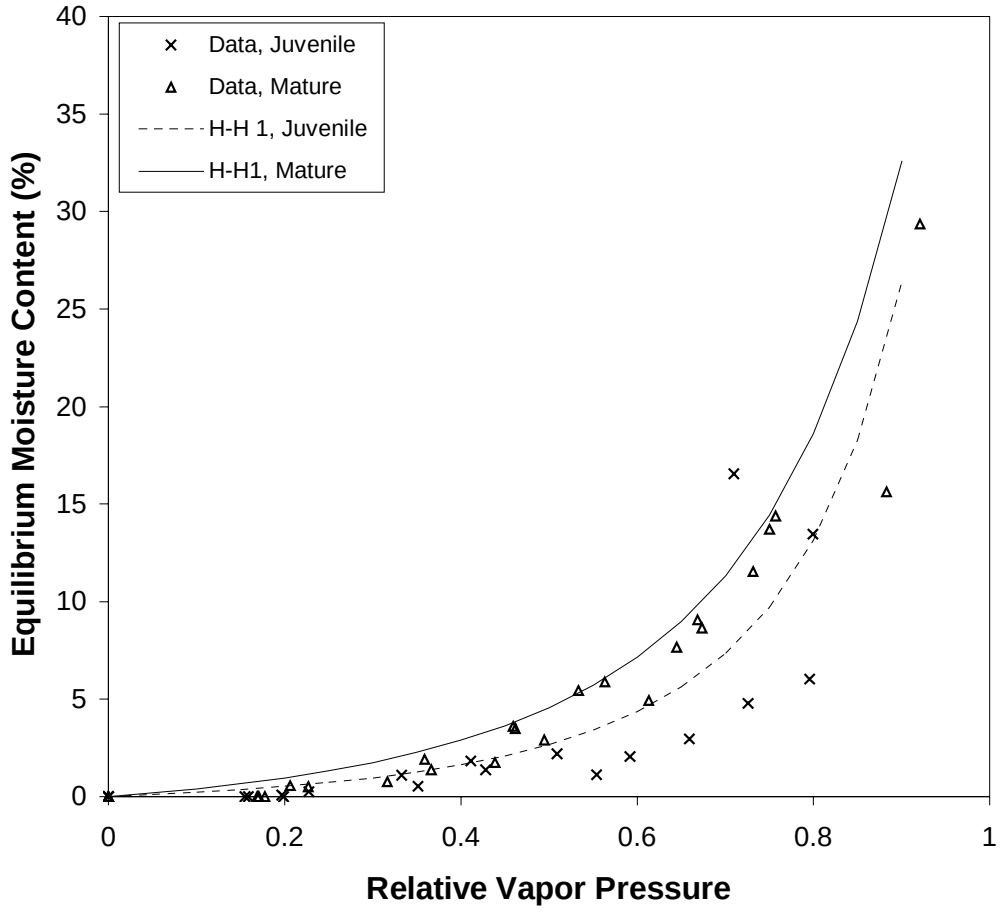

Figure 2.10. Desorption isotherm data for juvenile and mature aspen wood at 160 °C. Lines represent a nonlinear fit to the Hailwood-Horrobin 1-hydrate model.

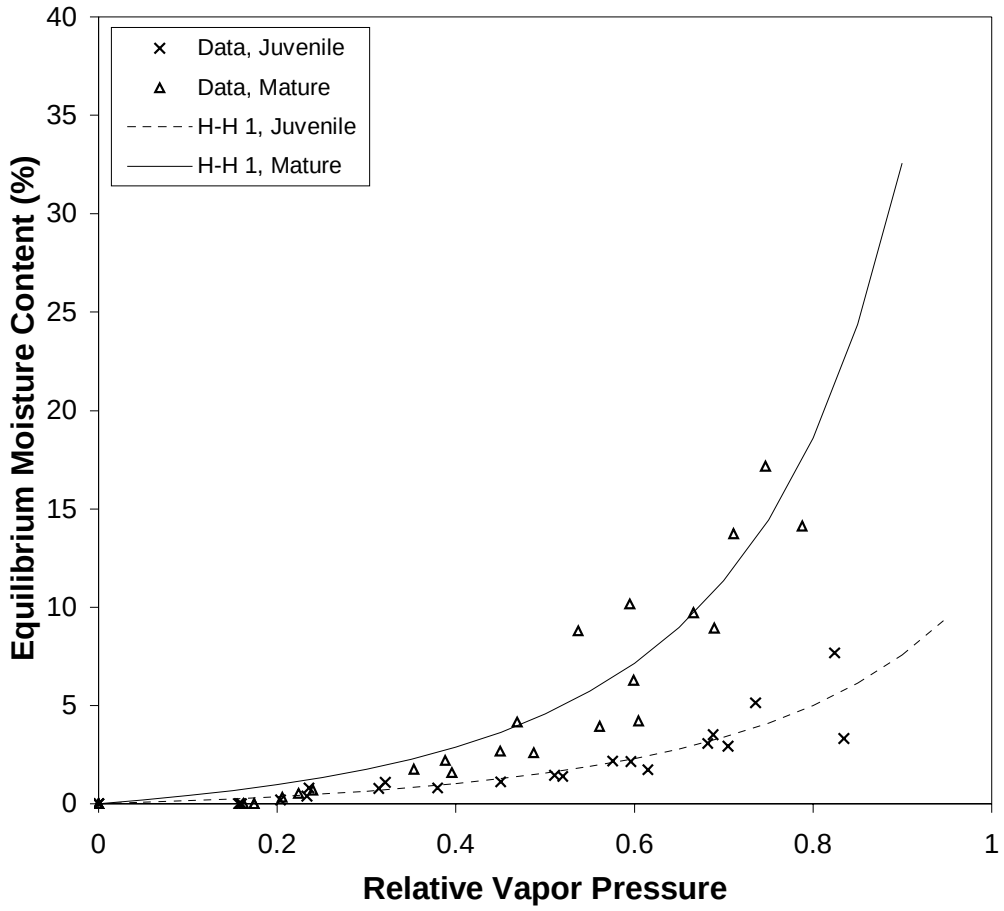

Figure 2.11. Desorption isotherm data for juvenile and mature loblolly pine wood at 160 °C. Lines represent a nonlinear fit to the Hailwood-Horrobin 1-hydrate model.

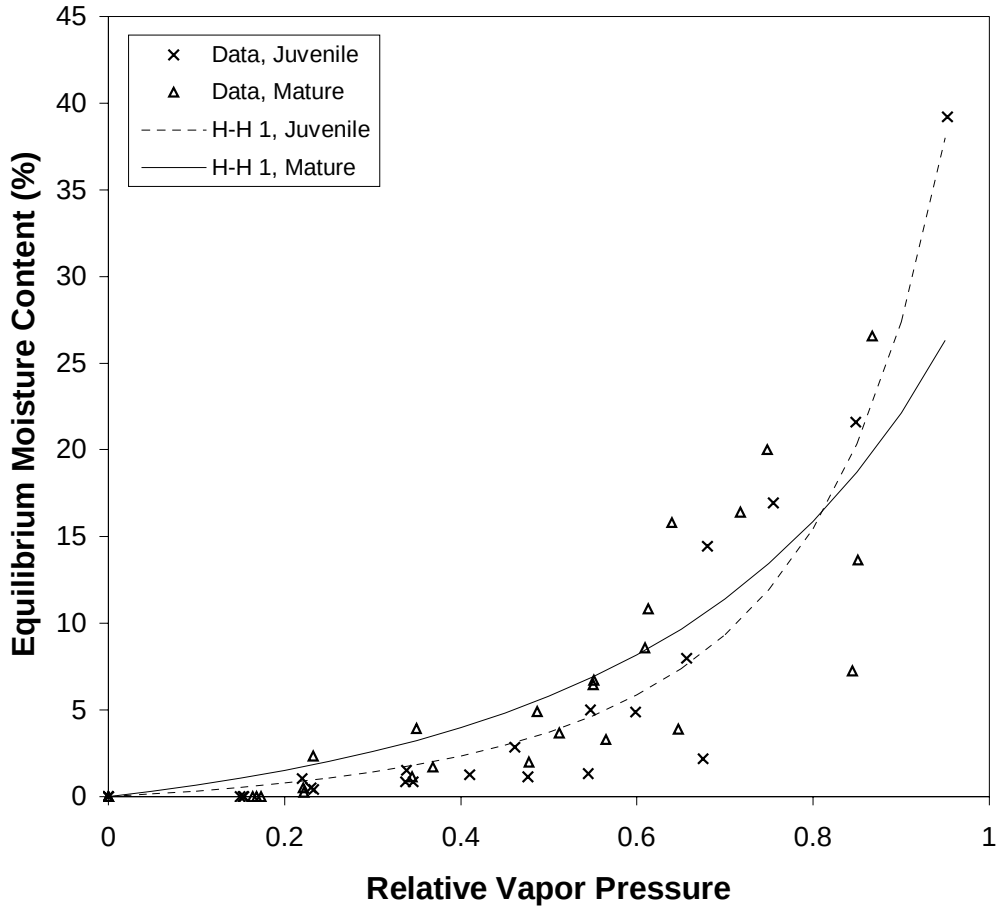

Figure 2.12. Desorption isotherm data for juvenile and mature yellow-poplar wood at 160 °C. Lines represent a nonlinear fit to the Hailwood-Horrobin 1-hydrate model**.**

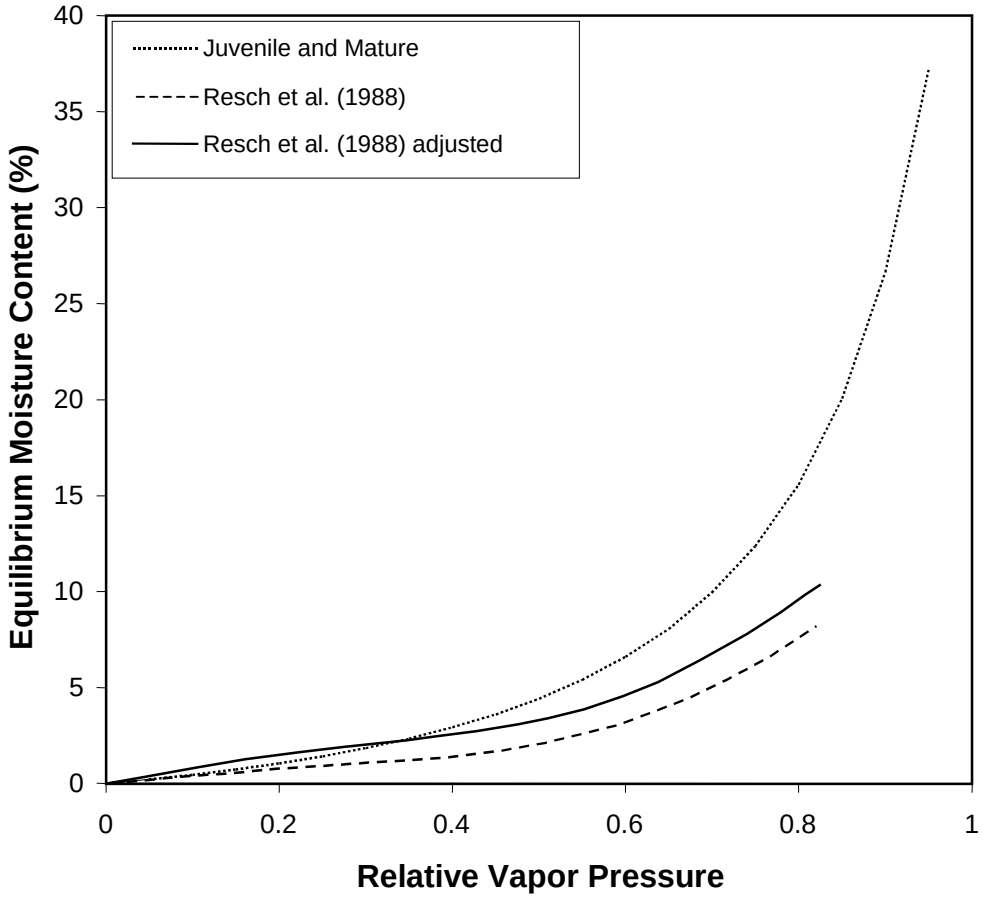

Figure 2.13. EMC for yellow-poplar wood at 160 °C. Data from combined mature and juvenile wood from this study in addition to data from Resch et al. (1988).

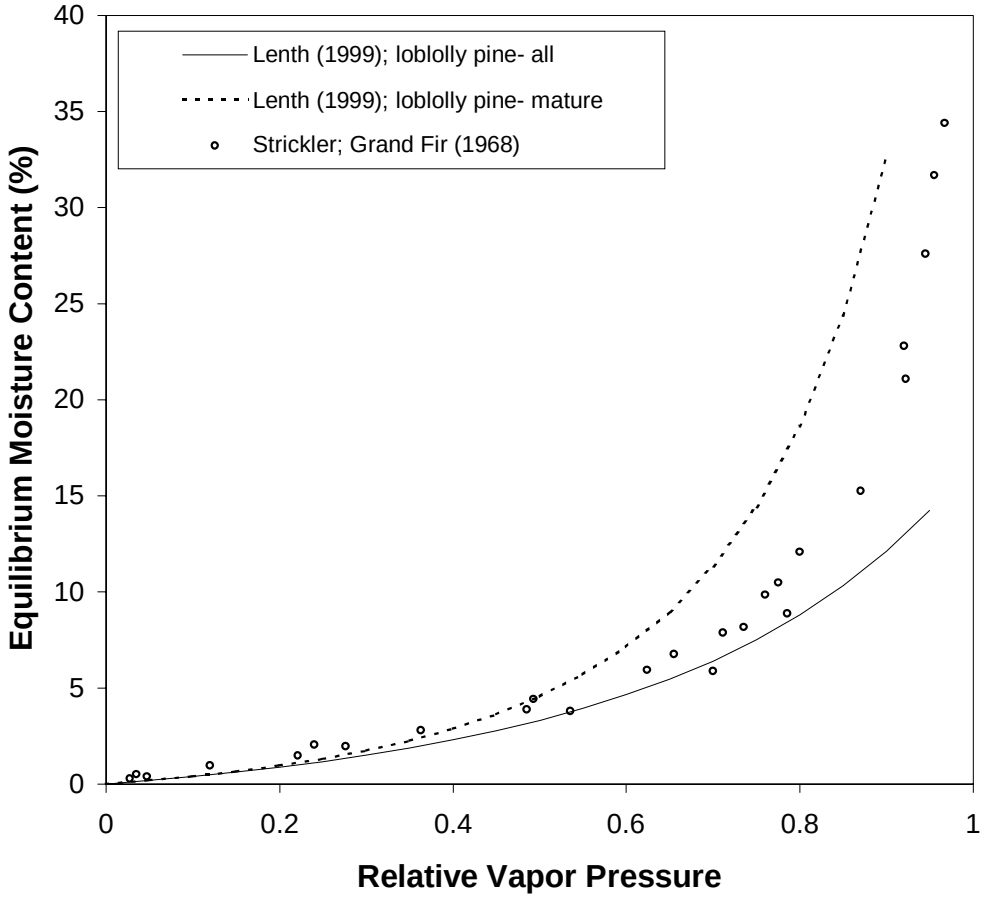

Figure 2.14. EMC for mature and combined mature and juvenile loblolly pine wood at 160 °C, in addition to data from Strickler (1968) for adsorption of grand fir at 150 and 170 °C.

CHAPTER 3. MOISTURE DEPENDENT SOFTENING BEHAVIOR OF WOOD

INTRODUCTION

The hot-press consolidation process used in the manufacture of wood-based composite products creates an environment which accentuates viscoelastic behavior. This viscoelastic behavior often results in densification from transverse compression of the constituent wood elements. Wood densification can have both permanent and recoverable components, which together have significant influence on the physical and mechanical properties of the composite product. It is known that the local environment of moisture content and temperature during hot-pressing influences densification, density gradient formation and non-recoverable strain. Furthermore, it has been observed that the increased density, and other physical or chemical changes, result in modified wood properties. These changes have considerable implications for improved product performance, yet their nature and the mechanisms responsible for them remain essentially unresolved.

The overall goal of this research effort is to characterize the viscoelastic behavior of wood as it pertains to conditions found during hot-pressing. This study employs a materials science approach to understanding the process of viscoelastic compression. This is fundamental research that will increase the understanding of material behavior during the manufacture of wood-based composites and provide insight for the development of new and improved products and processes using viscoelastic-thermal-compression (VTC). This research initiative has three sequential and interrelated components. The author feels these to be the necessary steps for understanding the phenomena involved in viscoelastic compression, and delineating the mechanisms through which this procedure can be harnessed into improved manufacturing technology.

The initial phase of this work involved investigations of the wood-water relationship at conditions relevant to the hot-pressing of wood composites. The focus of that work was to characterize the wood-water relationship in environments relative to wood-based composites manufacture. The research presented in this chapter built upon the knowledge gained in the high-temperature EMC study, an evaluation of the viscoelastic behavior of wood as a function of moisture content. This study investigated the thermal *softening* of the constituent wood polymers and the influence of wood moisture content on viscoelastic behavior. The viscoelastic behavior was probed through observation of the glass transition (T_g) temperature of *in situ* amorphous

components of wood via microdielectric analysis. The specific technical objective of this study was to characterize the glass transition behavior of wood as a function of moisture content at conditions relevant to wood-based composites manufacture. The results of this work will allow us to define optimum conditions for the viscoelastic thermal compression on wood.

BACKGROUND

Deformation of the wood component and development of density gradients during hot-pressing are very influential on resultant board properties. The time-dependent compression strain in a wood composite is influenced by temperature and moisture content changes during hot-pressing. The wood material may exhibit both glassy and rubbery phase behavior (Wolcott et al. 1990). Wood, though a complex natural polymeric composite material, exhibits physical and mechanical characteristics similar to simpler and more well defined synthetic polymers. Shutler (1992) found that moist yellow-poplar samples tested in compression exhibit the similar mechanical behavior to flexible polyurethane foams. Salmen (1984) and Kelley et al. (1987) have demonstrated application of the polymer science principal of time-temperature superposition to the softening of wood. Wolcott et al. (1990, 1994) extended this work by employing time-temperature-moisture content superposition as a method to explain the time dependent behavior of wood during the hot-pressing of wood-based composites.

Materials, such as wood, whose mechanical behavior is intermediate between that of solids and liquids are termed viscoelastic (Ferry 1980). Viscoelastic, amorphous polymers can exhibit a range of mechanical properties from linearly elastic to viscous dependent on the temperature, diluent concentration and time scale of the test (Ward 1983). The hemicelluloses, lignin, and non-crystalline cellulose components of the wood cell wall are amorphous and exhibit such viscoelastic characteristics in mechanical properties when exposed to increasing temperature, increasing moisture content, or very long times (Wolcott et al. 1990). The glassy state (Figure 3.1) of a polymer pertains to behavior at low temperatures, low diluent concentrations and high measurement frequencies and is often characterized by high modulus and brittle fracture (Wolcott et al. 1990). Lower modulus and high failure strains characterize the rubbery state, which refers to behavior at high temperatures, high diluent concentrations and low frequencies. Beyond the rubbery state, polymers such as thermoplastics will exhibit viscous flow, although it is believed that this behavior does not occur in wood prior to the onset of thermal degradation (Wolcott, et al. 1990).

Between the glassy and the rubbery states lies a region of transient behavior characterized by marked changes in properties resulting from small changes in temperature, diluent concentration or time. Considering any one of these amorphous polymers independently, the boundary between glassy (elastic) and rubbery (viscous) behavior is defined by a glass transition temperature, T_g, (Back and Salmen, 1982).

The glass transition temperature is defined as the temperature at which the available thermal energy of the polymer segments are sufficient to overcome the rotational energy barriers in the chain (Cowie, 1991). The transition from the glass to the rubbery state in polymers can be detected by observing rapid changes in mechanical or physical properties such as modulus, specific volume, heat capacity and dielectric behavior with increasing temperature. The term T_g generally refers to a temperature range or region where properties are rapidly changing, rather than a discrete temperature. Common analytical methods used to evaluate the glass transition of polymeric materials include both static and dynamic techniques. Differential scanning calorimetry (DSC), differential thermal analysis (DTA) and thermogravimetric analysis (TGA) are examples of static methods, whereas dynamic mechanical analysis (DMA/DMTA), dielectric thermal analysis (DETA) and torsional pendulum analysis represent common dynamic techniques for investigating the glass transition. Each technique probes different mechanical and/or molecular relaxations within the material, and observed values of T_g depend both on the technique and rate of measurement (Cowie, 1991). Dynamic techniques are further complicated by a strong influence of the frequency of the applied perturbation on the temperature of the observed transition. This frequency dependence can, however, be utilized advantageously to further investigate and differentiate relaxations and transitions in materials.

For characterizing the influence of moisture on softening behavior in hygroscopic materials such as wood, a problem exists in that common methods involve temperature scans, which, in an effort to detect a discontinuity in material response, cause a change of moisture content. It is well known that decreasing moisture content increases the T_g of amorphous polymers like lignin and hemicelluloses. Moisture content is reduced as temperature rises, thus driving the apparent T_g still higher. When the response to a mechanical stress is used to detect the T_g, as in dynamic mechanical analysis, the effects of declining moisture content become even more complex. If a mechanical stress is applied, desorption of a sample during testing could yield a reduced apparent Tg due to mechano-sorptive phenomena (Casey, 1987). If the moisture content is allowed to drift during

testing, the desired discontinuity becomes a subtle transition that may not be detectable before the wood polymer components begin to decompose (Wolcott et al., 1994). Some studies have been successful in maintaining saturation of sealed specimens as the temperature is increased (Salmen 1984; Irvine, 1984; Takahashi et al., 1998; Uhmeier et al., 1998). In order to maintain constant specimen moisture content, specimens must either be sealed, which interferes with most types of measurements, or experiments must be carried out in an environment that can maintain constant EMC conditions as the specimen temperature is elevated. Becker and Noack (1968) applied this approach to dynamic torsional measurements on beech wood, but their temperature scans were limited to 100 °C due to constraints of atmospheric pressure.

The hemicelluloses, lignin and amorphous cellulose components of wood have all been shown to exhibit thermal softening characteristic of the glass transition when isolated individually (Goring, 1963; Cousins, 1976; Salmen and Back, 1977; Back and Salmen, 1978; Irvine, 1984). While these results are important and some congruence exists among them, differing methods of extracting and preparing the wood constituents, as well as inconsistencies in techniques for detecting transitional behavior, limit their ability to describe the softening behavior of whole wood. It is also doubtful that the extracted compounds accurately represent the behavior of the *in situ* wood components. Since wood is a complex biological polymer composite with distinct molecular domains, the observed softening behavior of neat wood consists of one or more of rather broad transitions as determined by dynamic mechanical analysis (DMA), differential scanning calorimetry (DSC) and dielectric thermal analysis (DETA) (Salmen 1984; Wert, et al. 1984; Kelley et al. 1987). Where a single transition has been observed in solid neat wood, it is generally attributed to softening of *in situ* lignin (Chow and Pickles, 1971; Funakoshi, et al. 1979; Atack, 1981; Irvine, 1984; Östberg, et al. 1990; Takahashi, et al.1998; Uhmeier et al. 1998). Studies by Höglund, et al. (1976) and Becker and Noack (1968) have also reported softening behavior in wood, however they do not attribute it to specific wood constituents. In the range of –20 to 192 °C, two separate softening peaks have been observed by researchers using both dynamic and static mechanical methods for various species of solid wood with moisture contents from dry to saturation. These peaks have been attributed to relaxations in either a] the hemicellulose and lignin fractions, (Hillis and Rosa, 1978; Kelley, et al. 1987) or b] crystalline and amorphous regions in wood (Wert, et al 1984). Table 3.1. summarizes the softening temperatures reported for wood in the available literature.

Dielectric thermal analysis (DETA) is an increasingly popular technique for exploring molecular phenomena such as relaxations within polymers and is especially effective for observation of polar molecules where energy absorption is primarily due to reorientation of permanent dipoles (Hedvig, 1977). While dielectric analysis has been practiced for decades, modern microdielectric equipment provides for simultaneous acquisition of data across a wide range of frequencies using a variety of sensor configurations.

In DETA an oscillating, low voltage electrical field is applied to the sample. The sample acts as both a resistor and capacitor, displacing the electric charge. The complex dielectric constant ε^* can be determined by measuring the change in the amplitude and phase of the returning electrical current (Cowie, 1991). This principle is illustrated schematically in Figure 3.2. The complex dielectric constant (ε^*) can be further resolved into the dielectric permitivity (ε'), a measure of the electrical energy stored by the material, and the dielectric loss factor (ε''), an indication of the energy dissipated within the material (Cowie, 1991; Torgovnikov, 1993).

During a DETA experiment, atoms, ions, molecules and polar groups within the analyzed material align or attempt to align themselves with the direction of the applied electrical field. The relaxation times required for the displaced items to return to an unperturbed position when the field is removed give rise to distinct regimes of polarization for the material, which can be thought of as a spectrum of relaxation times. As a result, the dielectric properties of a material exhibit a strong dependence on the frequency of the applied electromagnetic field.

The dielectric response of wood and wood composites results primarily from ionic, dipole and interfacial polarizations (Torgovnikov 1993). *Ionic Polarization* results from the migration of charged ions in response to an external electric field. Relaxation times for ionic polarizations range from 10^{-13} to 10^{-12} seconds. *Dipole Polarization* is the rotation of polar molecules in the direction of an external electric field. The macromolecules cellulose, hemicellulose and lignin, as well as water, are subject to dipole polarization. Dipole polarization relaxation times range from 10^{-6} to 10^{-10} seconds. For this reason, dipole polarization manifests itself at frequencies less than 10^{10} Hz. *Interfacial Polarization* occurs between substances with different molecular or morphological properties at interfaces within heterogeneous materials such as wood. Relaxation times for interfacial polarizations range from 10^{-6} to 10^{-3} seconds (Torgovnikov 1993).

Qualitatively, the dielectric permitivity (ε') can be considered analogous to the mechanical loss compliance, while the dielectric loss factor (ε'') is more closely related to the mechanical

loss modulus than it is to the loss compliance (Cowie, 1991). However, the dielectric loss tangent ($\tan\delta = \varepsilon'' / \varepsilon'$) is the parameter that reflects most closely the response of the mechanical loss E''. Transitional behavior in solid materials is generally manifested as peaks in dielectric loss factor and tangent delta ($\varepsilon''/\varepsilon'$). When directly compared, DETA and DMTA measurements return comparable values for α and β transitions in polymers, and also exhibit similar characteristics when the frequency dependence of those transitions are investigated (McCrum et al., 1976; Wetton et al., 1986). DETA has shown to be complementary to the standard techniques of DSC and DMA for measuring relaxation phenomena in polymers (Rials 1992; Connolly and Tobias 1992). Eaton et al. (1976), Wert et al. (1984), and Mizumachi (1991) have used DETA to observe second order transitions in cellulose and its derivatives, wood, and wood polymer composites, respectively.

EXPERIMENTAL

Mature log sections of yellow-poplar (*Liriodendron tulipifera*) and loblolly pine (*Pinus taeda*) were obtained and cut into cants. These cants were further separated into juvenile, mature and intermediate portions. Juvenile wood was defined as the wood inside the tenth growth ring and mature wood as that material outside the thirtieth growth ring, as per Kretschmann and Bendsten (1992). The wood material was then end sealed and allowed to air dry at ambient laboratory conditions for approximately 12 months.

Specimens were created by cutting 3 to 4mm slices from the tangential surface of the seasoned cants. These slices were machined into veneers with a uniform thickness of 2mm in the radial direction using an abrasive planer. The veneers were then trimmed to dimensions of approximately 80 by 100 millimeters. Six replicate specimens of both mature and juvenile wood of each species were fabricated, for a total of 24 samples. Specimens were then separated into two groups of 12 samples, containing 3 replicates each of juvenile and mature wood for both species. Four testing conditions were investigated: 20, 12, 5, and 0 % moisture content. Higher moisture levels were not investigated because the DETA was unable to resolve consistent results at moisture levels above 20%. Each group of 12 specimens was be tested at two of the four moisture content conditions. The weight of the trimmed specimens was recorded and they were then dried in a convection oven at 102 °C to obtain the oven-dry weight as per ASTM Standard D4442, Method B. The perimeter edges of the dried samples were sealed with a 2mm layer of silicon sealant (Dow Corning™ 8641)

to prevent moisture loss during subsequent testing. The edge-sealed specimens were then oven-dried a second time at 102 °C. Half of the dried and edge-sealed specimens were allowed to equilibrate to a nominal EMC of 12% in an environment chamber at 20 (+/-)1 °C and 65 (+/-)2 % relative humidity. The remaining 12 were placed in another environment cabinet at 25 (+/-)1 °C and 95 (+/-)2 % relative humidity and equilibrated to a nominal EMC of 20%. Once the specimens reached equilibrium, they were sealed in plastic bags and left in their respective environments until testing. After being tested at 20% EMC, that group of 12 specimens was re-equilibrated to 5% nominal EMC in the laboratory before testing a second time. Likewise, after testing at 12% EMC, the remaining 12 specimens were dried at 102 °C in a convection oven and tested again in the oven-dry condition.

Dielectric thermal analysis was performed with a Eumetric System III MicroDielectrometer from Micromet Instruments. The dielectric properties of specimens were evaluated at frequencies ranging from 0.1 Hz to 100 kHz, dependent on the moisture content of the specimens. Specimens conditioned to higher moisture contents exhibited a more descriptive dielectric response at higher frequencies, whereas dry specimens were more responsive to lower frequencies. In the standard configuration of this instrument for bulk dielectric analysis, the test specimen is placed between two parallel electrodes and the gain and phase of an electrical signal passing through the test specimen is compared to a known capacitance. The area of the driven electrode divided by the distance between the electrodes is known as the A/D ratio, and is very influential on the magnitude of the measured dielectric properties. A high A/D ratio will yield a better resolution of dielectric constant (permitivity) and dielectric loss factor. For this project a specially designed electrode pair was used in order to provide a high A/D ratio and thus improve resolution of the dielectric measurements (Figure 3.3). The PTFE backed copper electrodes were created such that the upper electrode of the pair had a diameter of 5.3 cm. The upper electrode also incorporated a guard ring to reduce the effects of fringe fields on the dielectric measurements, and to utilize the noise suppressing circuitry of the dielectric analyzer. The lower electrode had a diameter of 8.1 cm. A type K thermocouple was fitted inside the PTFE backing of the receiving electrode, such that the temperature sensing element was within 2mm of the specimen surface, approximately aligned with the center of the specimen.

Temperature scans were carried out using an MP-1200/QC Programmable MiniPress networked with the Micromet™ System III microdielectric analyzer. The press had 4” x 8”

electronically heated platens and its computer control was integrated with the data acquisition and control features of the dielectric instrument. The electrode assembly described above was placed between the platens of the press, and the thermocouple was connected to the dielectric data acquisition system. The system was calibrated prior to each scan by measuring the dielectric properties of an air gap of fixed, known distance between the electrodes.

Equilibrated specimens were sealed in plastic bags until just prior to testing, at which time they were quickly weighed and placed between the electrodes. The press was closed under an air pressure of 276 kPa (40 lb/in^2). This yielded a net compressive force on the specimens of 7.6 kg/cm^2 (108 lb/in^2). The oven was pre-programmed to heat at 5 °C per minute and the temperature ramp and dielectric data acquisition were started simultaneously. Dielectric property data for the specimens at each of the six to eight measurement frequencies was collected simultaneously with temperature data, as the sample was heated. To minimize moisture loss during testing, the experiments were terminated when the specimen temperature reached 95 °C. At that time, the press was opened, and the specimens were immediately removed and weighed to quantify moisture lost during the test. This protocol was carried out for specimens at 20, 12, and 5 % EMC. The oven-dry specimens were heated to 225 °C before the experiments were terminated.

RESULTS AND DISCUSSION

The shortcoming of most previous work to characterize the moisture dependence of the glass transition(s) in wood is that they were unable to maintain constant moisture content of specimens during temperature scans. The method of edge-sealing specimens, when used with the dielectric technique in this study, was effective in limiting the moisture lost during experiments. Table 3.2 shows the moisture content of samples before and after the dielectric scans. Moisture loss was highest at the 20% EMC condition. It was believed that moisture loss occurred predominantly at the end of the test when the press was opened. The combined moisture barrier created by the sealed edges and the pressure of the electrodes on the flat surfaces of the specimens was sufficient to resist moisture transfer to the external environment while the hot press remained closed. The internal pressure which accumulated as the specimen was heated, likely resulted in some moisture "flashing" off as the press was opened. This hypothesis was supported by the immediate collection of condensation on the surface of the polyethylene bags which were used to transport the specimens

from the press to the laboratory balance. The small net loss at the 0% EMC condition resulted from thermal degradation of wood substance, since the temperature scans were extended to 225 °C in this treatment.

Figure 3.4 illustrates the dielectric behavior as a function of temperature for oven dry southern pine juvenile wood. Both the dielectric loss factor and the permitivity increase with temperature. An increase in the slope of the permitivity function beginning above 160 °C indicates that the polarization behavior of the material is changing at that point. Specifically, the amount of energy stored and subsequently released by the capacitive function of the material is increasing at a greater rate with temperature. The magnitude of the observed dielectric response increases with decreasing frequency. This is due to the fact that at each measurement frequency, only the polarization of entities within the material possessing characteristic relaxation times less than that measurement frequency can be observed. Lower frequencies allow more time for displaced entities to relax themselves between cycles. Figure 3.4 shows dielectric behavior characteristically exhibited by the wood specimens in this study. Figures illustrating the dielectric permitivity and loss factor as a function of temperature and moisture content for southern pine mature, yellow-poplar juvenile and yellow-poplar mature wood are included in Appendix I.

Discontinuities in the dielectric behavior of polymers are more easily observed by examining the dielectric loss tangent (tanδ), which is equal to the loss factor divided by the permitivity. Secondary transitions in polymers are generally associated with peaks in tanδ (Cowie, 1991; McCrum, et al. 1967). Figures 3.5 - 3.8 show the dielectric tanδ response observed for southern pine juvenile wood at 0, 5, 12, and 20 percent moisture content, respectively. This plot is characteristic of all sample types that were studied. Additional figures illustrating the dielectric tangent delta response as a function of temperature and moisture content for southern pine mature, yellow-poplar juvenile and yellow-poplar mature wood are included in Appendix I. The other three wood types exhibited similar behavior, with the peak temperatures shifted slightly up or down. Each figure displays data collected at the six frequencies of measurement for which the tanδ function exhibits the most activity. Peaks in the tanδ function correspond to the temperature at which a dielectric softening (i.e. a relaxation process) was observed at that frequency in the sample. At 1 Hz, a maxima in tanδ corresponding to this super-ambient relaxation process can be observed in Figure 3.5 near 200 °C for southern pine juvenile wood at 0 % M.C. and near 90 °C in Figure 3.6 at 5% M.C. The relaxation near 200°C for dry wood at 1 Hz agrees with the reported range of 192 -

235 °C for a glass transition of *in situ* wood polymers by dynamic mechanical means (Sadoh, 1981; Funakoshi et al. 1979; and Wert et al. 1984). For any given frequency, the temperature at which a peak in tanδ occurs is shifted towards lower temperatures as moisture level increases. This trend has been reported by all researchers who have studied the softening or relaxation behavior of wood across a range of moisture contents (Table 3.1). The influence of moisture on the dielectric behavior of wood was also manifested in the fact that the frequencies at which relaxation processes can be observed, increased as moisture content was increased. Increasing moisture level also has the effect of broadening the peaks representing a dielectric relaxation. To some extent, this phenomena has also been reported for other techniques used to investigate the glass transition of wood (Salmen, 1984; Kelley et al. 1987). In the DETA this peak broadening represents the contribution of an increasing number of polarizing species to the dielectric response. The breadth of the relaxation peaks must be kept in mind when interpreting the results at high moisture levels.

The frequency dependence of a relaxation process can be evaluated by investigating the relationship of measurement frequency with the temperature corresponding to the maximum value of tanδ (T_{max}). Plots of the reciprocal of T_{max} against the logarithm of frequency at all moisture levels for juvenile and mature wood of southern pine and yellow-poplar, respectively, are provided in Figures 3.9 and 3.10. The data points representing the peak temperatures for each specimen type align themselves predominantly in a linear fashion with log frequency. Increasing the moisture level tends to shift the slope of the relationship, with the reciprocal temperature decreasing more rapidly with increasing frequency as moisture level was increased. For southern pine (Figure 3.9) the juvenile wood tends to exhibit slightly lower values of 1000/T, corresponding to higher tanδ peak temperatures, than the mature wood. This suggests that the softening temperature associated with this dielectric relaxation in southern pine is higher for juvenile wood than for mature wood. In yellow-poplar, this trend is reversed. At this time, there is no obvious explanation for this inversion, but it may be due to differences in the polarizability of the types of lignin found in the two species, and the relative proportions of the wood constituents present in the juvenile and mature material.

A common method of quantifying the frequency dependence of a relaxation process is after the method of Arrhenius, which involves plotting the log of the measurement frequency against the reciprocal of T_{max}. This is essentially the inverse of the plots in Figures 3.9 and 3.10. The slope of this plot is then related to the apparent activation energy of the relaxation process through the form of the Arrhenius equation given below:

$$\log f = \frac{\log f_o - E_a}{RT} \qquad [3.1]$$

Here f is the frequency of measurement, f_o is a pre-exponential factor, E_a is the apparent activation energy, R is the gas constant and T is the tanδ peak temperature in Kelvin. Units for E_a are in terms of the gas constant R.

Figures 3.11 and 3.12 display Arrhenius plots for the frequency dependence of the super-ambient dielectric relaxation process. The strong and well defined frequency dependence of the observed dielectric relaxation delineates it as a secondary transition, while the temperature range at which it is observed further suggests that is an α transition. Table 3.3 lists the slope and intercept of linear fits to the relationships shown in Figures 3.11 and 3.12. The calculated apparent activation energies for southern pine and yellow-poplar mature wood, juvenile wood and the two wood types combined, at each of the four moisture conditions, are also provided in Table 3.3. A test for independence between regression lines (Neter and Wasserman, 1974) revealed the Arrhenius relationships for mature and juvenile wood to be statistically independent at a significance level of $\alpha < 0.005$ for both southern pine and yellow-poplar at all four moisture conditions.

The apparent activation energies determined for the observed relaxation process tend to decrease with increasing moisture content, and range from near 50 kJ/mole at 20% moisture content to approximately 140 kJ/mole for dry wood. These activation energies are much lower than the values for the *in situ* α transition (T_g) of lignin of 339 kJ/mole (MC = 15%) reported by Kelley et al. (1987) and 395 kJ/mole (water saturated) by Salmen (1984), both using the DMTA. For polymers in general, the apparent activation energy for a glass transition is thought to be greater than or equal to around 40 kJ/mole, with a tendency to increase with increasing T_g (Salmen, 1984). Activation energies of 117 kJ/mole (dielectric) and 104 kJ/mole (mechanical) have been reported for the α transition near 80 °C of side-branched polyethylene (McCrum, et al. 1967). Dielectrically and mechanically observed α transitions in the same material generally yield equivalent E_a values (McCrum, et al. 1967). The activation energies generated in the presented work are more on the order of those reported for the sub-ambient β transitions in wood. Using the DMTA, Kelley et al. (1987) observed a β transition at –90 to –75 °C, for which they determined an activation energy of 102 kJ/mole. Eaton et al. (1976) observed a similar β transition in cellulose using DETA, with values of E_a ranging from 84 kJ/mole (13% M.C.) to 146 kJ/mole (5% M.C.). However, β

transitions are generally observed well below ambient temperature and are associated with site exchange of moisture in hydrophilic polymers (Eaton et al., 1976; Kelley et al, 1987).

Figure 3.13 displays the temperature of the observed relaxation at 1 Hz as a function of moisture content. Relaxation temperature values at 1 Hz were obtained from the regression equations for log frequency against $1000/T_{max}$. At 1 Hz, the data points at 20% moisture content represent extrapolated values based on the regression parameters reported in Table 3.3, as the DETA temperature scans did not extend to sub-ambient conditions. The data recorded in this study does not exhibit the plateau at 5 – 10% M.C. observed by some for *in situ* α transition(s) in wood (Irvine, 1984; Kelley et al. 1987; Ostberg, et al. 1990). The decrease in the temperature of the relaxation process is curvilinear with moisture content, but it continues to decrease above 10%, similar to the behavior reported by Irvine (1984) for isolated hemicellulose and by Back and Salmen (1982) for isolated amorphous cellulose and hemicellulose.

Also included in Figure 3.13 are the T_g versus moisture content relationships for the α_1 (lignin) and α_2 (hemicellulose) secondary transitions reported by Kelley et al. (1987) as summarized by the Kwei model. The Kwei model has been used by several researchers (Kelley, et al. 1987; Wolcott, et al. 1990) to describe the depression of the T_g in wood due to increasing moisture content and has the form:

$$T_g = \frac{(W_1 T_{g1} + kW_2 T_{g2})}{(W_1 + kW_2) + qW_1 W_2}, \qquad [3.2]$$

where W and T_g represent the weight fraction and glass transition temperature of the polymer(1) and diluent(2) (Kelley et al. 1987). The constants q and k represent adjustable parameters accounting for secondary interactions and free volume considerations respectively. There has been some question regarding the validity of applying this model to the T_g(s) of a natural polymeric system as complex as wood. Consequently, it was not fit to the data in this study.

The relationship of relaxation temperature with moisture content observed in this work is quite similar to that reported for the T_g of hemicellulose by Kelley et al. (1987), especially at moisture contents up to 10%. Unfortunately they were unable to resolve an apparent activation energy for this relaxation process at a measurement frequency that could be compared to the results of this study. The agreement between these results, however, suggests that the observed dielectric relaxation may be the glass transition of the *in situ* hemicelluloses and the amorphous component of cellulose, or indeed a net relaxation of all the amorphous components combined.

Similar agreement between transitions reported by DMTA and DETA techniques has been reported for glass transitions in other polymers (McCrum, 1967; Wetton et al. 1984). While the two techniques have been shown to be complementary, it is likely that they respond differently to increases in the amount of moisture in a material. The dynamic bending properties evaluated by the DMTA are likely to achieve a level of diminishing returns where additional increases in moisture no longer influence the material behavior. This relationship is akin to the influence of the fiber saturation point on the mechanical strength of wood. The magnitude of the relaxations probed by the DMTA make it sensitive to motions in polymer chain segments. The plasticization effect of water on these chain segments will likely be much greater for the initial layer of water molecules, and subsequently less for each additional layer as the forces attracting the water molecules to the substrate decrease. This behavior is certainly tied closely to the sorptive behavior of the polymer diluent system. Thus the T_g of the less sorptive lignin would plateau at a lower moisture content than that of the more sorptive hemicellulose, as indicated by the results of Kelley et al. (1987). This idea is supported by results on the softening of isolated lignin and carbohydrates, in which the lignin T_g reaches a plateau with increasing moisture content, while the T_g of hemicellulose and amorphous cellulose continue to decline markedly as moisture levels increase above 20% (Salmen and Back 1977; Irvine, 1984). The dynamic motion of polymer chain segments evaluated by the DMTA may also be restricted by confines within the wood structure, or by association with inflexible components in the wood cell wall, such as crystalline cellulose.

DETA on the other hand, will respond differently to changing levels of moisture. The dielectric response of wood consists mainly of dipolar and interfacial polarizations. Since the plasticizing water molecules are themselves dipoles, as well as contributors to interfacial polarization (Torgovnikov, 1993), addition of water will have a complex effect on the dielectric response of hydrophilic polymers. The proximity of the polarizing dipoles to the backbone, and the amount to which they are influenced by the configurational motions of the polymer chain will directly affect the correlation between dielectric and mechanical properties (Ferry, 1980). The accumulation of additional water will add more dipoles to the material which are decreasingly responsive to the motions of the polymer backbone. This would suggest that the correlation between DMTA and DETA decreases with increasing moisture content. The dielectric response may not reflect a “plateauing” effect with increasing moisture, more likely to be observed is a continued decline in the relaxation temperature of the polymer-plasticizer

system with increasing levels of water. Using DETA, the delineation of the behavior of moisture from that of the polymer-diluent system is obviously complex and interpretation of results is further disadvantaged by the lack of similar studies for comparison. However, the obvious frequency dependence of the observed relaxations, and the modest agreement with transition temperatures observed using other techniques, lends merit and validity to the identification of the observed relaxations as glass transitions of wood polymers.

An equivalence between time and temperature in their influence on viscoelastic response has been thoroughly demonstrated for amorphous polymers (Ferry, 1980; Aklonis and Macknight, 1983; Cowie, 1991). The time-temperature superposition (TTSP) principle was developed to reduce the amount of experimental effort required in determining time dependent material properties. This technique can also be employed to evaluate the compliance of experimental results with theoretical relationships for amorphous polymers. Application of TTSP has been demonstrated to be effective for wood at various levels of hydration (Salmen, 1984, Kelley, et al. 1987; Wolcott, et al. 1994).

At moisture levels of 0, 5 and 12 %, curves of log permitivity were shifted horizontally along the log frequency axis to a reference temperature corresponding to that experimental temperature closest to the observed 1 Hz relaxation temperature (T_g). At 20 % moisture content, the lowest experimental temperature (near 40 °C) was chosen as a reference temperature, because the 1 Hz extrapolation of the observed T_g was well below the range of temperature over which permitivity data collected. Master curves for the permitivity of yellow-poplar juvenile wood at the four different moisture levels are given in Figures 3.14 through 3.17. The master curves for the other three wood types are provided in Appendix II. At 0 and 20 % moisture content the master curves appear very smooth, while a moderate amount of scatter exists in those generated at 5 and 12 %. Similarly to the procedure of Salmen (1984) and Kelley et al. (1987), vertical shifts were not performed. The method for vertical correction was derived from the kinetic theory of rubber elasticity, and thus its bearing on the dielectric response of a complex material such as wood is questionable. The shift factors used in generating the master curves are plotted against the difference between the measurement temperature and the reference temperature (T-T_{ref}), and displayed in the upper right hand corner of Figures 3.14 through 3.17 and AII.1- AII.12.

Glassy, amorphous polymers are expected to comply with the Williams-Landel-Ferry (WLF) equation above their T_g up to T_g + 100 °C. For an arbitrarily chosen reference temperature, the WLF equation has the form (Aklonis and MacKnight (1983):

$$\log a_T = \frac{-C_1(T - T_{ref})}{C_2 + (T - T_{ref})} \qquad [3.3]$$

Here log a_T is the shift factor, C_1 is a constant proportional to the fractional free volume of the polymer system (f_g) at the glass transition, and C_2 is a constant which relates the free volume and its coefficient of thermal expansion (α_f). When $T_{ref} = T_g$, values of C_1 and C_2 determined by fitting the WLF equation to the shift factor data can determine the suitability of the WLF and associated free volume relationships for describing the viscoelastic relaxation process in question. Table 3.5 collects the values of C_1 and C_2 as well as corresponding estimates of f_g and α_f obtained by a Levenberg Marquardt nonlinear regression of the WLF equation on the shift factor data. Parameters of the fit to the WLF equation are reported for master curves at 5, 12 and 20 % moisture content. At 0 %, the limits of temperature within which the data was obtained were insufficient for the generation of shift factors in the range of application for the WLF equation, which is T_g to T_g + 100°C. In table 3.4 the "universal" constants reported by Aklonis and Macknight (1983) for $T_{ref} = T_g$ are given for comparison as are corresponding values of f_g and α_f (Young and Lovell, 1991). Also provided in Table 3.4 are the parameters of an empirical linear fit to the shift factor data for all moisture contents. In Figures 3.14 – 3.17 and AII.1 – AII.12, the fitted WLF equation is superimposed onto the shift factor plots of master curves obtained from experiments at 5, 12, and 20 % moisture content, whereas the linear fit is superimposed on those master curves from the 0 % moisture content specimens.

The shift factors do appear to be effectively described by linear empirical models, and the slope values are in reasonable agreement with those reported at lower moisture levels by Wolcott (1989) for relaxation modulus and creep compliance in wood. The increased deviation from those results with increasing moisture content can be explicated with the same arguments used previously to explain differences between the results of mechanical and dielectric analyses. Reasonable agreement between the values of the fitted WLF constants and the "universal" constants suggests that the observed viscoelastic process does follow WLF behavior. The shift factor plots inset in the master curves illustrate this association. The WLF constants in Table 3.5 are also somewhat in agreement with those reported by Salmen (1984) for water saturated wood

(C_1 = 18.18, C_2 = 77.2) and Kelley et al. (1987) for wood plasticized with ethyl formamide. The experimentally determined values for the fractional free volume at T_g (f_g, Table 3.4) of the samples tested are considerably lower than the universal value reported for amorphous polymers of 0.025 (Young and Lovell, 1991) and that observed for water saturated wood by Kelly et al. (1987) of 0.024. It must again be noted that influence of the measurement technique certainly bears upon this comparison. Values of f_g tend to increase with increasing moisture content. This trend follows the intuitive idea that the free volume of the system increases as it is swollen with adsorbed moisture. With regard to the thermal expansion coefficient of the free volume (α_f), there are no trends apparent with regard to wood type or moisture level.

Reasonable compliance with the WLF equation, and moderate agreement between the constants derived from the dielectric experiments with those reported for mechanical tests on a similar system, suggest that the observed dipole response involves changes in backbone configuration that are associated with the glass transition (Ferry, 1980). Corroborated by the evidence found in its frequency dependence, the temperature dependence of the shift factors suggest that the observed dielectric relaxation represents a secondary material transition. The fact that no β or lower transitions have been observed for wood in or above the ambient temperature range, indicates that this relaxation is an α transition. Furthermore, the fact that the observed relaxation is coincident at low moisture levels with the reported T_g of in situ wood polymers, leads to the belief that this relaxation process represents the glass transition of hemicellulose and the amorphous cellulose components or a relaxation of all amorphous components of wood. It is postulated that these wood components will dominate the dielectric response of wood in the conditions studied due to: 1] their greater proportion of dipolar groups, 2] the proximity of these dipoles to the backbone chain, and 3] their degree of coupling with the conformational motions of the backbone polymer chain (Ferry, 1980).

The nature of the DETA technique, however, makes it difficult to differentiate which individual *in situ* components are responsible for the observed dispersion. The DETA is also not ideally suited for measurements in polymer systems where high moisture levels create a heavy dipolar response that can cloud observation of the targeted relaxation. As moisture levels increase in a hydrated system, the dispersion of the observed dielectric behavior is most likely a manifestation of the “gross” dipolar response of all of the hygroscopic polymer components and their bound moisture to the applied electrical field.

CONCLUSIONS

Dielectric thermal analysis (DETA) was used to observe moisture dependent relaxation behavior in juvenile and mature wood of southern pine and yellow-poplar. This dielectric relaxation process exhibited the frequency dependence and Williams Landel Ferry (WLF) compliance characteristic of an α (glass) transition. The observed T_g was consistent with reported values for wood, in particular those for hemicellulose and amorphous cellulose components of wood at low to moderate moisture contents. However at higher moisture levels, the DETA was not sensitive enough to polymer chain behavior to definitively differentiate the relaxation behavior of the individual amorphous wood components from the dipolar activity of the adsorbed water.

The moisture dependence of the observed transition was significantly different for mature and juvenile wood. At moisture levels up to 12 %, yellow-poplar juvenile wood exhibited a lower T_g than mature wood. For southern pine this trend was inexplicably reversed. The time temperature superposition principle (TTSP) was shown to effectively demonstrate frequency – temperature equivalence for the dielectric response of wood up to 20 % moisture content.

This work adds new information to the knowledge base regarding material behavior during the manufacture of wood-based composites. These results can be combined with those from the previous chapter to provide further insight into response of wood to hot-pressing environments, and will assist in further clarifying the complex influence of moisture on the thermal softening of wood.

CHAPTER 3 TABLES:

Table 3.1. Reported softening temperatures for wood.

Source	Technique	Species	Measurement Frequency (Hz)	Moisture Content (%)	Softening Temperature[a] T_g (°C)
Kelley et al., 1987	DMTA	spruce	1	30	60
				20	60
				10	80
				5	115
Salmen, 1984	DMTA	spruce	0.05	saturated	82
			0.5		85
			5		95
			20		100
Atack, 1982	Torsional Pendulum	spruce	1[a]	saturated	85
Becker and Noack, 1968	Torsional Pendulum	beech	0.5 – 3	saturated	80
				26	85
				20.5	95
Höglund et al., 1976	Torsional Pendulum	various	1[a]	saturated	80
			10[a]		110
Sadoh, 1981	Torsional Pendulum	birch	0.02	saturated	80
			0.5	dry	235
Wert et al., 1984	Torsional Pendulum	spruce	1	dry	132 & 192
Hillis and Rosa, 1978	Static Torsion	pine	N/A	saturated	80 & 92

[a] approximate values

Table 3.1 (continued). Reported softening temperatures for wood.

Source	Technique	Species	Measurement Frequency (Hz)	Moisture Content (%)	Softening Temperature[a] T_g (°C)
Takahashi et al., 1998	Radial Compression	various	N/A	saturated	80
Uhmeier et al., 1998	Radial Compression	spruce	N/A	saturated	85
Funakoshi et al., 1979	DTA	birch	N/A	dry	210
Irvine, 1984	DTA	Eucalyptus	N/A	25	62
				16	68
				12	82
				7	108
Östberg et al., 1990	DSC	spruce	N/A	25	60
				20	60
				17	60
				15.5	61
				13	63
				11.5	65
				8	70
				8	73
				7	81
				6.5	86

[a] approximate values

Table 3.2. Average values of moisture content for specimens before and after dielectric experiments. Standard deviations in parentheses.

	Nominal EMC (%)											
	0[a]			5			12			20		
Wood Type	in	out	change	in	out	change	in	out	change	in	out	change
Southern pine												
juvenile	0.0 (0.0)	-0.8 (0.2)	-0.8 (0.2)	5.1 (0.6)	4.4 (0.4)	-0.7 (0.2)	11.4 (1.2)	8.9 (1.3)	-2.5 (0.2)	19.1 (0.6)	15.1 (0.4)	-4.0 (0.2)
mature	0.0 (0.0)	-1.1 (0.5)	-1.1 (0.5)	6.4 (0.1)	4.6 (0.3)	-1.7 (0.2)	13.1 (0.1)	9.8 (0.2)	-3.3 (0.2)	19.6 (0.4)	14.9 (0.9)	-4.8 (0.8)
Yellow-poplar												
juvenile	0.0 (0.0)	-1.4 (0.3)	-1.4 (0.3)	6.0 (0.3)	4.8 (0.2)	-1.2 (0.1)	12.1 (0.8)	9.2 (0.5)	-2.8 (0.3)	19.0 (0.3)	14.9 (0.1)	-4.1 (0.3)
mature	0.0 (0.0)	-0.8 (0.2)	-0.8 (0.2)	6.6 (0.4)	5.1 (0.3)	-1.5 (0.5)	13.0 (0.3)	10.0 (0.3)	-3.0 (0.1)	19.8 (0.4)	14.9 (0.5)	-4.9 (0.2)

[a] net loss at 0% EMC reflects loss of wood substance due to thermal degradation.

Table 3.3. Parameters of the Arrhenius relationship for frequency dependence of the super-ambient dielectric relaxation in southern pine and yellow-poplar.

M. C. (%)	Species	Wood Type	log frequency vs 1000/T (K^{-1}) slope	intercept	Activation energy (ΔE_a, $kJ \cdot mole^{-1}$)
0	southern pine	juvenile	-6.42	13.46	122.93
		mature	-5.68	12.22	108.76
		combined	-5.67	13.46	108.57
	yellow-poplar	juvenile	-7.58	13.12	145.14
		mature	-6.43	16.34	123.12
		combined	-6.22	13.17	119.10
5	southern pine	juvenile	-4.01	10.98	76.78
		mature	-4.58	13.11	87.70
		combined	-4.18	11.81	80.04
	yellow-poplar	juvenile	-6.60	19.77	126.38
		mature	-5.06	14.73	96.89
		combined	-5.63	16.75	107.80
12	southern pine	juvenile	-5.49	18.60	105.12
		mature	-4.40	15.75	84.25
		combined	-4.68	16.35	89.61
	yellow-poplar	juvenile	-4.65	16.66	89.04
		mature	-6.03	20.35	115.46
		combined	-5.76	19.73	110.29
20	southern pine	juvenile	-2.71	11.85	51.89
		mature	-3.27	13.75	62.61
		combined	-2.75	12.02	52.66
	yellow-poplar	juvenile	-3.35	13.88	64.15
		mature	-2.83	12.13	54.19
		combined	-3.01	12.75	57.63

Table 3.4. Parameters of both the fitted WLF equation and a linear fit to the shift factor data.

Wood type	Moisture Content	WLF Parameters C_1	C_2	f_g	α_f	Linear Fit Parameters slope	R^2
Southern pine	0	--	--			-0.02	0.92
juvenile	5	6.7	281.9	0.065	$2.3e^{-4}$	-0.03	0.99
	12	5.9	234.8	0.074	$3.2e^{-4}$	-0.02	0.99
	20	5.5	388.2	0.079	$2.0e^{-4}$	-0.01	0.99
Southern pine	0	--	--			-0.02	0.90
mature	5	5.7	191.2	0.076	$3.9e^{-4}$	-0.03	0.98
	12	4.6	191.8	0.094	$4.9e^{-4}$	-0.02	0.99
	20	2.6	135.7	0.167	$1.2e^{-3}$	-0.01	0.98
Yellow-poplar	0	--	--			-0.04	0.97
juvenile	5	2.94	66.4	0.148	$2.2e^{-3}$	-0.04	0.99
	12	2.05	71.5	0.212	$2.9e^{-3}$	-0.02	0.93
	20	3.00	179.8	0.144	$6.3e^{-4}$	-0.01	0.90
Yellow-poplar	0	--	--			-0.03	0.92
mature	5	7.3	194.3	0.059	$3.0e^{-4}$	-0.04	0.99
	12	3.4	117.0	0.128	$1.1e^{-3}$	-0.02	0.98
	20	3.6	234.8	0.121	$5.1e^{-4}$	-0.01	0.99
	universal[a]	17.4	51.6	0.025	$4.8e^{-4}$	--	--

[a] Aklonis and MacKnight (1983), Young and Lovell (1991).

CHAPTER 3 FIGURES

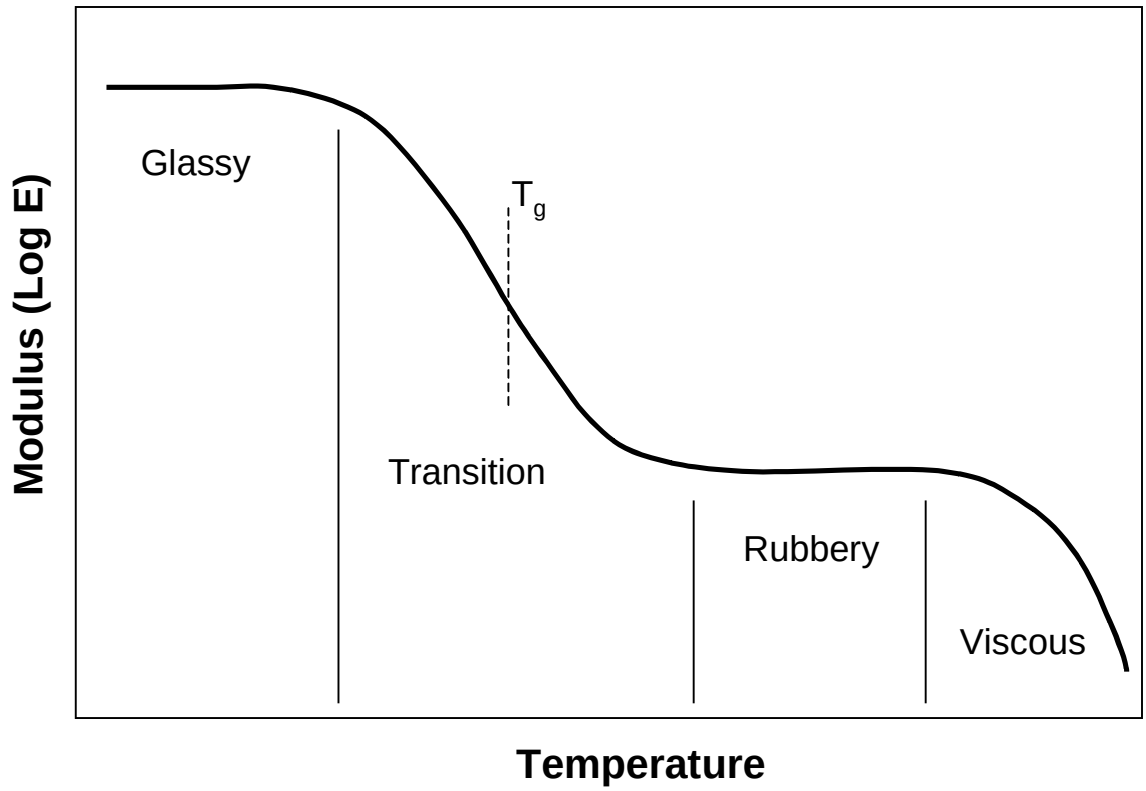

Figure 3.1. Variation of relaxation modulus with temperature for an amorphous polymer.

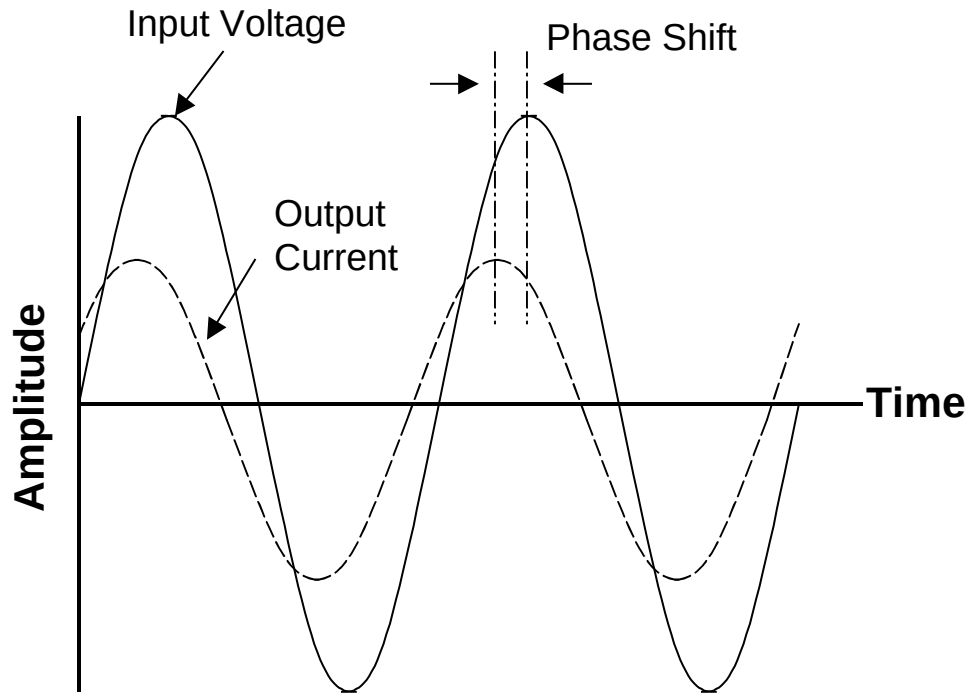

Figure 3.2. Schematic representation of the behavior of input voltage and out put current in DETA.

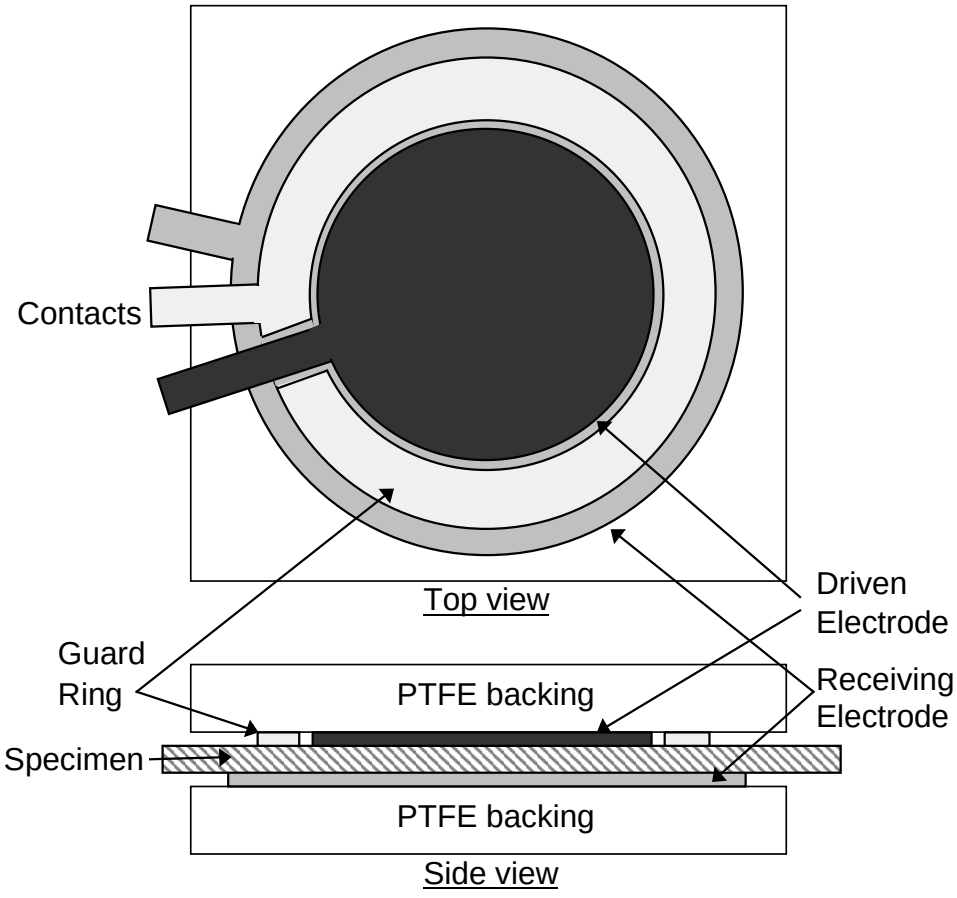

Figure 3.3. Schematic diagram of dielectric electrode assembly.

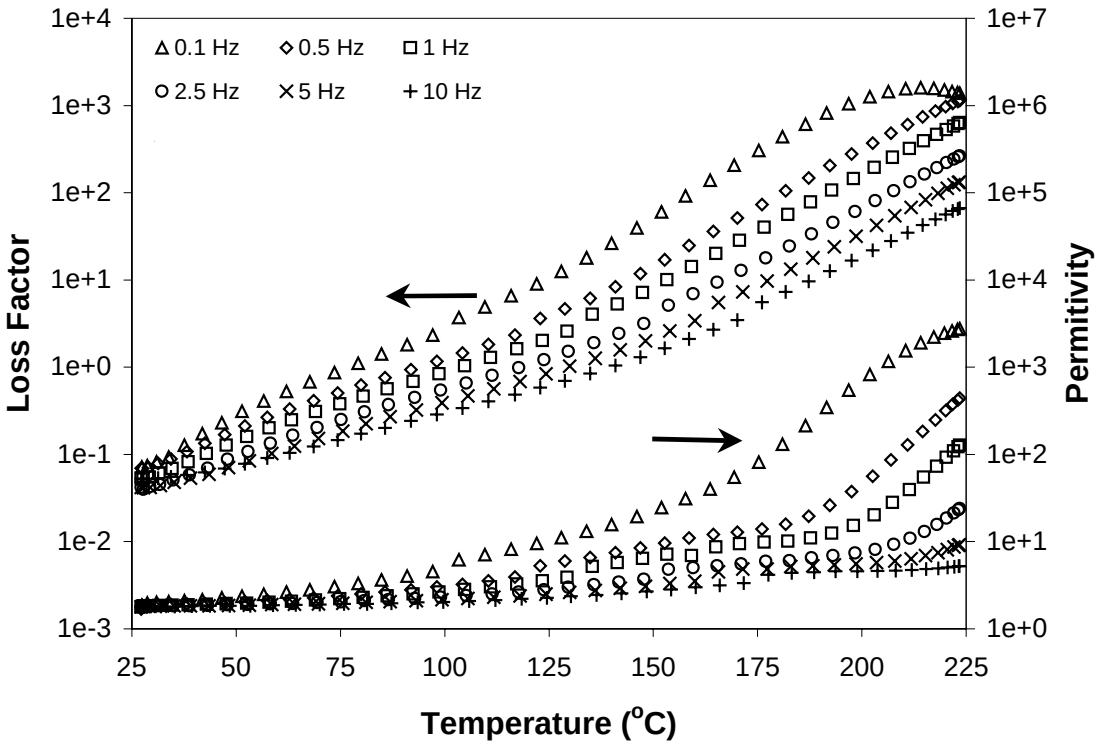

Figure 3.4. Dielectric permitivity (right axis) and dielectric loss factor (left axis) verses temperature for southern pine juvenile wood at 0% moisture content. Six measurement frequencies are shown.

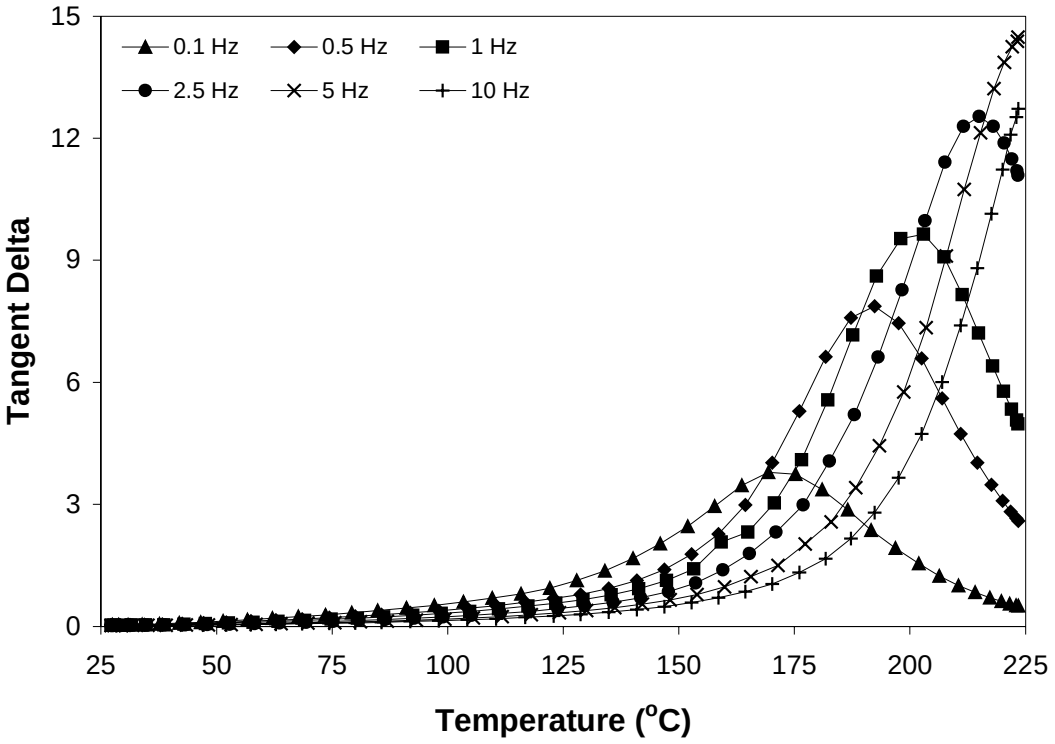

Figure 3.5. Dielectric loss tangent verses temperature for southern pine juvenile wood at 0% moisture content. Six measurement frequencies are shown.

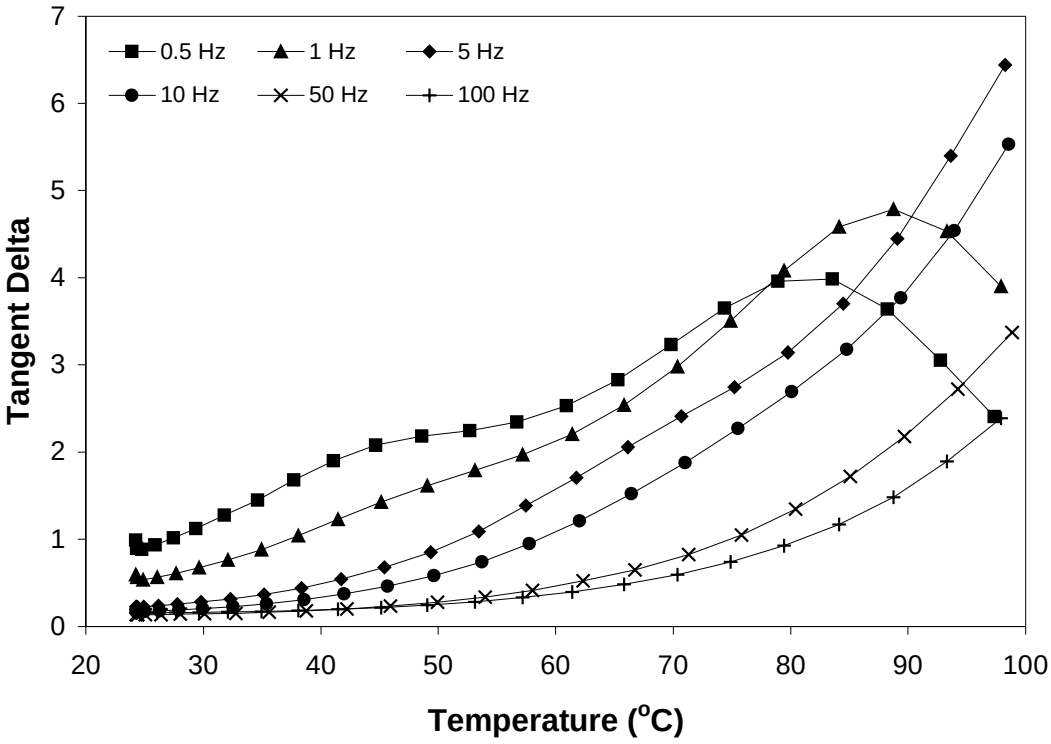

Figure 3.6. Dielectric loss tangent verses temperature for southern pine juvenile wood at 5% moisture content. Six measurement frequencies are shown.

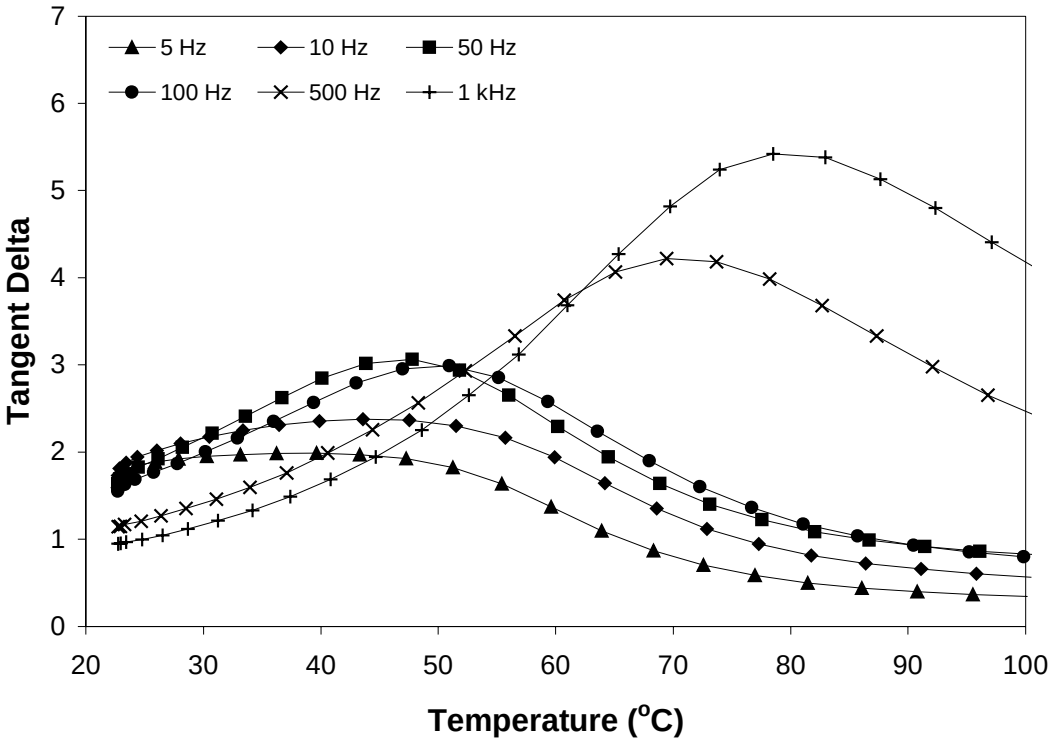

Figure 3.7. Dielectric loss tangent verses temperature for southern pine juvenile wood at 12% moisture content. Six measurement frequencies are shown.

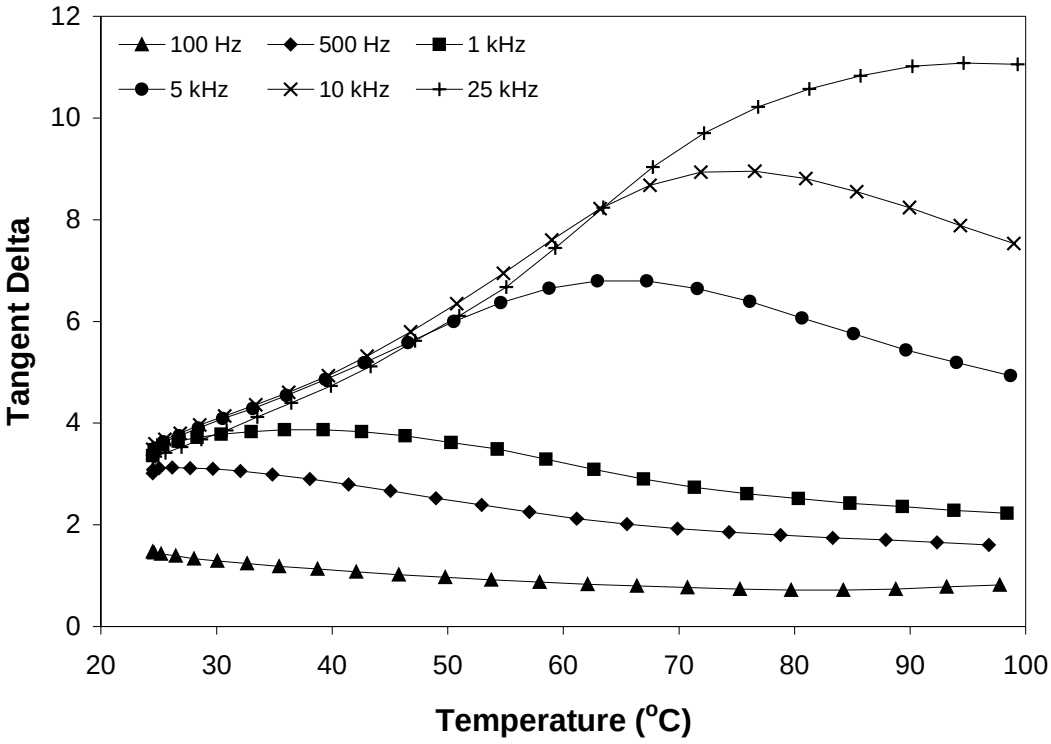

Figure 3.8. Dielectric loss tangent verses temperature for southern pine juvenile wood at 20% moisture content. Six measurement frequencies are shown.

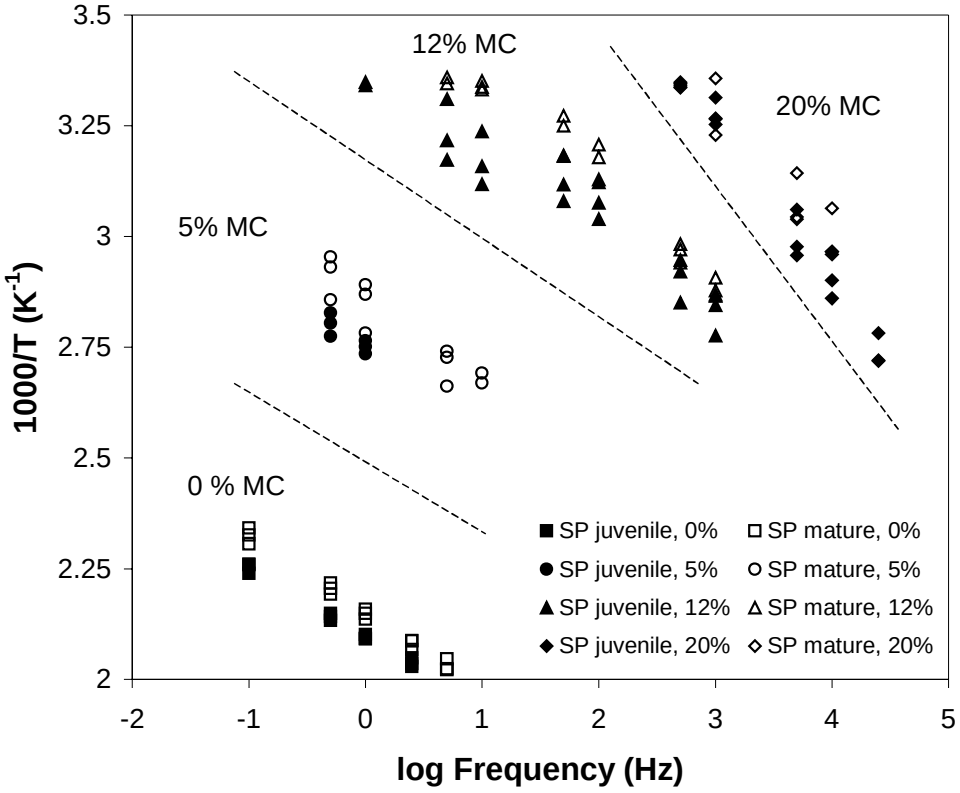

Figure 3.9. Plot of reciprocal absolute temperature against log frequency for the T_{max} of the dielectric relaxation process in southern pine at 0, 5, 12, and 20 % moisture content.

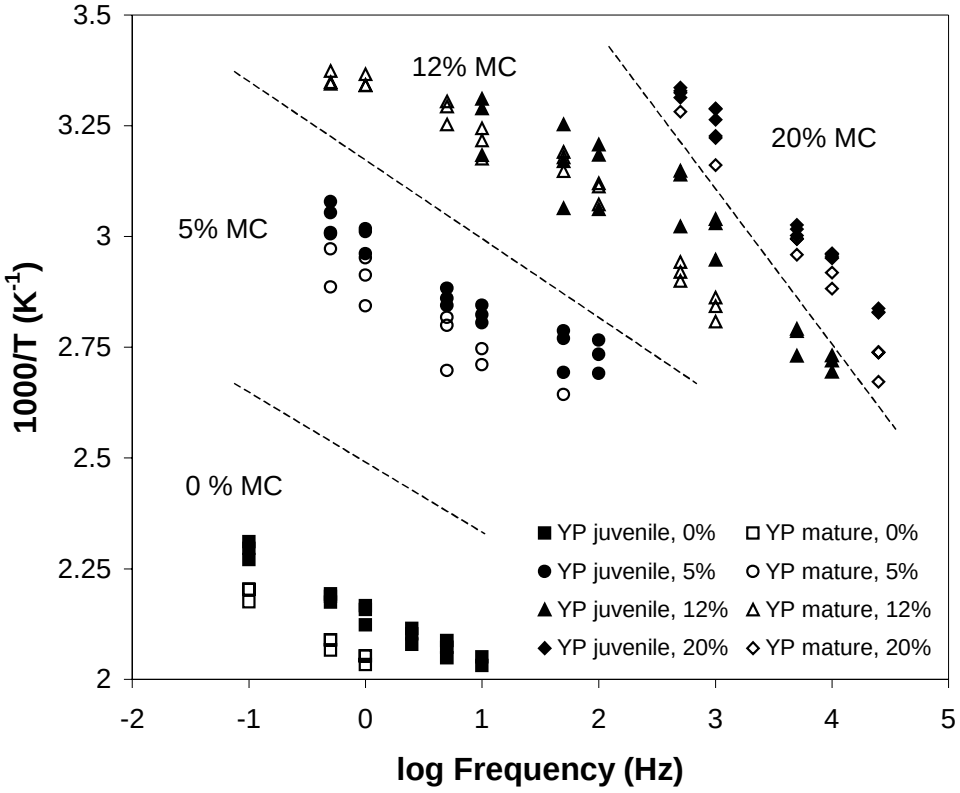

Figure 3.10. Plot of reciprocal of absolute temperature against log frequency for the T_{max} of the dielectric relaxation process in yellow-poplar at 0, 5, 12, and 20 % moisture content.

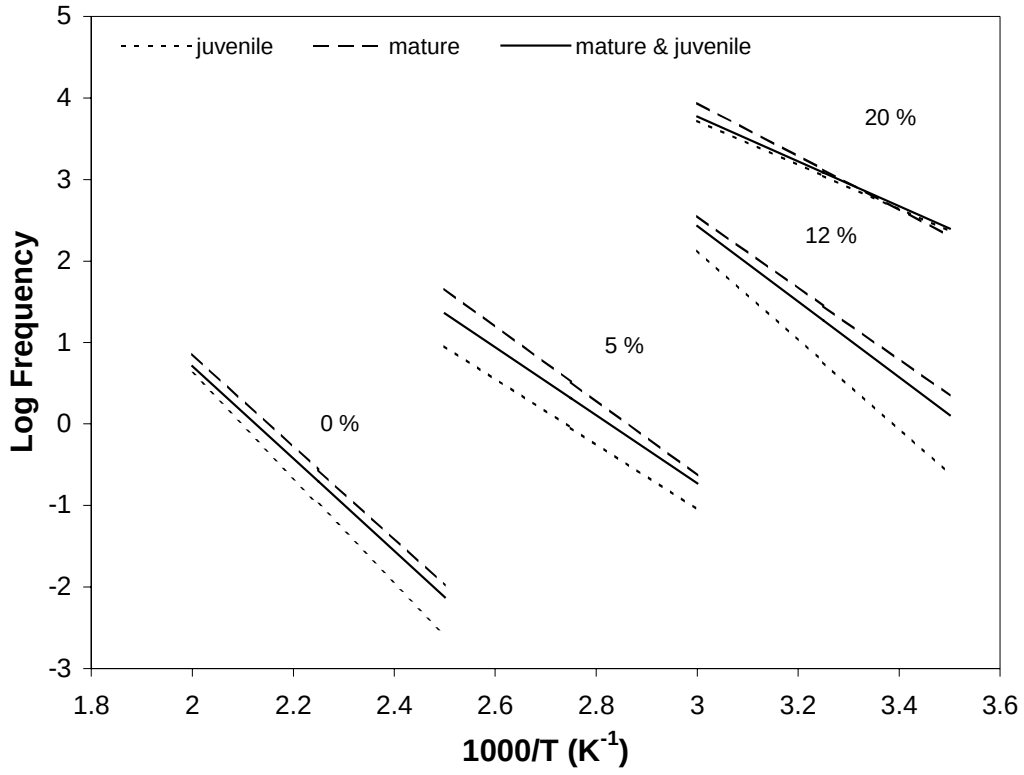

Figure 3.11. Arrhenius plot of log frequency against reciprocal of absolute temperature for the T_{max} of the dielectric relaxation process in southern pine at 0, 5, 12, and 20 % moisture content.

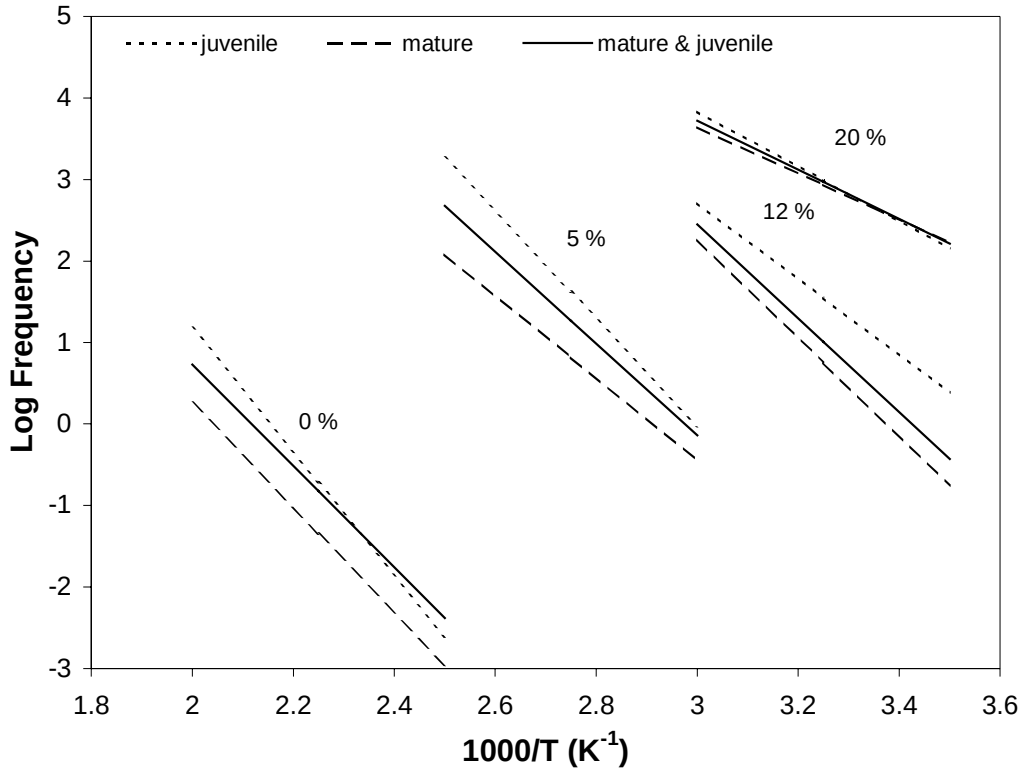

Figure 3.12. Arrhenius plot of log frequency against reciprocal of absolute temperature for the T_{max} of the dielectric relaxation process in yellow-poplar at 0, 5, 12, and 20 % moisture content.

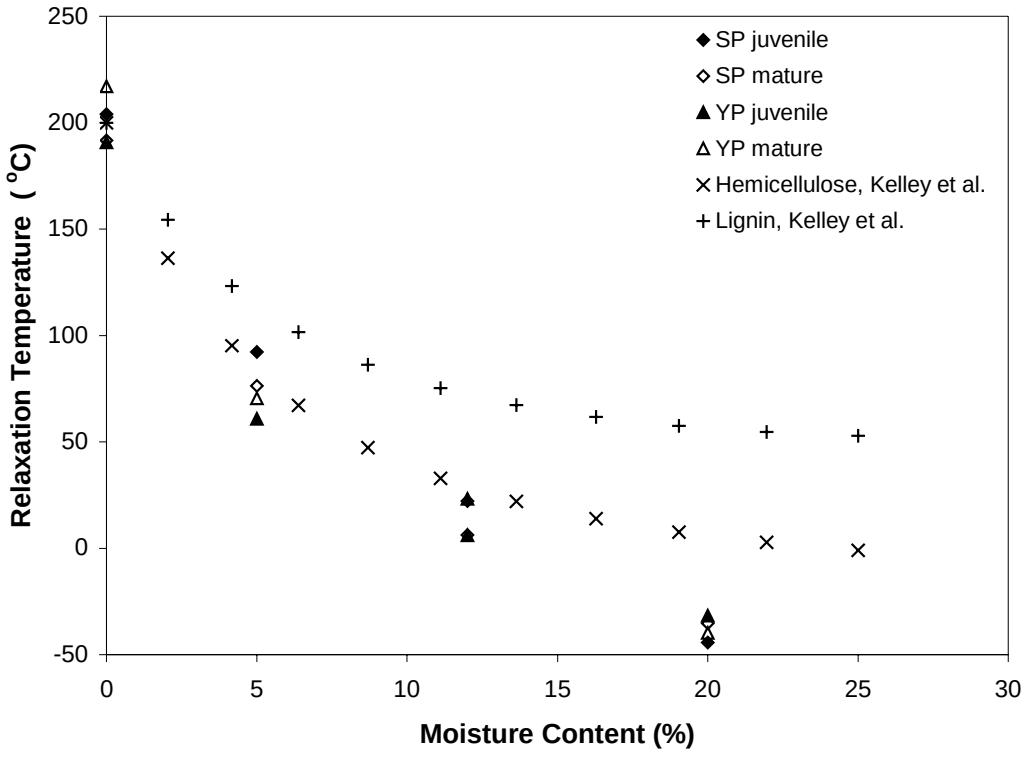

Figure 3.13. Plot of relaxation temperature at 1 Hz against moisture content. Lines represent data of Kelley et al. (1987) summarized by the Kwei model.

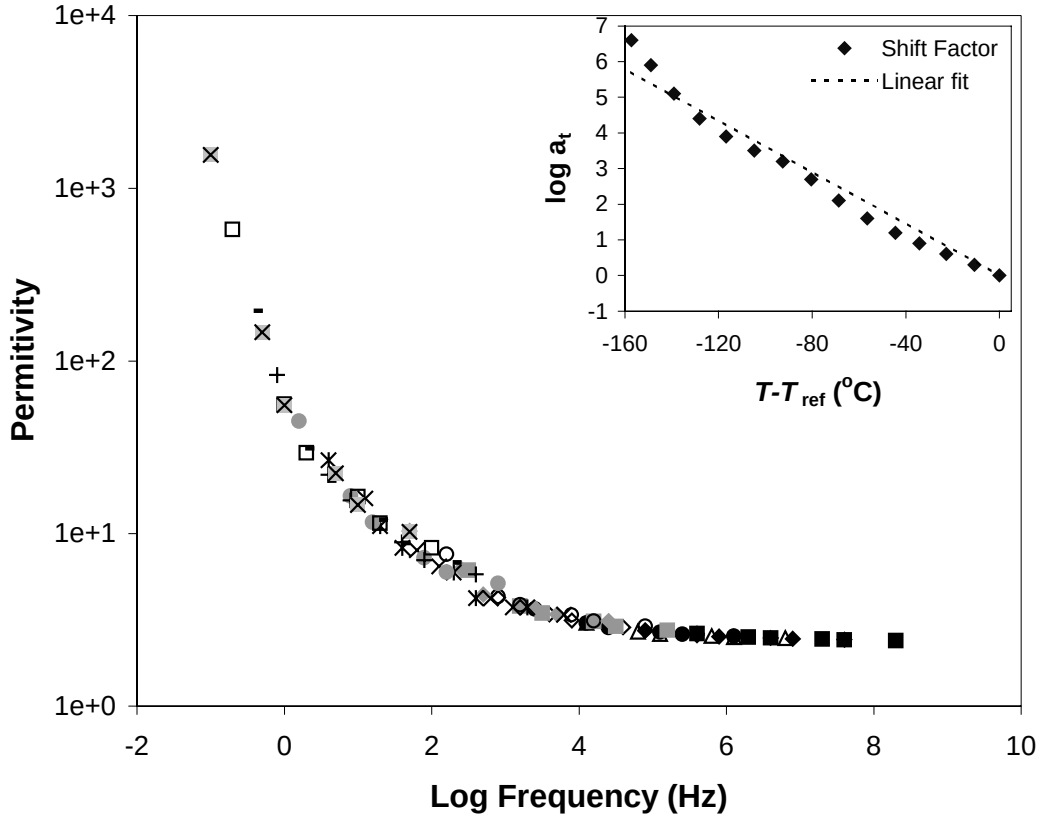

Figure 3.14. Master curve for permitivity versus log frequency for yellow-poplar juvenile wood at 0% moisture content. The observed T_g of 198 °C is used as the reference temperature.

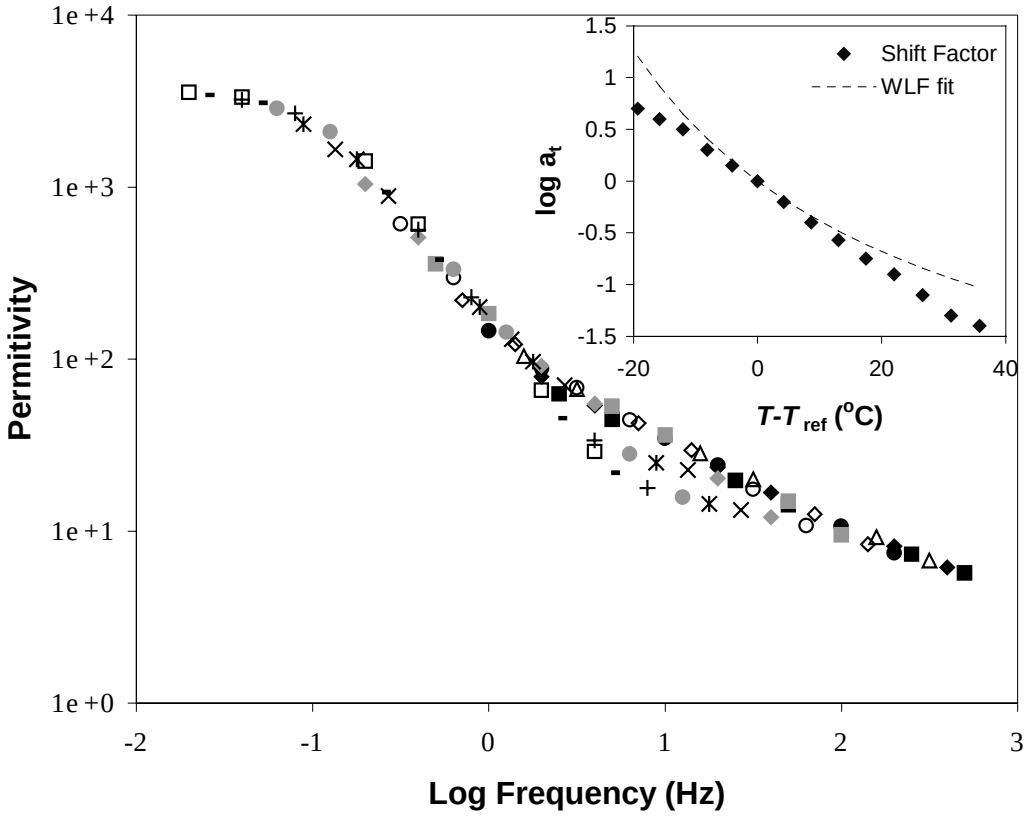

Figure 3.15. Master curve for permitivity versus log frequency for yellow-poplar juvenile wood at 5% moisture content. The observed T_g of 61 °C is used as the reference temperature.

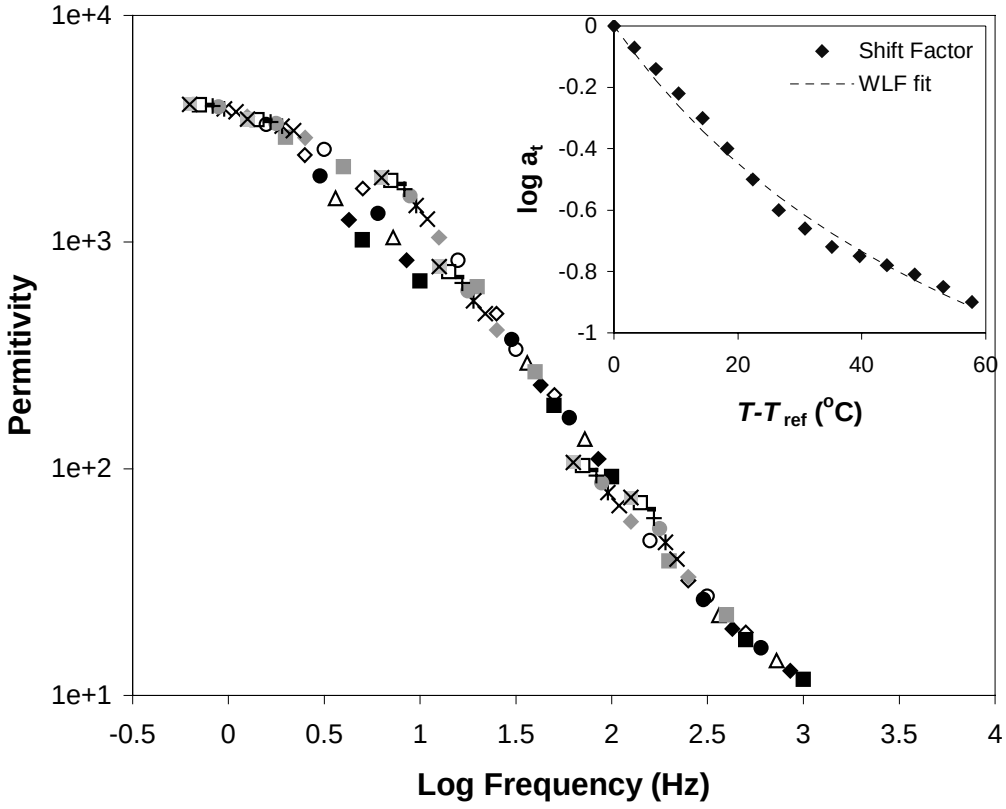

Figure 3.16. Master curve for permitivity versus log frequency for yellow-poplar juvenile wood at 12% moisture content. 40 °C was used as the reference temperature.

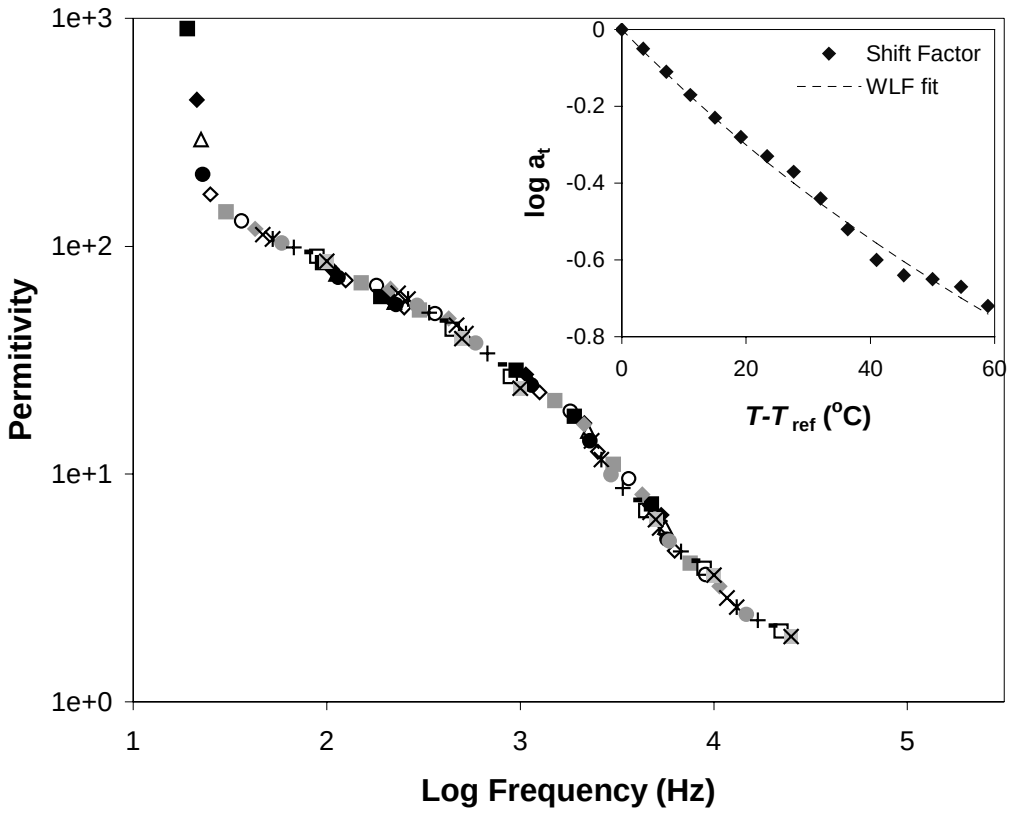

Figure 3.17. Master curve for permitivity E' versus log frequency for yellow-poplar juvenile wood at 20% moisture content. 40 °C was used as the reference temperature.

LITERATURE CITED

Aklonis, J.J. and W.J. MacNight. 1983. Introduction to Polymer Viscoelasticity. J. Wiley and Sons. New York.

Armstrong, J.P., C. Skaar, and C. deZeeuw. 1984. The efffect of specific gravity on several mechanical properties of some world woods. Wood Sci. Tech. 18:137-146.

Atack, D. 1981. Dynamic mechanical loss properties of wood. Philos. Mag. A. 43(3):619-625.

Back, E.L., and N.L. Salmen. 1982. Glass transitions of wood components hold implications for molding and pulping processes. Tappi 65(7):107-110.

Barrett, David J. and R.M. Kellog (1986) Lumber quality from second growth managed forests. Proceedings of a Cooperative Technical Workshop on Juvenile Wood. FPRS/SAF Volume 1.

Becker, H. and D. Noack. 1968. Studies on the dynamic torsional viscoelasticity of wood. Wood Sci. Tech. 2:213-230.

Bendsten, Alan B. (1978) Properties of wood from improved and intensively managed trees. For. Prod. J. 28(10): 61-72.

_____, and J. Senft. (1986) Mechanical and anatomical properties in individual growth rings of plantation-grown eastern cottonwood and loblolly pine. Wood and Fiber Sci. 18(1): 23-38.

Casey, L.J. 1987. Changes in wood-flake properties in relation to heat, moisture and pressure during flakeboard manufacture. MS Thesis V.P.I. & S.U. Blacksburg, VA.

Christensen, G.N. and K.E. Kelsey. 1959. The sorption of water vapor by the constituents of wood. Holz Roh- Werkstoff. 17(5):89-204.

Chow, S.Z., and K.J. Pickles. 1971. Thermal softening of wood and bark. Wood and Fiber. 3,166-178.

Connolly, M. and B. Tobias. 1992. Thermoset cure by dynamic mechanical, dielectric and calorimetric methods. Amer. Lab. 24(1): 38-42.

Cousins, W.J. 1976. Elastic modulus of hemicellulose as related to moisture content. Wood Sci. Tech. 10:9-17.

___. 1978. Young's modulus of hemicellulose as related to moisture content. Wood Sci. Tech. 12:161-167.

Cowie, J.M.G. 1991. Polymers: Chemistry and physics of modern materials, 2nd ed. Blackie Academic and Professional, New York.

Eaton, R.F., T.H. Tran, M. Shen, T.F. Schatzki, and E. Menefee. 1976. Water dependent beta relaxations in cellulose and its derivatives. Polymer Prepr. 17(2):54-58.

Engelhardt, F. 1979. Investigations on the sorption of water vapour by beech at temperatures ranging from 110 to 170 °C. Holz Roh- Werkstoff. 37(3):99-112.

Fengel, D. and G. Wegener. 1989. Wood: Chemistry, Ultrastructure, Reactions. Walter de Gruyter. New York.

Ferry, J.D. 1980. Viscoelastic properties of polymers, 3rd ed. John Wiley and Sons, New York, NY.

Funakoshi, H., N. Shiraishi, M. Norimoto, T.Akoi, H. Hayashi, and T. Yokota. 1979. Studies on the thermoplasticization of wood. Holzforshung. 33(5):159-166.

Geimer, R., R.J. Mahoney, S.P. Loehnertz, and R.W. Meyer. 1985. Influence of processing-induced damage on strength of flakes and flakeboards. F.P.L. Res. Paper #463. U.S.D.A. Forest Products Lab. Madison, WI.

Goring, D.A.I. 1963. Thermal softening of lignin, hemicellulose and cellulose. Pulp Paper Mag. Can. 64(12):517-527.

Grumach, M. 1951. The equilibrium moisture content of wood in superheated steam. CSIRO, Div. For. Prod., Proj. S 17 Prog. Rep.

Hahn, R.A. 1966. Theoretical considerations in the drying of wood at pressures above atmospheric. For. Prod. J. 16(4):25-32.

Hailwood, A.J. and S. Horrobin. 1946. Absorption of water by polymers: analysis in terms of a simple model. Trans. Faraday Soc. 42B:84-102.

Hedvig, P. 1977. Dielectric spectroscopy of polymers. John Wiley and Sons. New York.

Hillis. W.E., and A.N. Rosa. 1978. The softening temperatures of wood. Holzforshung. 32(2):68-73.

Hillis, W.E. 1984. High temperature and chemical effects on wood stability, part I: General considerations. Wood Sci. Tech. 18:281-293.

Höglund, H., U. Sohlin, and G. Tistad. 1976. Physical properties of wood in relation to chip refining. Tappi 59(6):144-147.

Hsu. W.E., W. Schwald, J. Schwald, and J.A. Shields. 1988. Chemical and physical changes required for producing dimensionally stable wood-based composites. Wood Sci. Tech. 22:281-289.

Humphrey, P.E. and A.J. Bolton. 1989. The hot pressing of dry-formed wood-based composites Part II. A simulation model for heat and mass transfer, and typical results. Holzforshung. 43(3):199-206.

Irvine, G.M. 1984. The glass transitions of lignin and hemicellulose and their measurement by differential thermal analysis. Tappi 67(5):118-121.

Jeffries, R. 1960. The sorption of water by cellulose and eight other textile polymers, part III. The sorption of water vapor by textile polymers at 120 ° and 150 ° C. Jour. Text. Inst. 51(11):T441.

Kaar. 1991. The complete analysis of wood polysaccharides using HPLC. J. Wood Chem. Tech. 11(4):447:469

Kamke, F.A. and M.P. Wolcott. 1991. Fundamentals of flakeboard manufacture: Wood-moisture relationships. Wood Sci. Tech. 25:57-71.

Kamke, F.A., and L.J. Casey 1989. Fundamentals of flakeboard manufacture: Internal mat conditions. For. Prod. J. 38(6)38-44.

Kauman, W.G. 1956. Equilibrium moisture content and drying control in superheated steam drying. For. Prod. J. 6(9):328-332.

Kelley, S.S. T.G. Rials, and W.G. Glasser. 1987. Relaxation behavior of the amorphous components of wood. J. Mat. Sci. 22:617-624.

Keylwerth, R. 1949. Fundamentals of high-temperature drying of wood. Holz Zentrabl. 75(76):953-954.

Kohlman, F. and L. Malmquist. 1952. Research on seasoning sawn pine timber at high temperatures. Medd. Sven. Traforskn. Inst. Avd. 23.

Kretschmann, D.E. and B.A. Bendsten. 1992. Ultimate tensile stress and modulus of elasticity of fast-grown plantation loblolly pine lumber. Wood and Fiber Sci. 24(2):189-203.

Ladell, J.L. 1957. High temperature kiln drying of eastern Canadian softwoods. West. For. Prod. Lab. Tech. Note 2. Vancouver, B.C., Can.

Lutz, J.F. 1974. Drying of veneer to a controlled moisture content by hot-pressing and steaming. USDA For. Ser. Res. Pap. FPL 227. For. Prod. Lab. Madison, WI.

McCrum, N.G., B.E. Read, and G. Williams. 1967. Anelastic and dielectric effects in polymeric solids. John Wiley and Sons, New York.

Mizumachi, H. 1991. Wood-Polymer Composites. In: Wood and Cellulosic Chemistry. Marshall Dekker, New York.

Neter, J. and W. Wasserman. 1974. Applied linear statistical models. Richard D. Irwin Inc., Homewood, IL

Östberg, G., L. Salmen and J. Terlecki. 1990. Softening temperature of moist wood by differential scanning calorimetry. Holzforshung. 44(3):223-225.

Panshin, A.J., and C. de Zeeuw. 1980. Textbook of Wood Technology. McGraw-Hill Co. New York.

Price, E.W. 1976. Determining tensile properties of sweetgum veneer flakes. For. Prod. J. 26(10):50-53.

Pugel, A.D., E.W. Price and C.Y. Hse. 1990b. Composites from southern pine juvenile wood. Part 2: Durability and dimensional stability. For. Prod. J. 40(3):57-61.

Resch, H., M.L. Hoag, and H.N. Rosen. 1988. Desorption of yellow-poplar in superheated steam. For. Prod. J. 38(3):13-18.

Rials, T.J. 1992. Cure Analysis of Phenol-Formaldehyde Resins by Microdielectric Spectroscopy. In Viscoelasticity of Biomaterials. Eds. W.G. Glasser and H. Hatakeyama, ACS Symposium Series 489. ACS, Washington D.C. 18: 282.

Rosen, H.N. 1980. Psychrometric relationships and equilibrium moisture content of wood at temperatures above 212 F. Wood and Fiber 12(3):153-171.

Sadoh, T. 1981. Viscoelastic properties of wood in swelling systems. Wood Sci. Tech. 15:57-66.

Salmen, L., and E.L. Back. 1977. The influence of water on the glass transition of cellulose. Tappi 60(12):137-140.

Salmen, N. L. 1984. Viscoelastic properties of in situ lignin under water-saturated conditions. J. Mat. Sci. 19:3090-3096.

Shutler, E.L. 1992. Relating the compression and recovery of polymeric cellular materials to the dimensional stability of wood composites. M.S. Thesis, W.V.U. Morgantown, WV.

Siau, J.F. 1971. Flow in wood. Syracuse University Press, Syracuse, NY.

_____. 1984. Transport processes in wood. Springer-Verlag, New York.

_____. 1995. Wood: influence of moisture on physical properties. Dept. Wood Sci. & For. Prod. Blacksburg, VA.

Simpson, W.T. 1971. Equilibrium moisture content prediction for wood. Forest Prod. J. 21(5):48-49.

_____. 1973. Predicting equilibrium moisture content of wood by mathematical models. Wood and Fiber. 5(1):41-49.

_____. 1980. Sorption theories applied to wood. Wood and Fiber. 12(3):183-195.

_____ and H.N. Rosen. 1981. Equilibrium moisture content of wood at high temperatures. Wood and Fiber. 13(3):150-158.

Skaar, C. 1972. Water in wood. Syracuse University Press, Syracuse, NY.

_____. 1976. In: Gerhards, C.C. and J.M. McMillan (eds): High-temperature drying effects on mechanical properties of softwood lumber. pp. 113-127. USDA For. Serv., For. Prod. Lab., Madison, WI.

_____. 1988. Wood-water relations. Springer-Verlag, New York.

Strickler, M.D. 1968. High temperature relations of grand fir. For. Prod. J. 18(4):69-75.

Sturany, H. 1952. The Schilde air-free steam dryer for wood. Hol Roh- Werkst. 10:358-362.

Takahashi, K., T. Morooka and M. Norimoto. 1998. Thermal softening of wet wood in the temperature range of 0 to 200°C. Wood Research, 85:78-80.

Torgovnikov, G.I. 1993. Dielectric Properties of Wood and Wood-Based Materials. Springer-Verlag. Berlin. 196 pp.

Uhmeier, A., T. Morooka and M. Norimoto. 1998. Influence of thermal softening and degradation on the radial compression behavior of wet spruce. Holzforshung, 52(1):77-81.

Urquhart, A.R., and A.M. Williams. 1924. The moisture relations of cotton: the effect of temperature on the absorption of water by soda-boiled cotton. Jour. Text. Inst. 15:T559.

U.S. Forest Products Laboratory. 1974. Wood Handbook. U.S. Dept. Ag., Ag. Hndb. 72, For. Prod. Lab., Madison, WI.

Ward, I.M. 1983. Mechanical properties of solid polymers, 2nd ed. Wiley-Interscience. New York, NY.

Wert, C.A., M. Weller and D. Caulfield. 1984. Dynamic loss properties of wood. J. Appl. Phys. 56(9):2453-2458.

Wetton. R.E., M.R. Morton, and A. M. Rowe. 1986, *Incomplete reference*. International Laboratory. 70.

Wolcott, M.P. 1989. Modeling viscoelastic cellular materials for the pressing of wood composites. Ph.D. Dissertation, V.P.I. and S.U. Blacksburg, VA.

_____, F.A. Kamke, and D.A. Dillard. 1990. Fundamentals of flakeboard manufacture: Viscoelastic behavior of the wood component. Wood and Fiber Sci. 22(4)345-361.

_____, ___, and ___. 1994. Fundamental aspects of wood deformation pertaining to manufacture of wood-based composites. Wood and Fiber Sci. 26(4):496-511.

Young, R.J. and P.A. Lovell. 1991. Introduction to polymers, 2nd ed. Chapman and Hall, London.

APPENDIX I

Dielectric properties of southern pine juvenile, yellow-poplar juvenile, and yellow-poplar mature wood specimens as a function of temperature and moisture content.

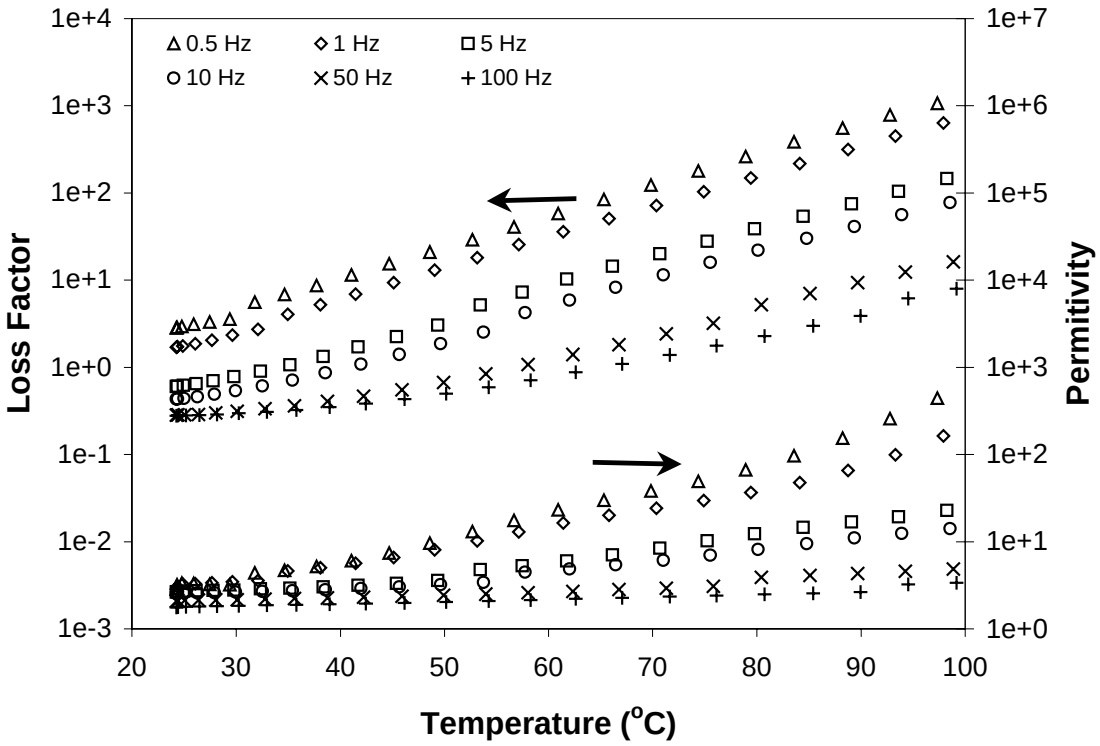

Figure AI.1. Dielectric permitivity (right axis) and dielectric loss factor (left axis) verses temperature for southern pine juvenile wood at 5% moisture content. Six measurement frequencies are shown.

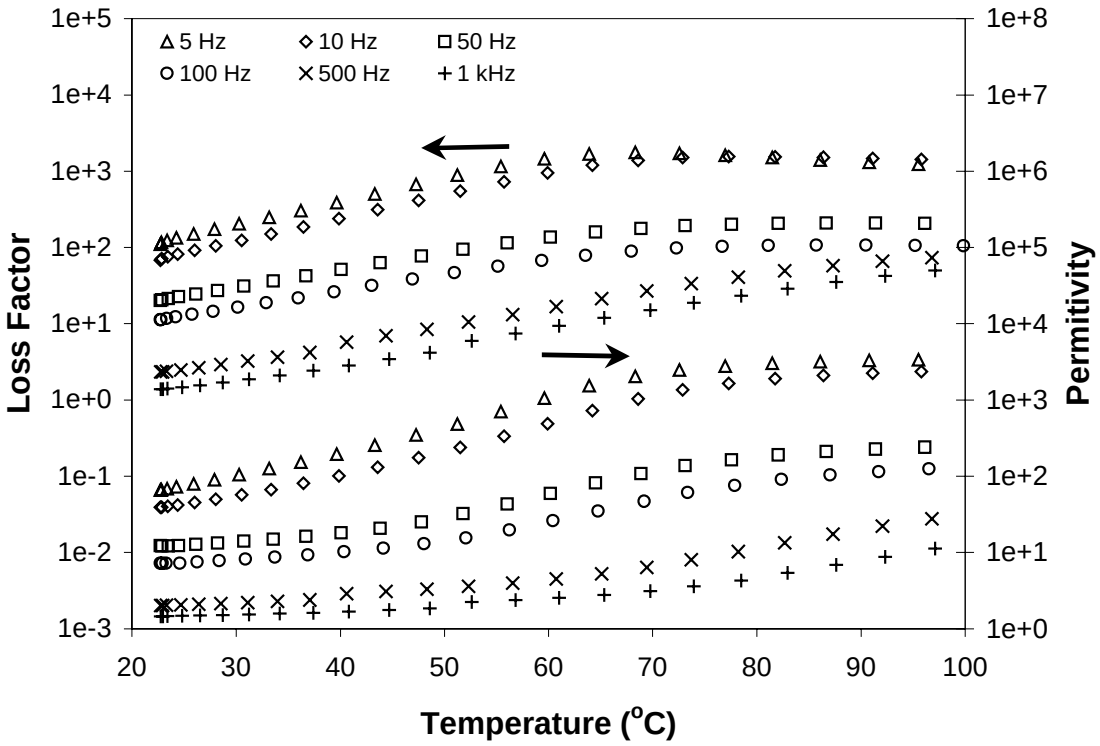

Figure AI.2. Dielectric permitivity (right axis) and dielectric loss factor (left axis) verses temperature for southern pine juvenile wood at 5% moisture content. Six measurement frequencies are shown.

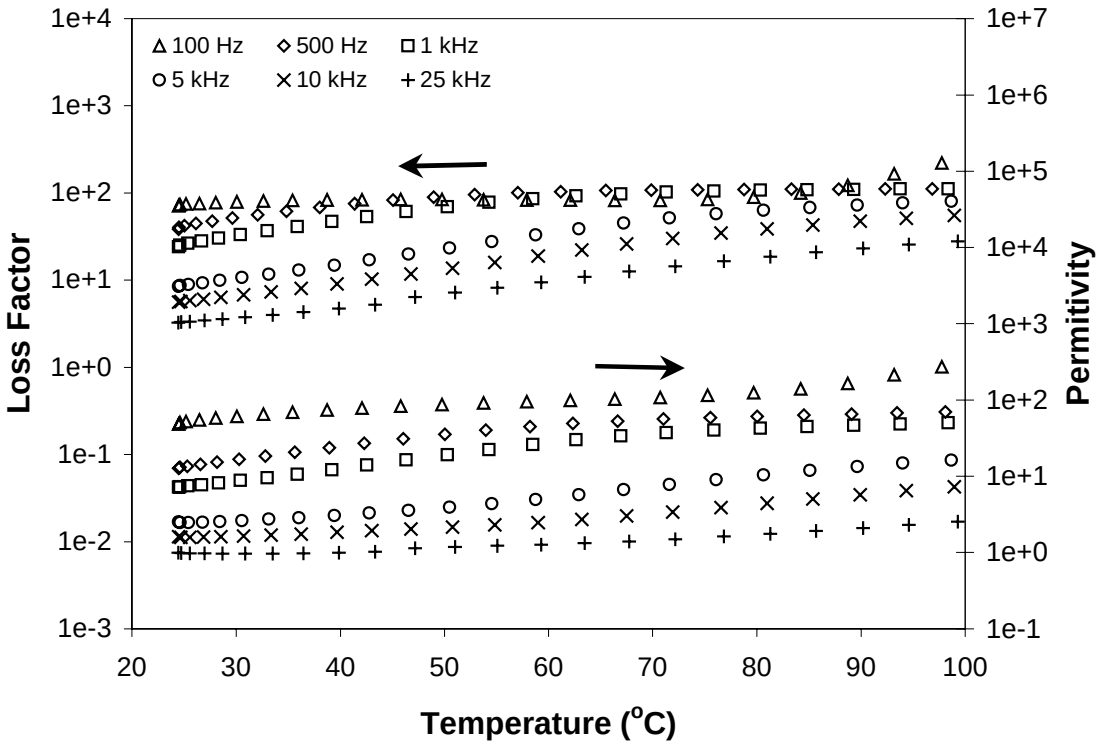

Figure AI.3. Dielectric permitivity (right axis) and dielectric loss factor (left axis) verses temperature for southern pine juvenile wood at 20% moisture content. Six measurement frequencies are shown.

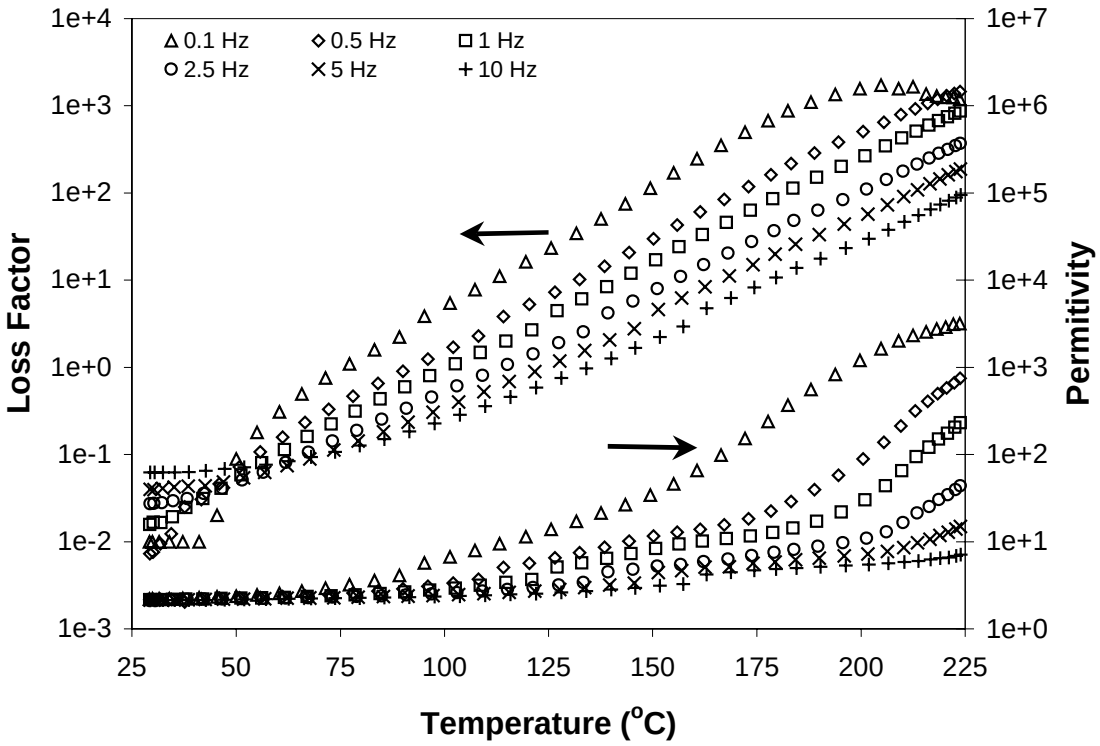

Figure AI.4. Dielectric permitivity (right axis) and dielectric loss factor (left axis) verses temperature for southern pine mature wood at 0% moisture content. Six measurement frequencies are shown.

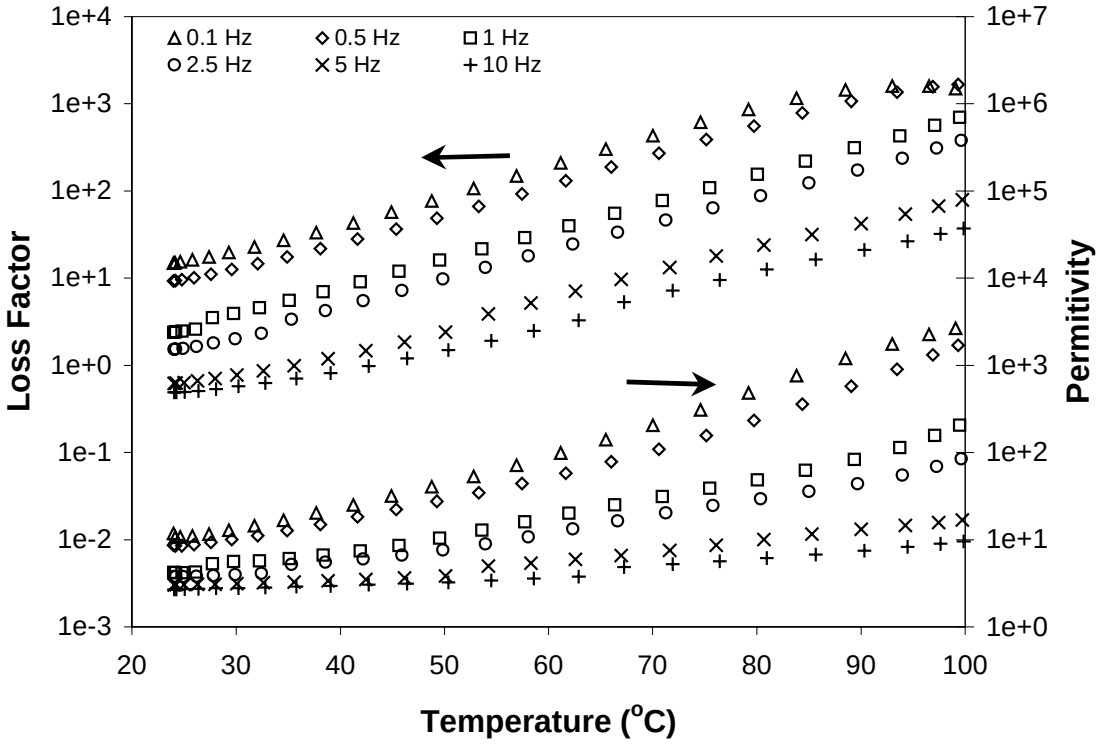

Figure AI.5. Dielectric permitivity (right axis) and dielectric loss factor (left axis) verses temperature for southern pine mature wood at 5% moisture content. Six measurement frequencies are shown.

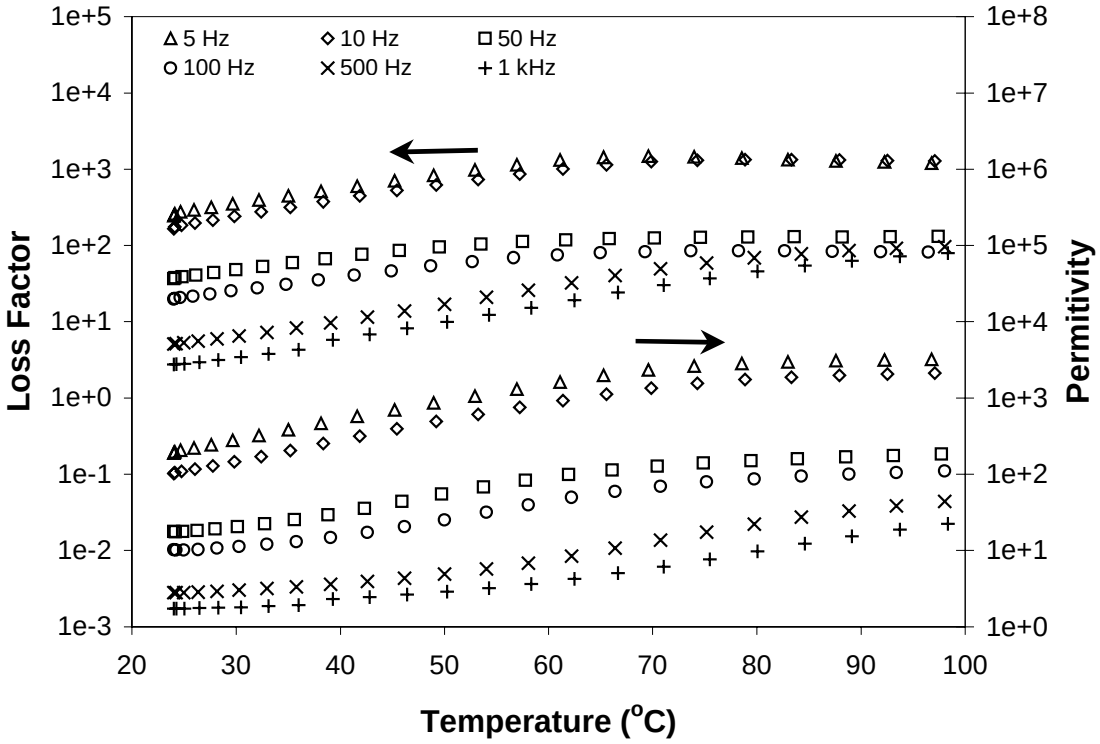

Figure AI.6. Dielectric permitivity (right axis) and dielectric loss factor (left axis) verses temperature for southern pine mature wood at 12% moisture content. Six measurement frequencies are shown.

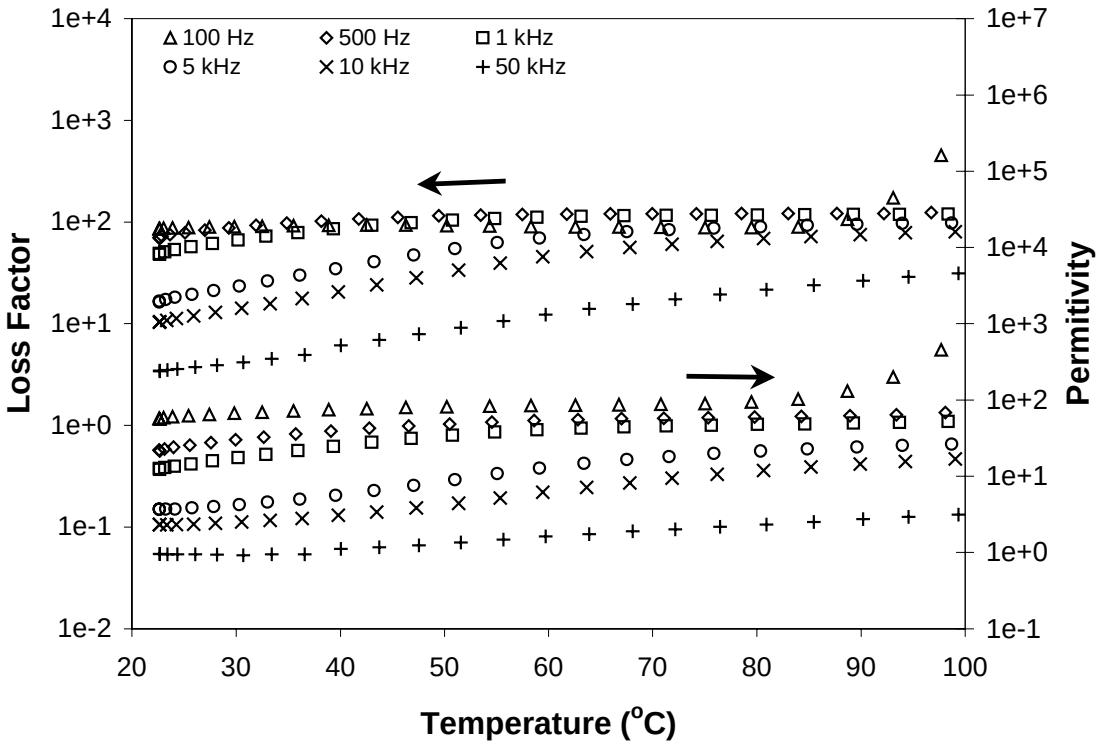

Figure AI.7. Dielectric permitivity (right axis) and dielectric loss factor (left axis) verses temperature for southern pine mature wood at 20% moisture content. Six measurement frequencies are shown.

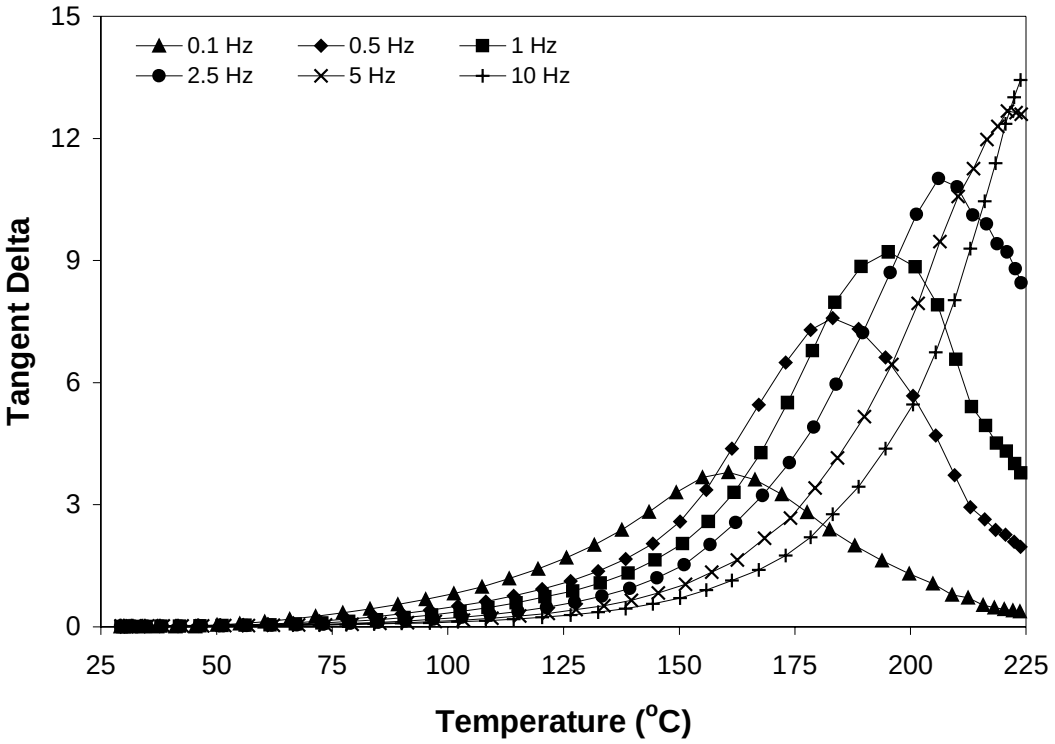

Figure AI.8. Dielectric tangent delta verses temperature for southern pine mature wood at 0% moisture content. Six measurement frequencies are shown.

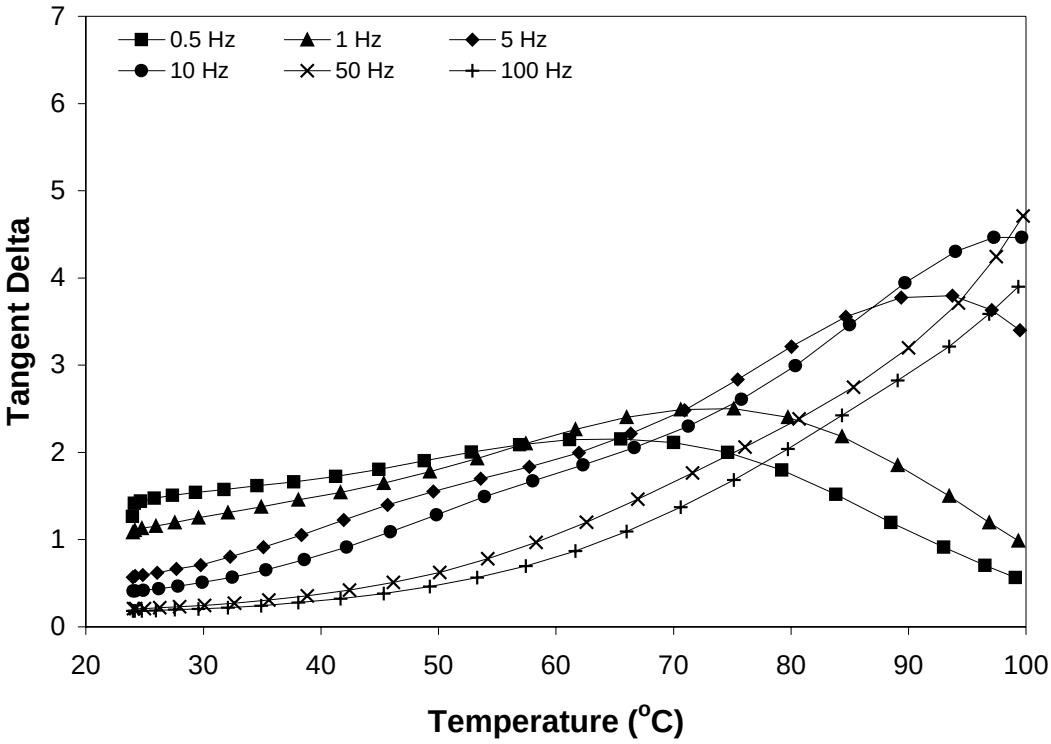

Figure AI.9. Dielectric tangent delta verses temperature for southern pine mature wood at 5% moisture content. Six measurement frequencies are shown.

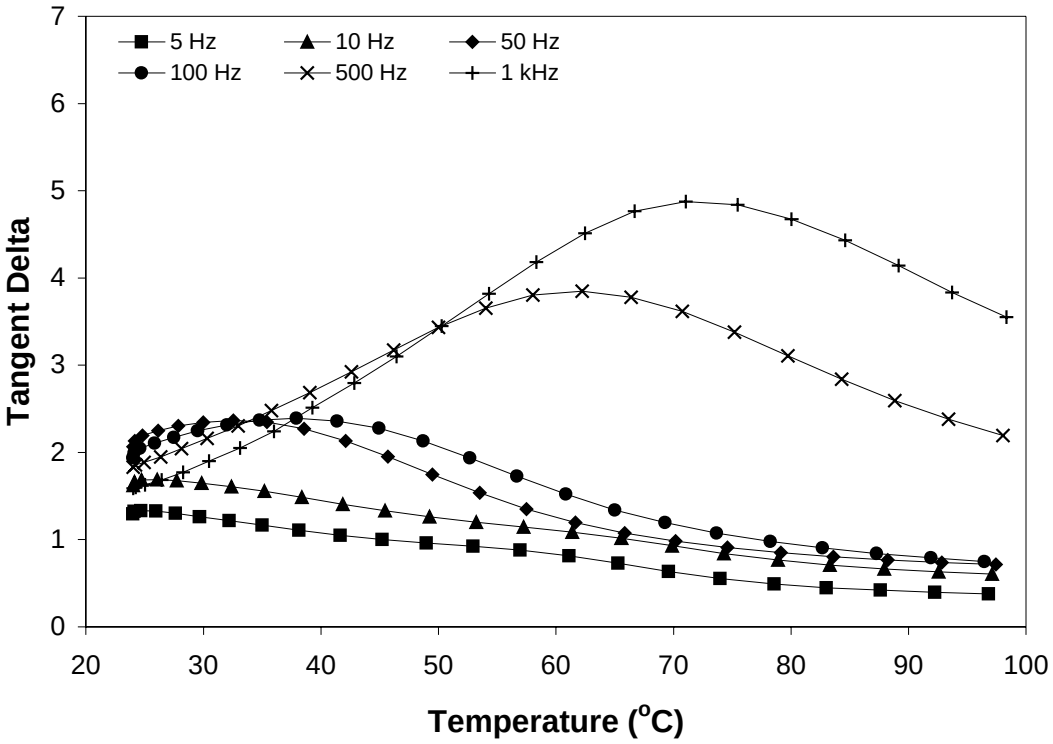

Figure AI.10. Dielectric tangent delta verses temperature for southern pine mature wood at 12% moisture content. Six measurement frequencies are shown.

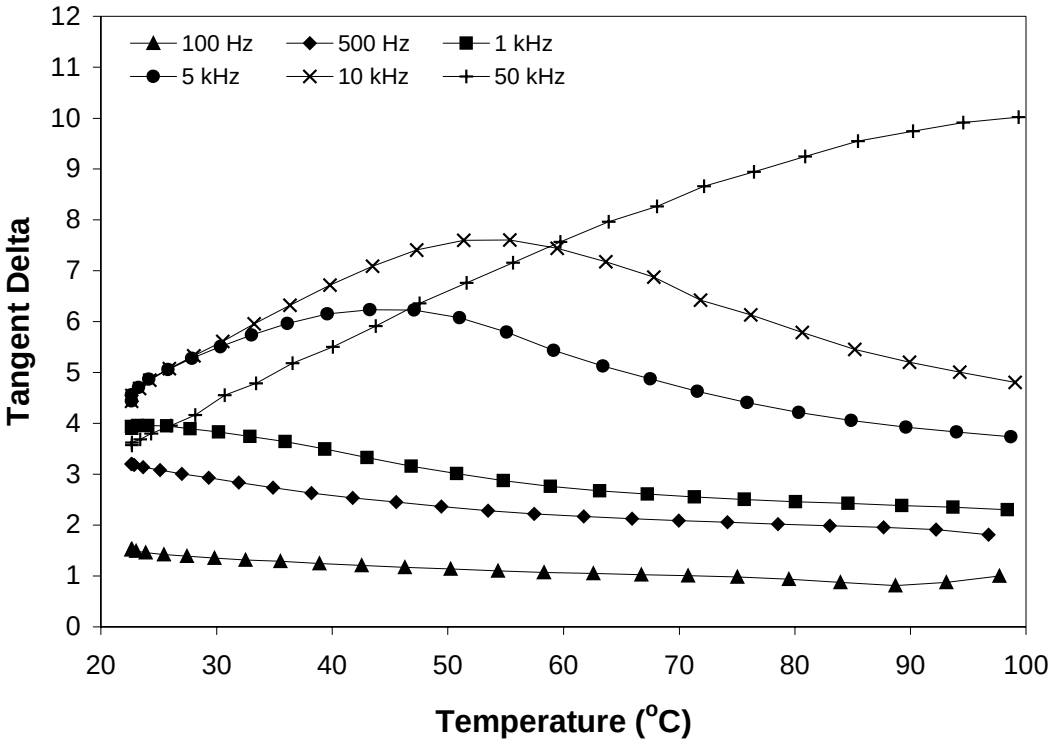

Figure AI.11. Dielectric tangent delta verses temperature for southern pine mature wood at 20% moisture content. Six measurement frequencies are shown.

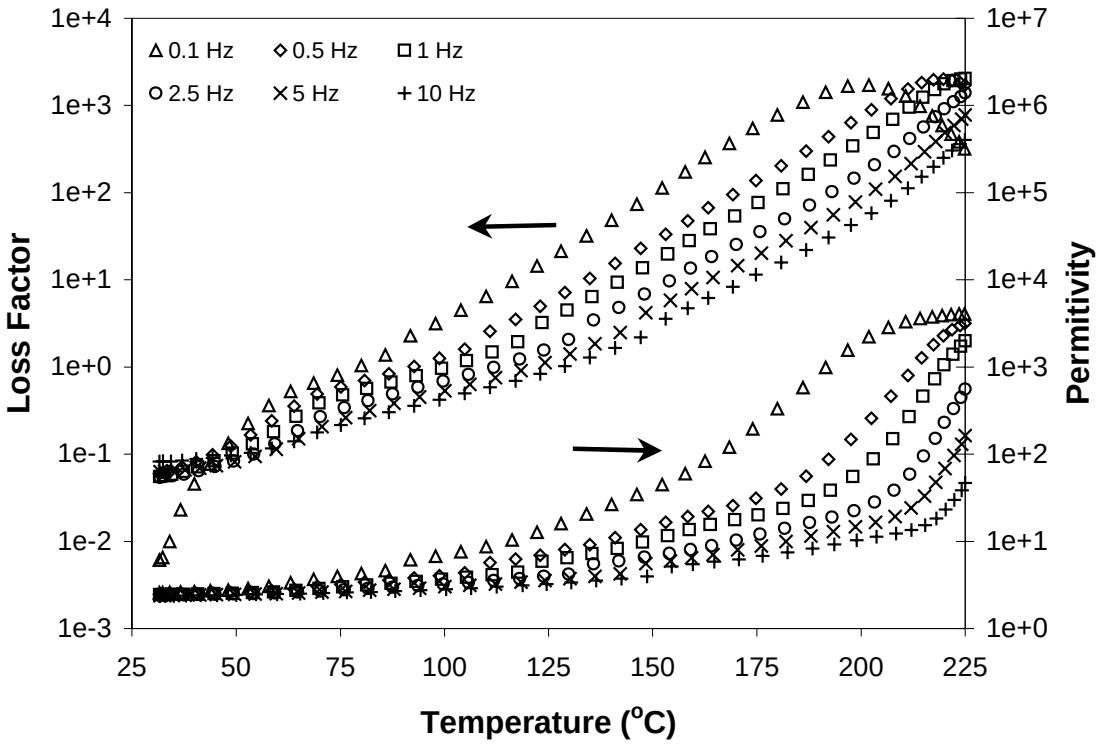

Figure AI.12. Dielectric permitivity (right axis) and dielectric loss factor (left axis) verses temperature for yellow-poplar juvenile wood at 0% moisture content. Six measurement frequencies are shown.

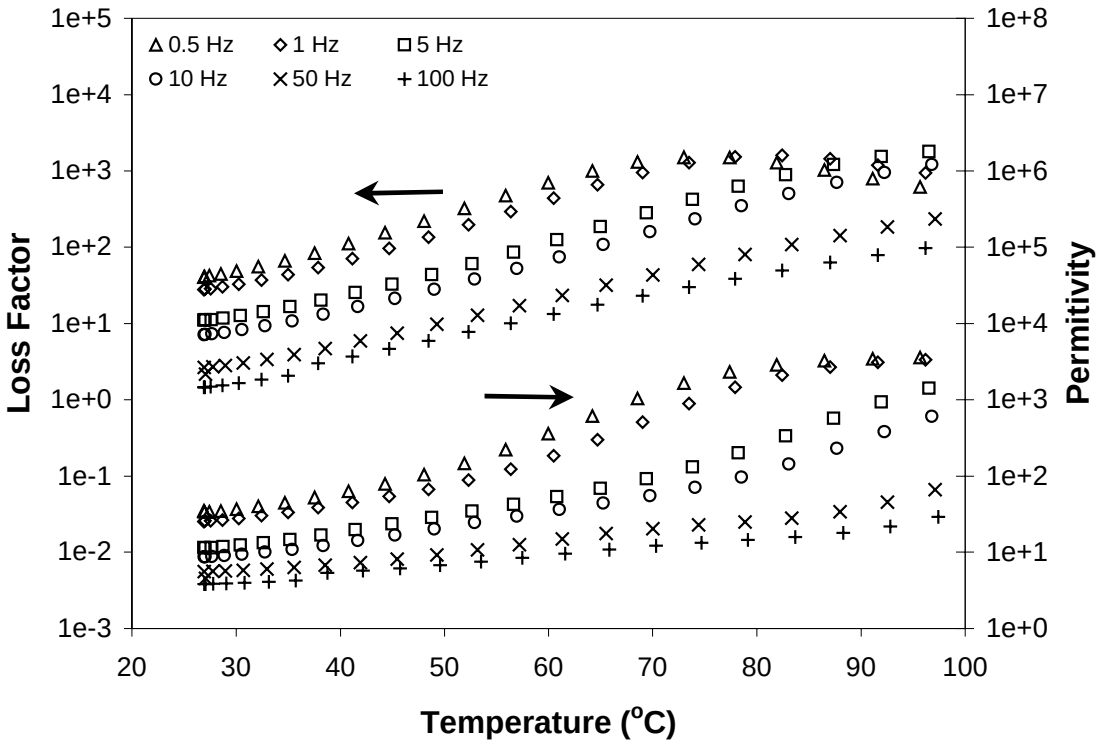

Figure AI.13. Dielectric permitivity (right axis) and dielectric loss factor (left axis) verses temperature for yellow-poplar juvenile wood at 5% moisture content. Six measurement frequencies are shown.

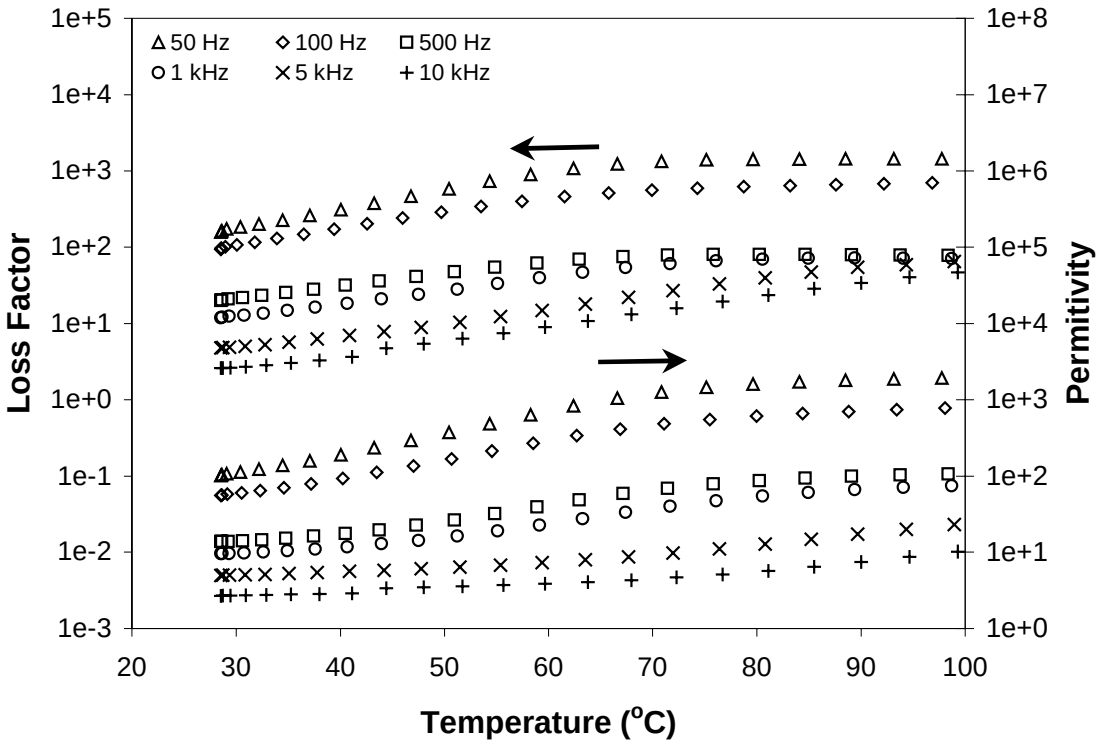

Figure AI.14. Dielectric permitivity (right axis) and dielectric loss factor (left axis) verses temperature for yellow-poplar juvenile wood at 12% moisture content. Six measurement frequencies are shown.

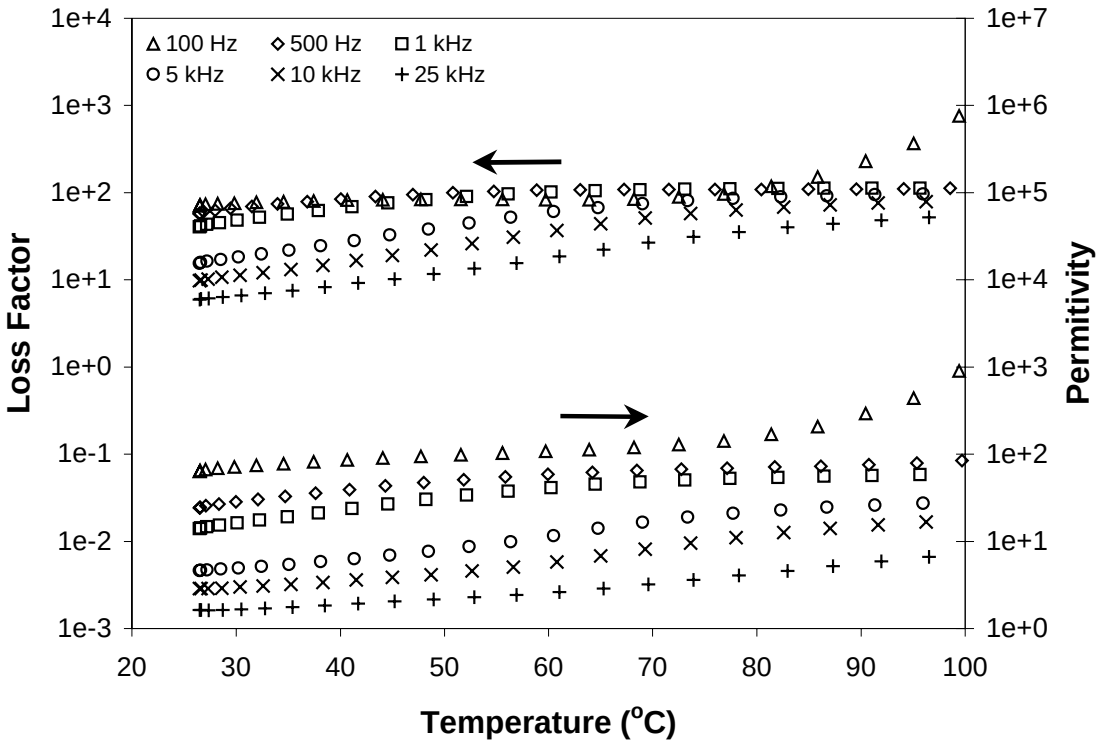

Figure AI.15. Dielectric permitivity (right axis) and dielectric loss factor (left axis) verses temperature for yellow-poplar juvenile wood at 20% moisture content. Six measurement frequencies are shown.

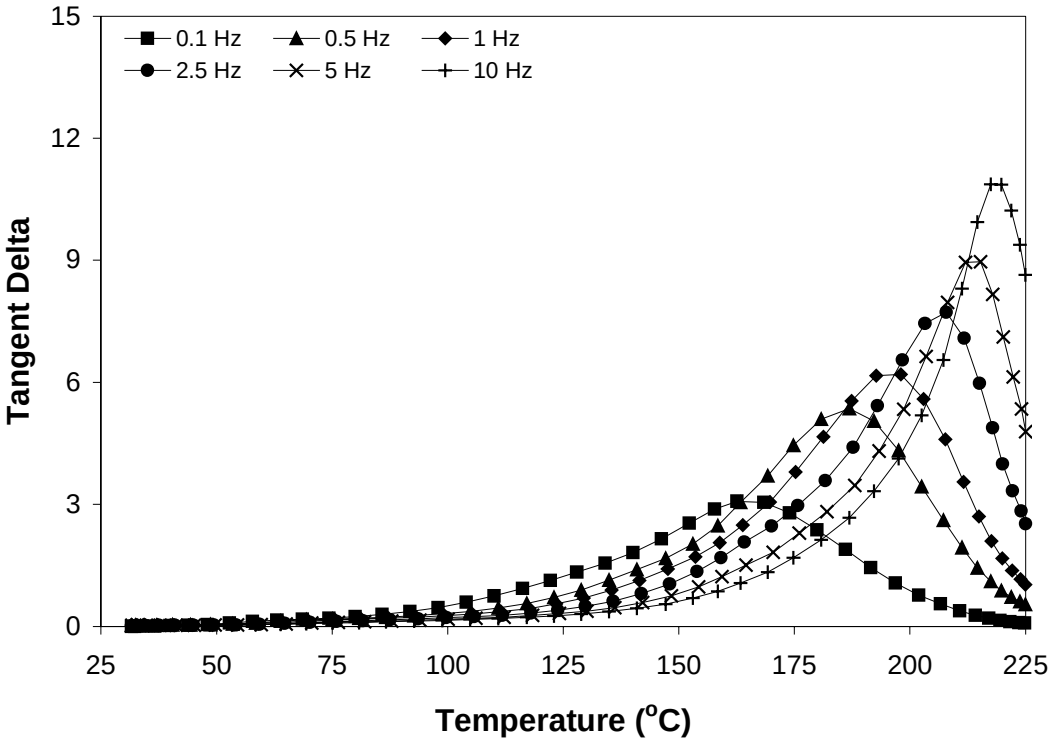

Figure AI.16. Dielectric tangent delta verses temperature for yellow-poplar juvenile wood at 0% moisture content. Six measurement frequencies are shown.

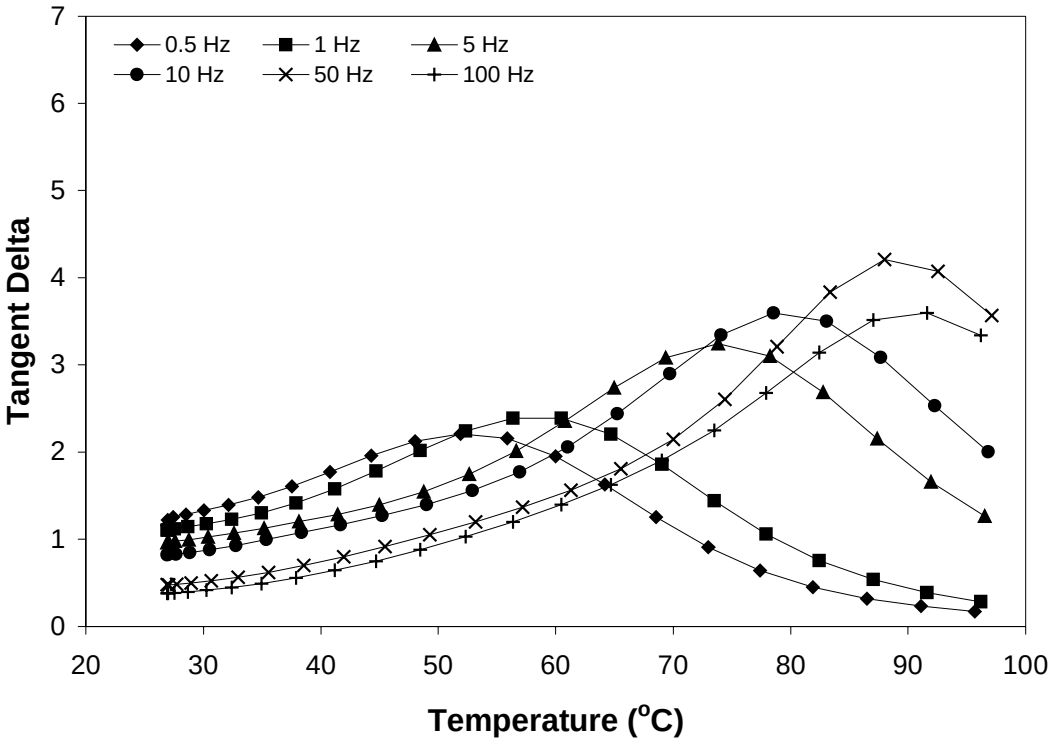

Figure AI.17. Dielectric tangent delta verses temperature for yellow-poplar juvenile wood at 5% moisture content. Six measurement frequencies are shown.

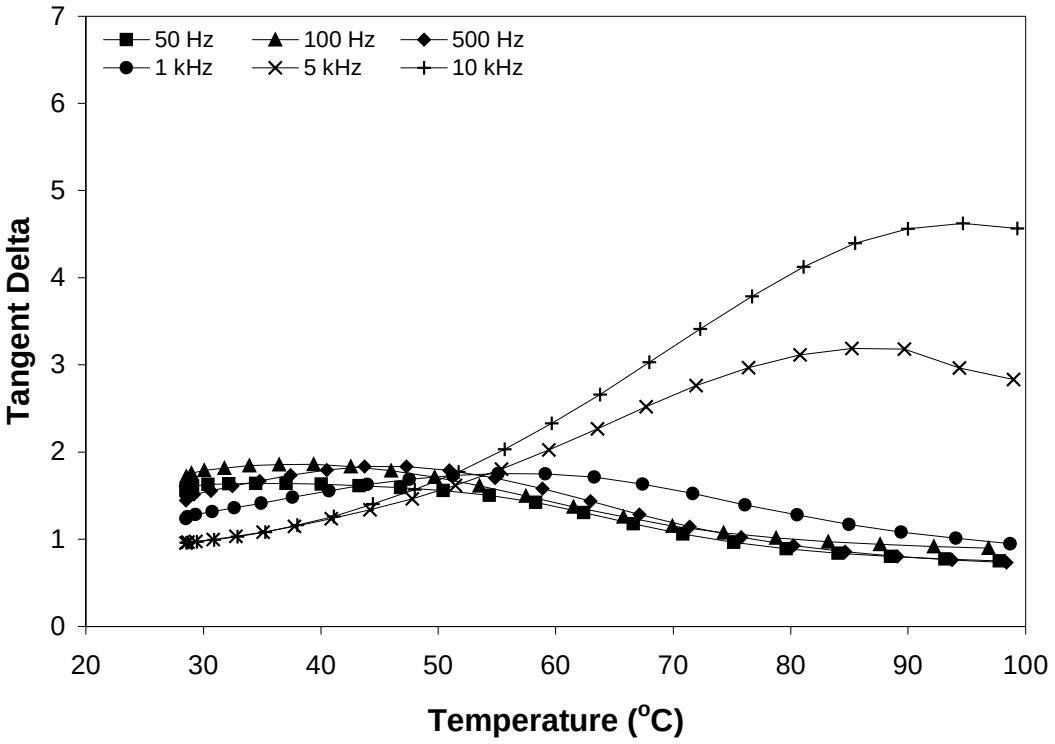

Figure AI.18. Dielectric tangent delta verses temperature for yellow-poplar juvenile wood at 12% moisture content. Six measurement frequencies are shown.

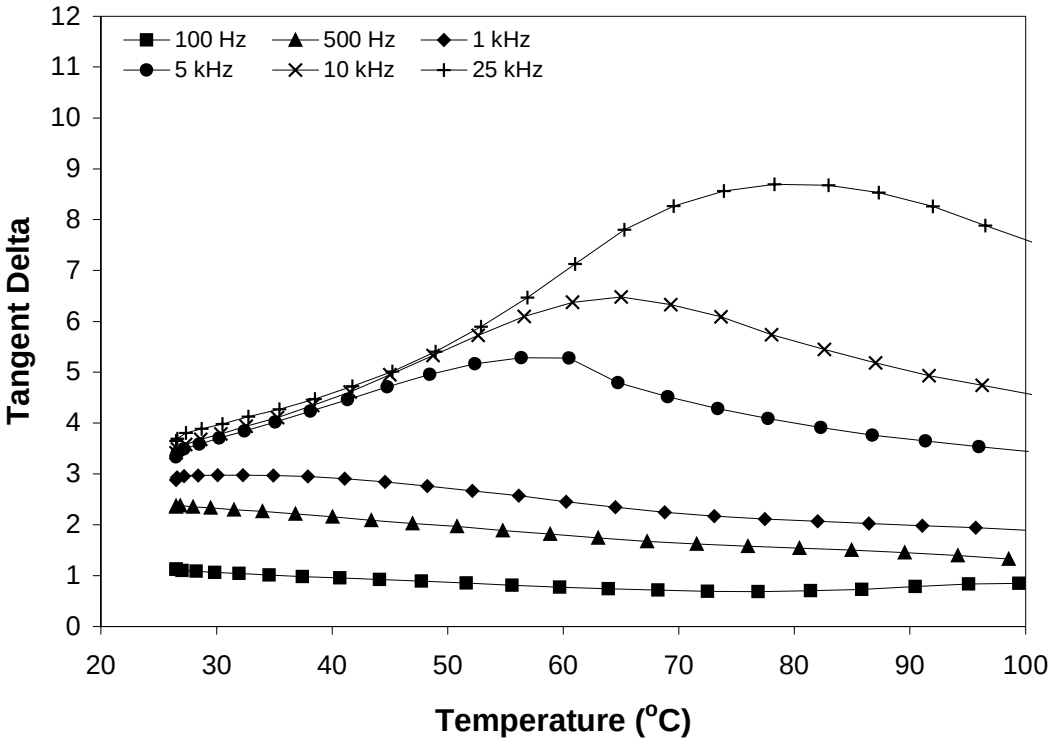

Figure AI.19. Dielectric tangent delta verses temperature for yellow-poplar juvenile wood at 20% moisture content. Six measurement frequencies are shown.

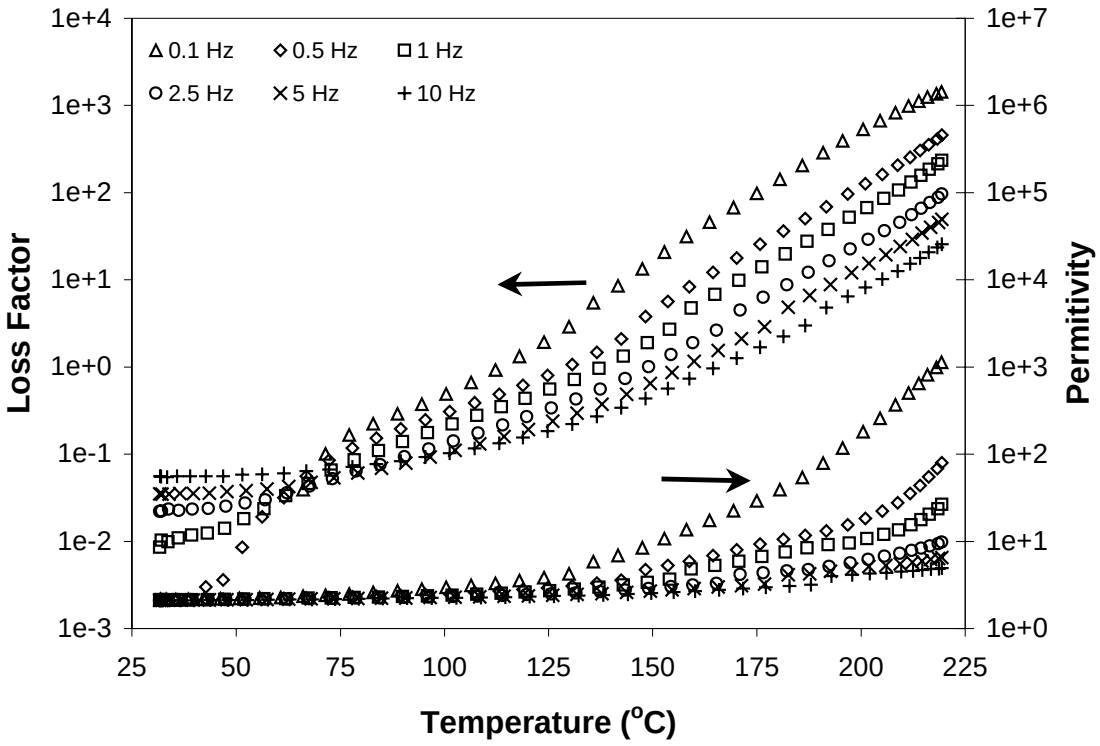

Figure AI.20. Dielectric permitivity (right axis) and dielectric loss factor (left axis) verses temperature for yellow-poplar mature wood at 0% moisture content. Six measurement frequencies are shown.

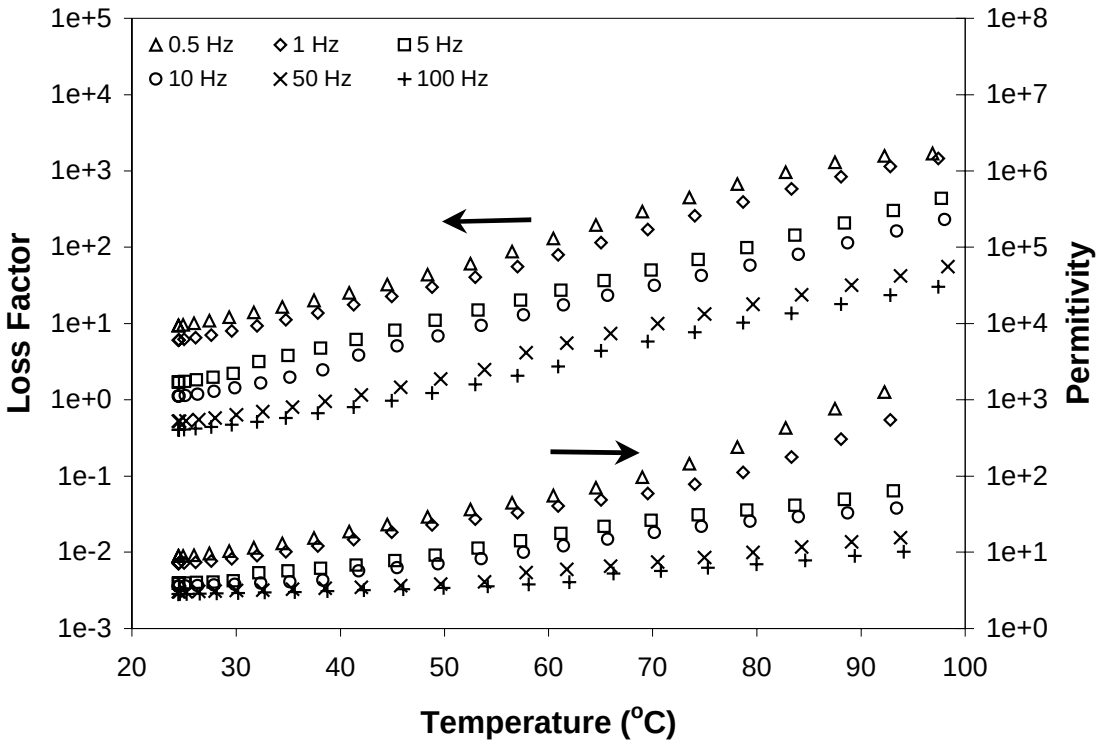

Figure AI.21. Dielectric permitivity (right axis) and dielectric loss factor (left axis) verses temperature for yellow-poplar mature wood at 5% moisture content. Six measurement frequencies are shown.

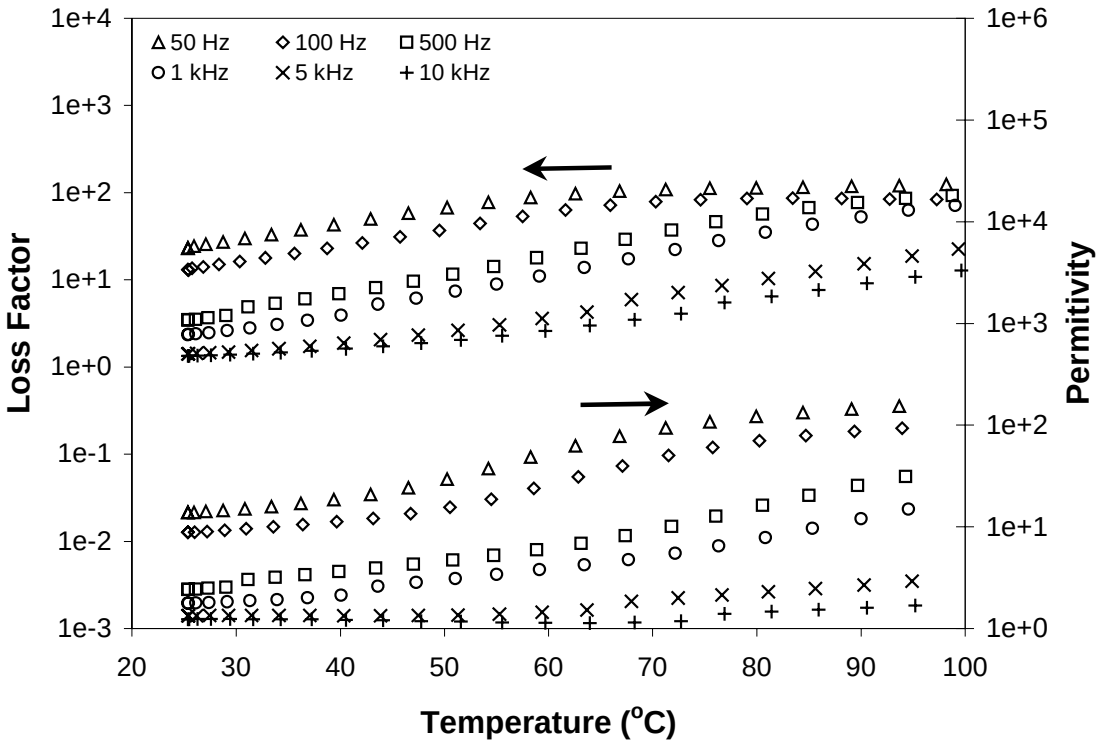

Figure AI.22. Dielectric permitivity (right axis) and dielectric loss factor (left axis) verses temperature for yellow-poplar mature wood at 12% moisture content. Six measurement frequencies are shown.

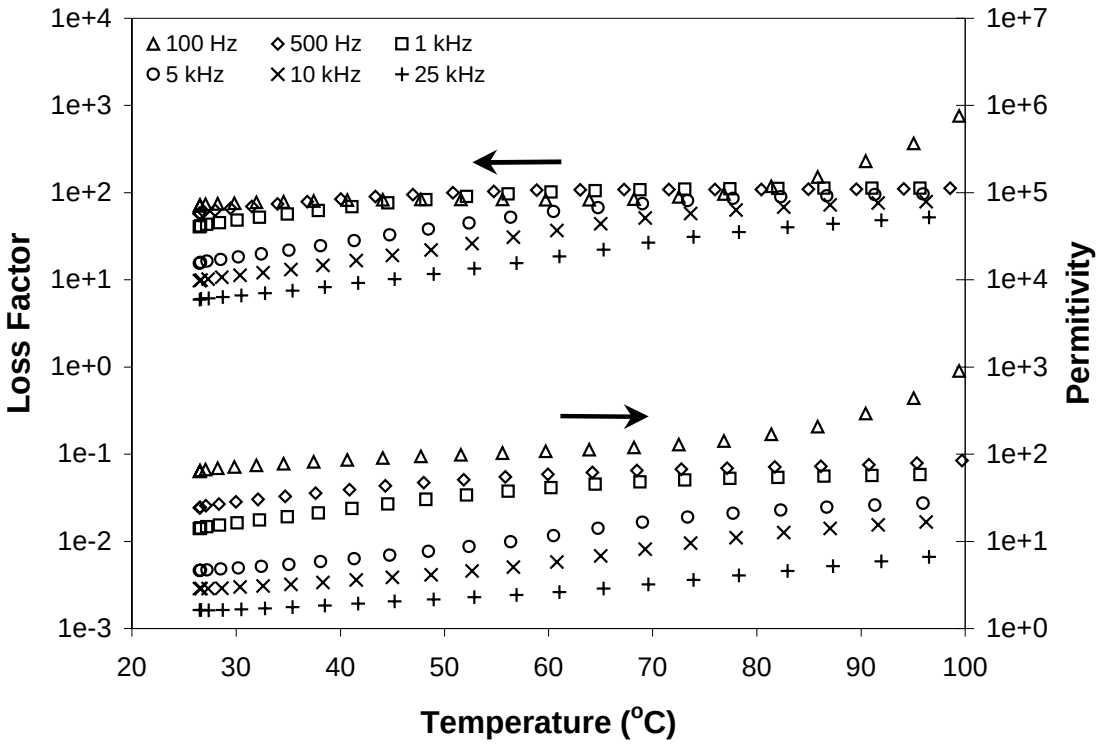

Figure AI.23. Dielectric permitivity (right axis) and dielectric loss factor (left axis) verses temperature for yellow-poplar mature wood at 20% moisture content. Six measurement frequencies are shown.

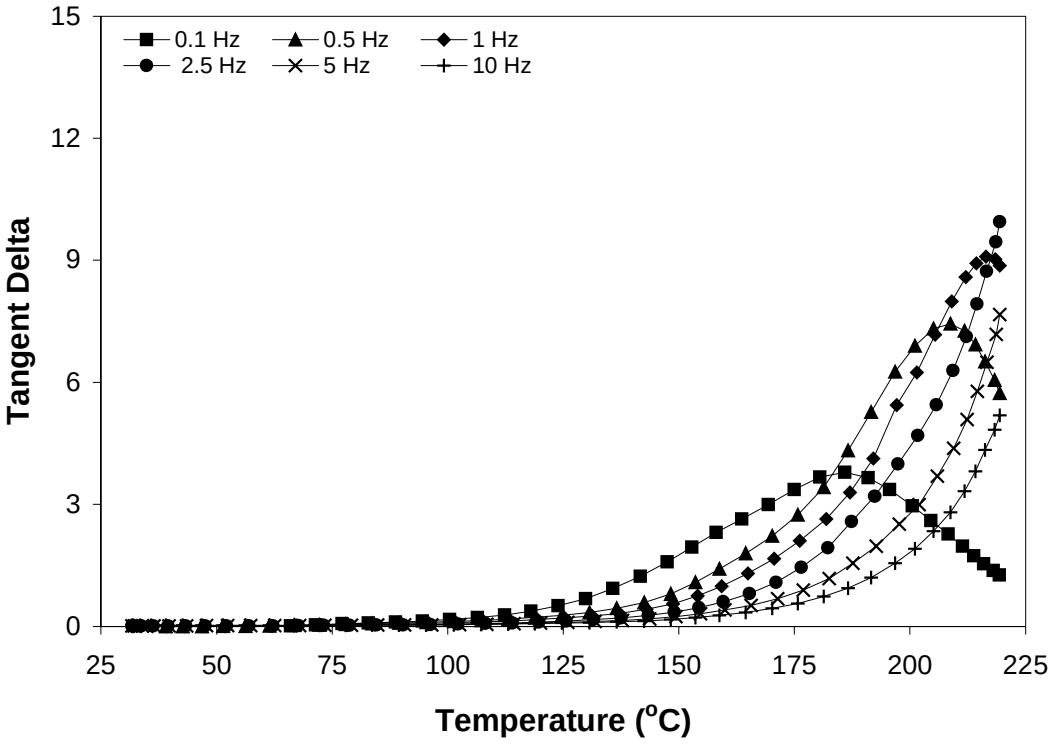

Figure AI.24. Dielectric tangent delta verses temperature for yellow-poplar mature wood at 0% moisture content. Six measurement frequencies are shown.

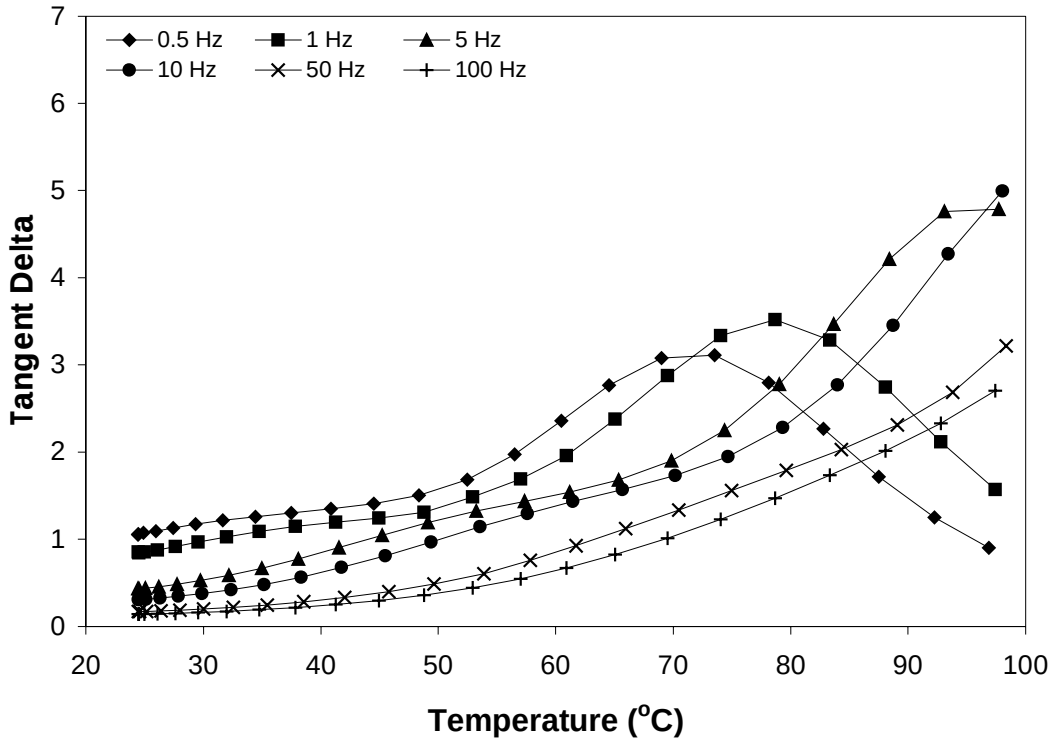

Figure AI.25. Dielectric tangent delta verses temperature for yellow-poplar mature wood at 5% moisture content. Six measurement frequencies are shown.

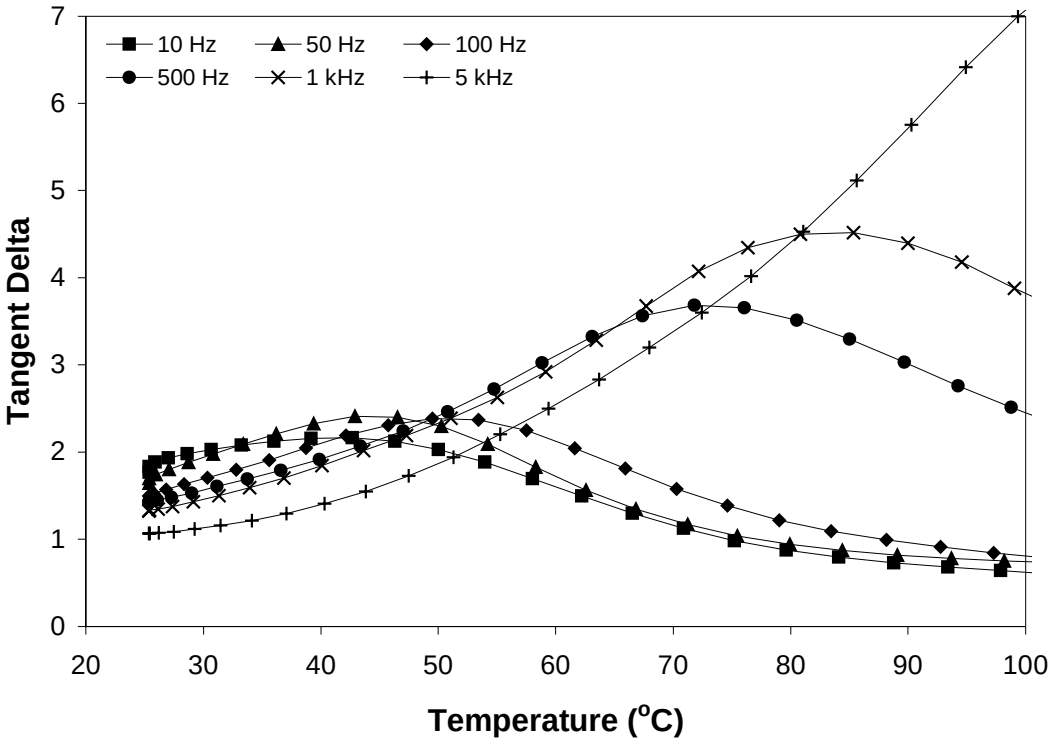

Figure AI.26. Dielectric tangent delta verses temperature for yellow-poplar mature wood at 12% moisture content. Six measurement frequencies are shown.

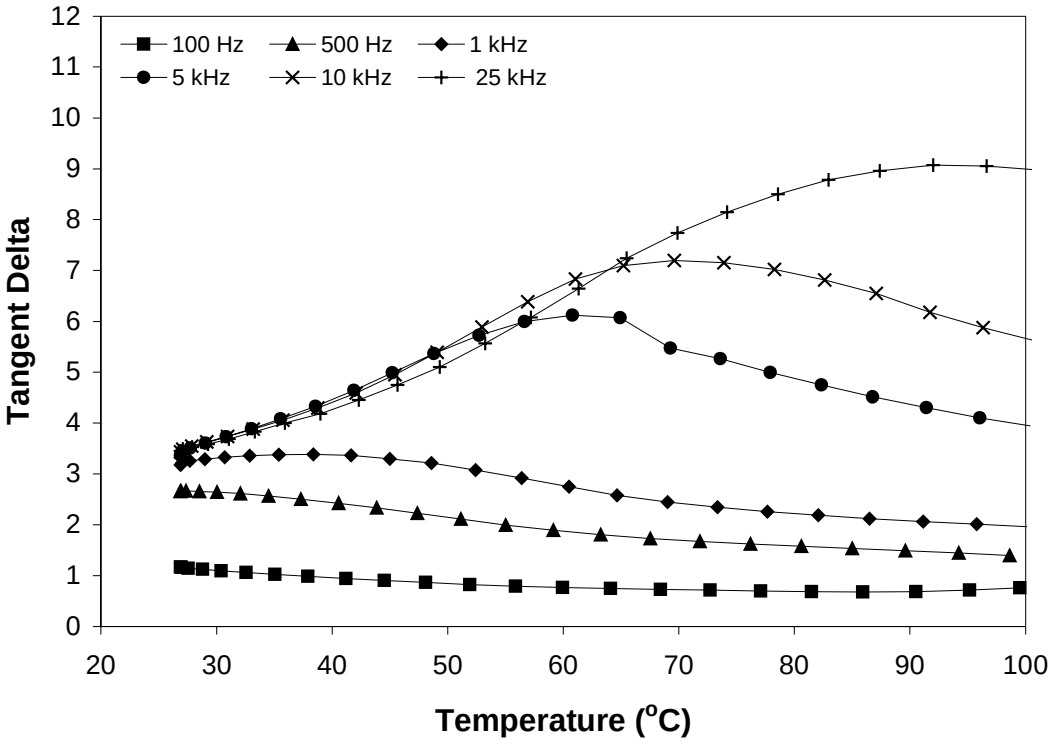

Figure AI.27. Dielectric tangent delta verses temperature for yellow-poplar mature wood at 20% moisture content. Six measurement frequencies are shown.

APPENDIX II

Time – temperature superposition of the dielectric permitivity for southern pine juvenile, southern pine mature, and yellow-poplar mature wood specimens at 0, 5, 12 and 20 percent moisture content.

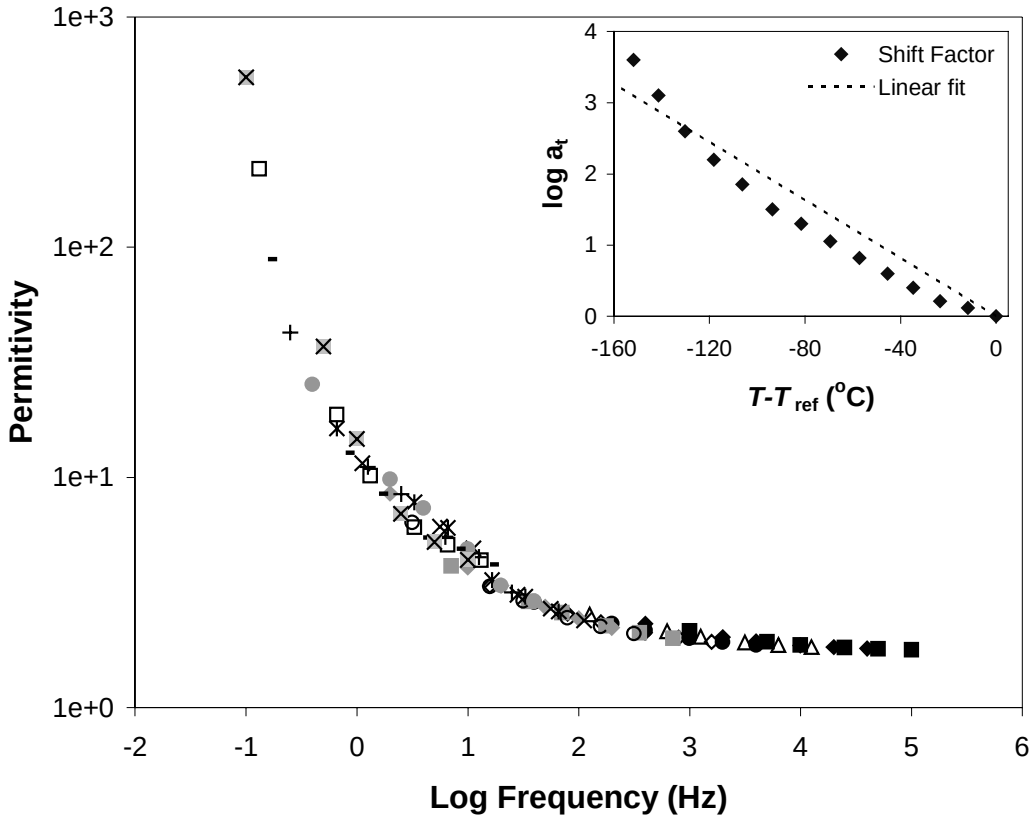

Figure AII.1. Master curve of dielectric permitivity versus log frequency for southern pine juvenile wood at 0% moisture content. The reference temperature used was 200 °C.

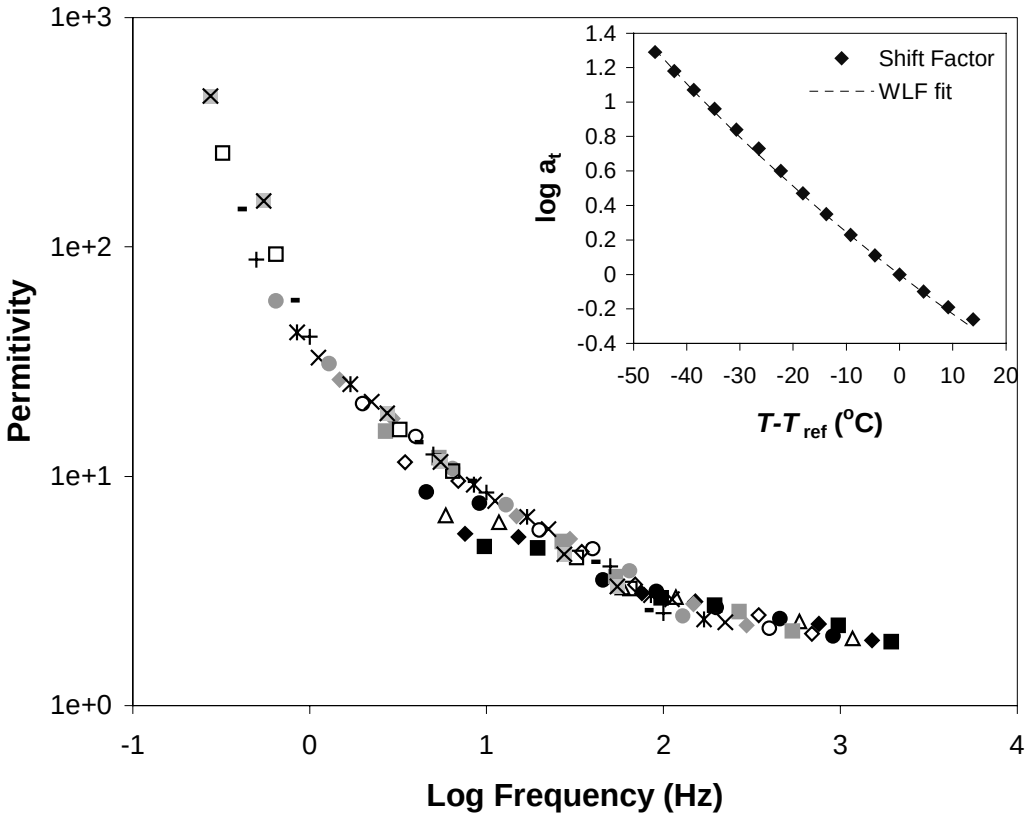

Figure AII.2. Master curve of dielectric permitivity versus log frequency for southern pine juvenile wood at 05% moisture content. The reference temperature used was 86 °C.

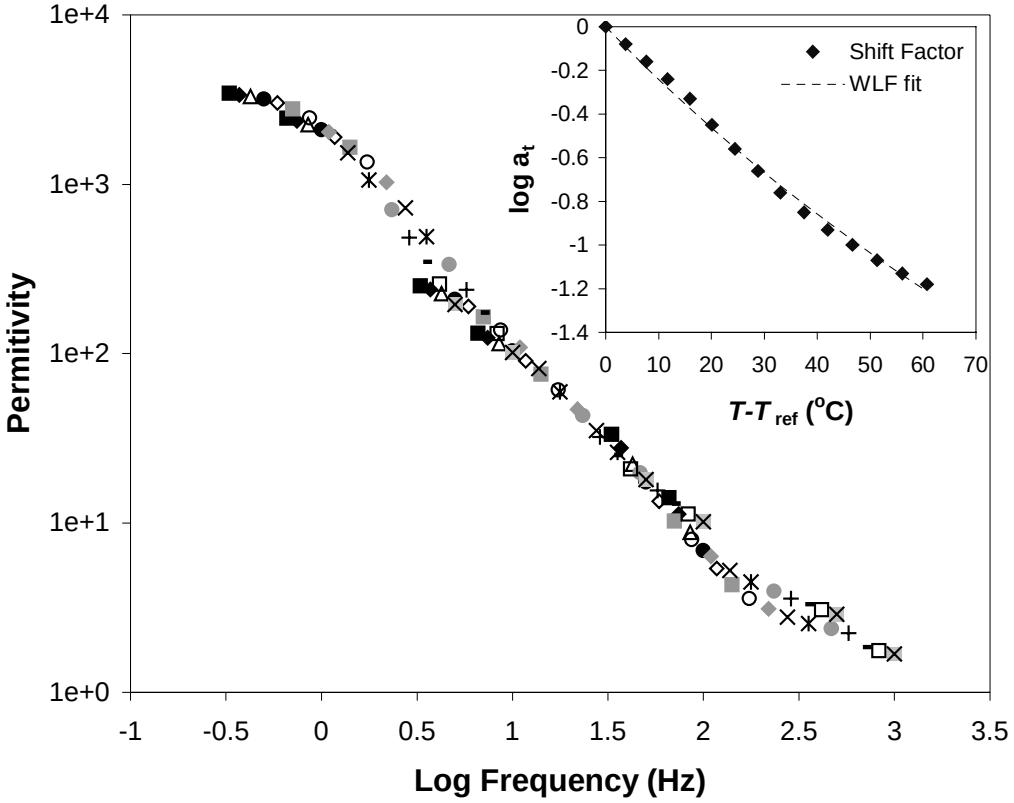

Figure AII.3. Master curve of dielectric permitivity versus log frequency for southern pine juvenile wood at 12% moisture content. The reference temperature used was 40 °C.

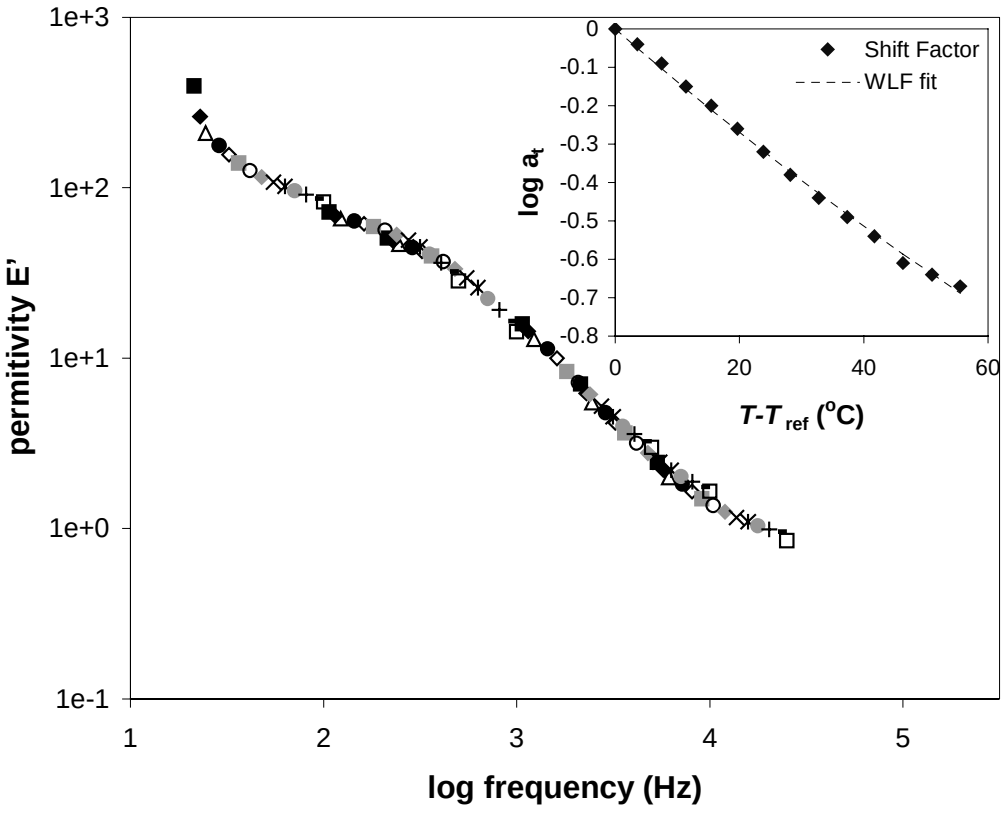

Figure AII.4. Master curve of dielectric permitivity versus log frequency for southern pine juvenile wood at 20% moisture content. The reference temperature used was 43 °C.

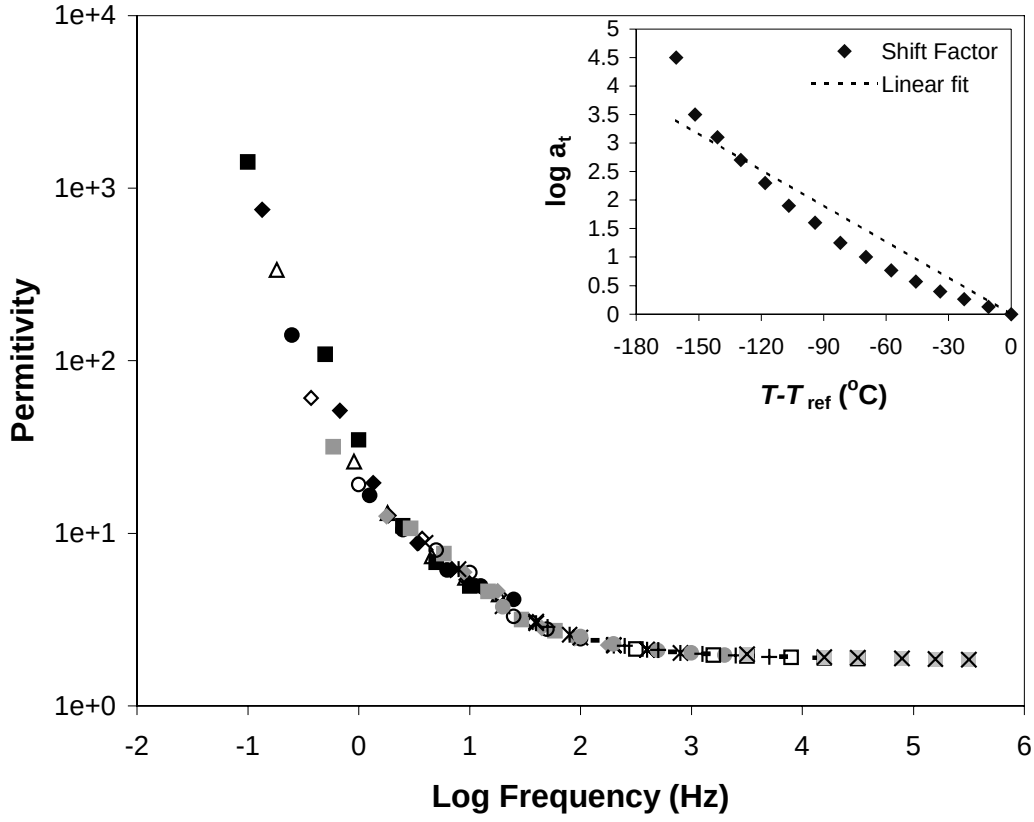

Figure AII.5. Master curve of dielectric permitivity versus log frequency for southern pine mature wood at 0% moisture content. The reference temperature used was 200 °C.

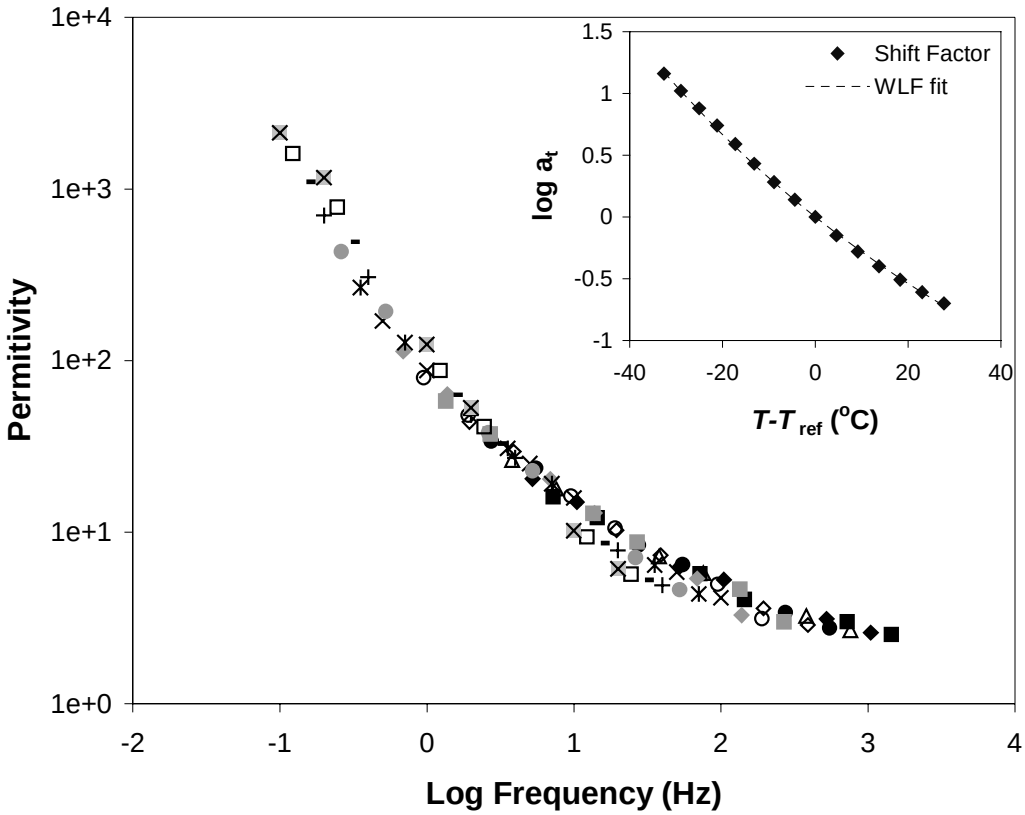

Figure AII.6. Master curve of dielectric permitivity versus log frequency for southern pine mature wood at 05% moisture content. The reference temperature used was 74 °C.

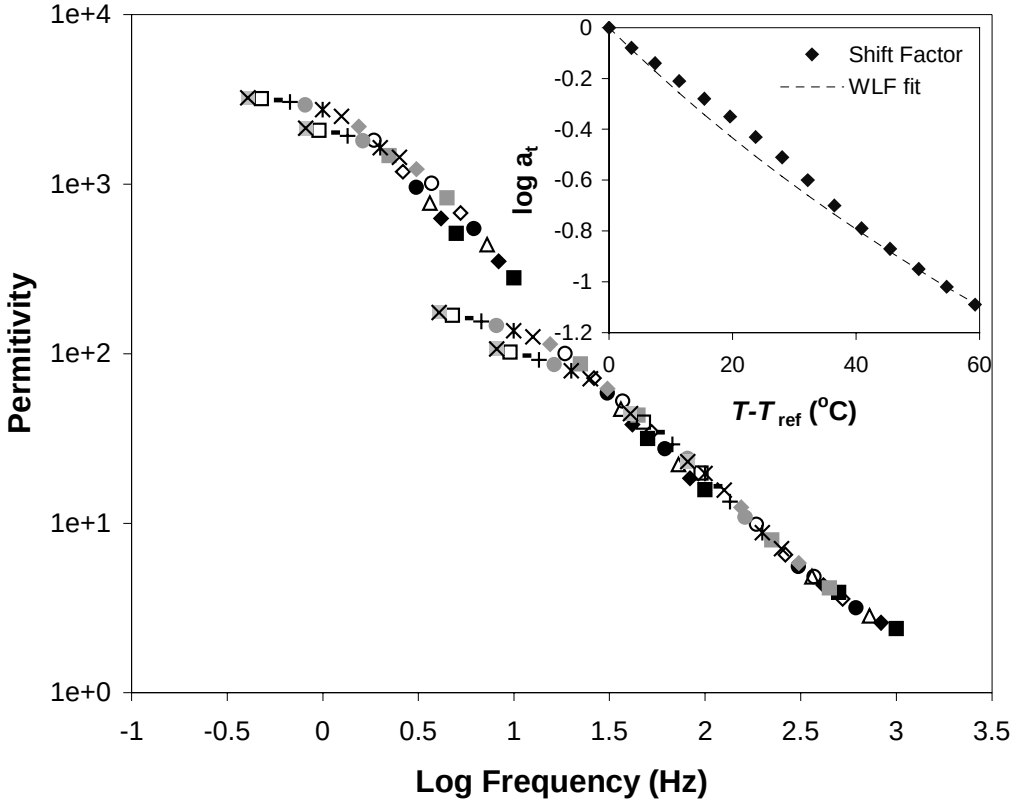

Figure AII.7. Master curve of dielectric permitivity versus log frequency for southern pine mature wood at 12% moisture content. The reference temperature used was 42 °C.

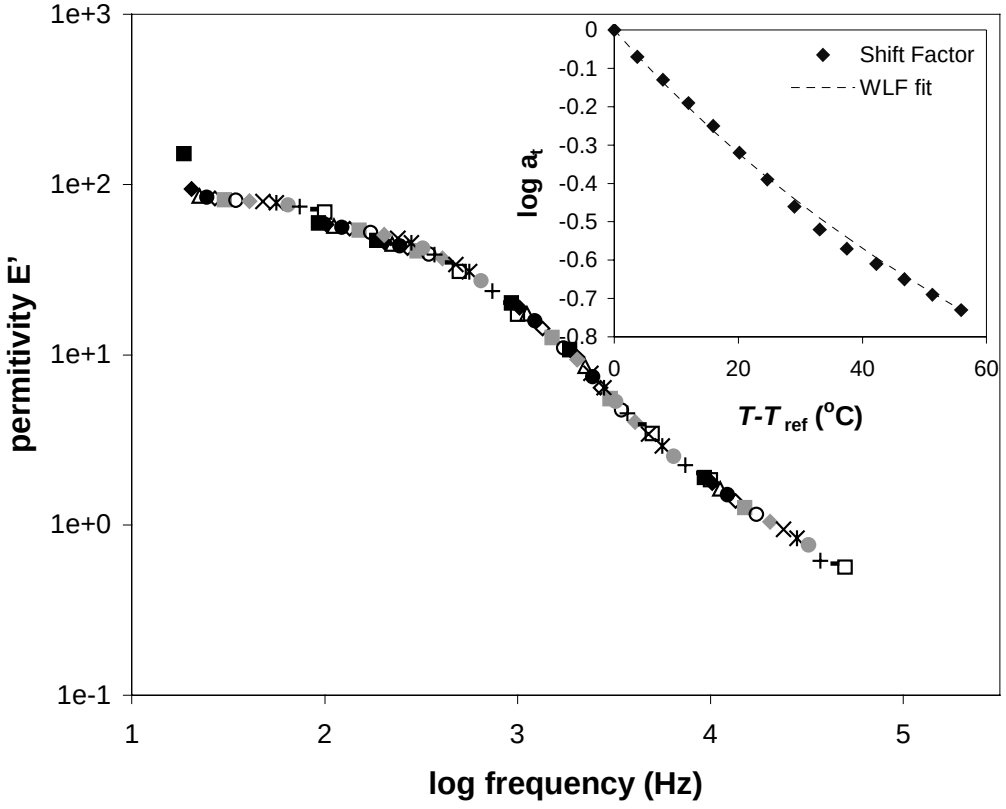

Figure AII.8. Master curve of dielectric permitivity versus log frequency for southern pine mature wood at 20% moisture content. The reference temperature used was 43 °C.

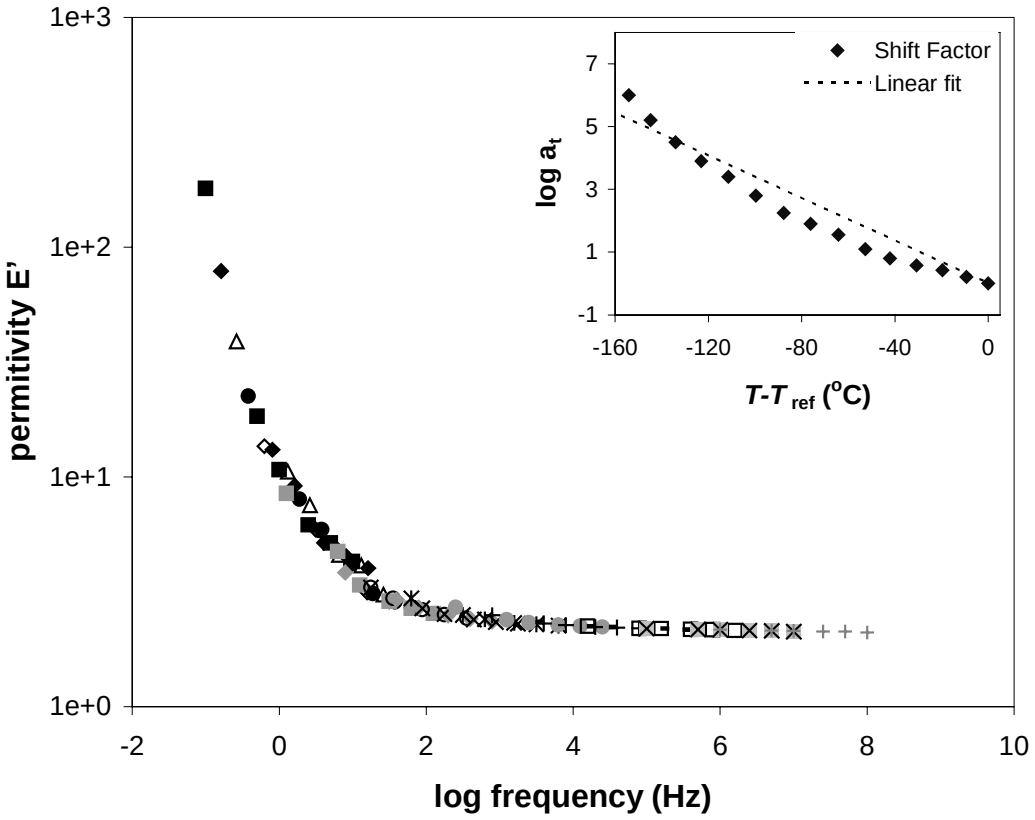

Figure AII.9. Master curve of dielectric permitivity versus log frequency for yellow-poplar mature wood at 0% moisture content. The reference temperature used was 200 °C.

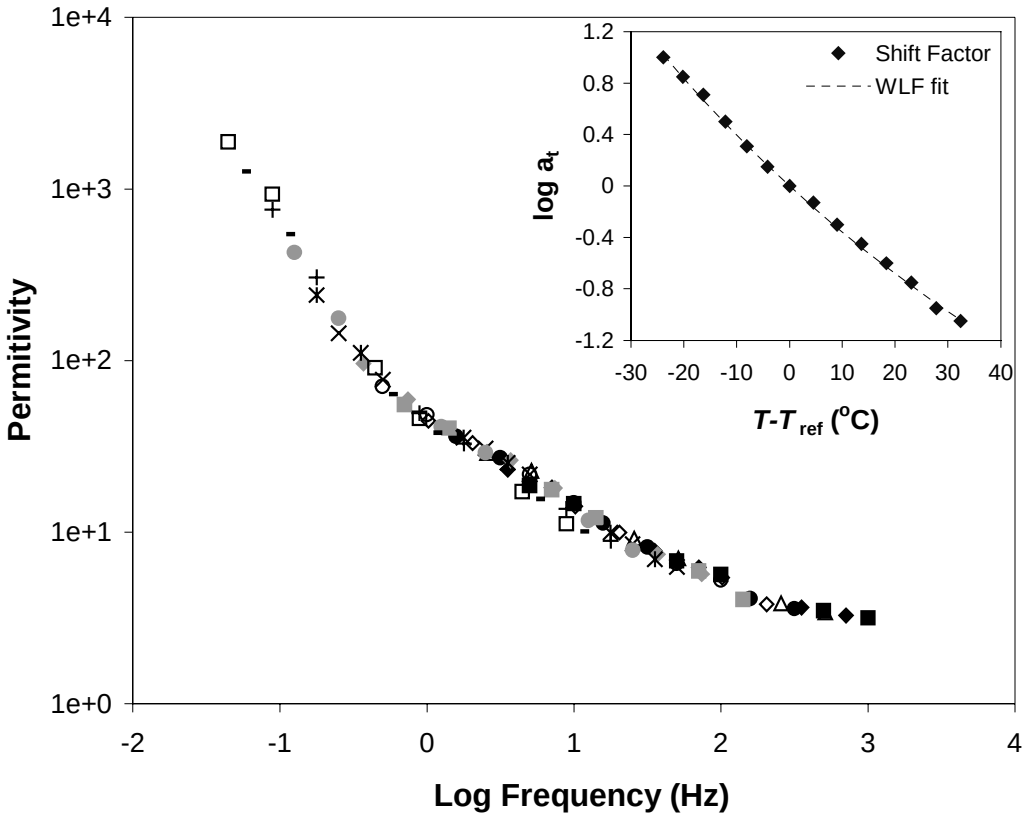

Figure AII.10. Master curve of dielectric permitivity versus log frequency for yellow-poplar mature wood at 05% moisture content The reference temperature used was 65 °C.

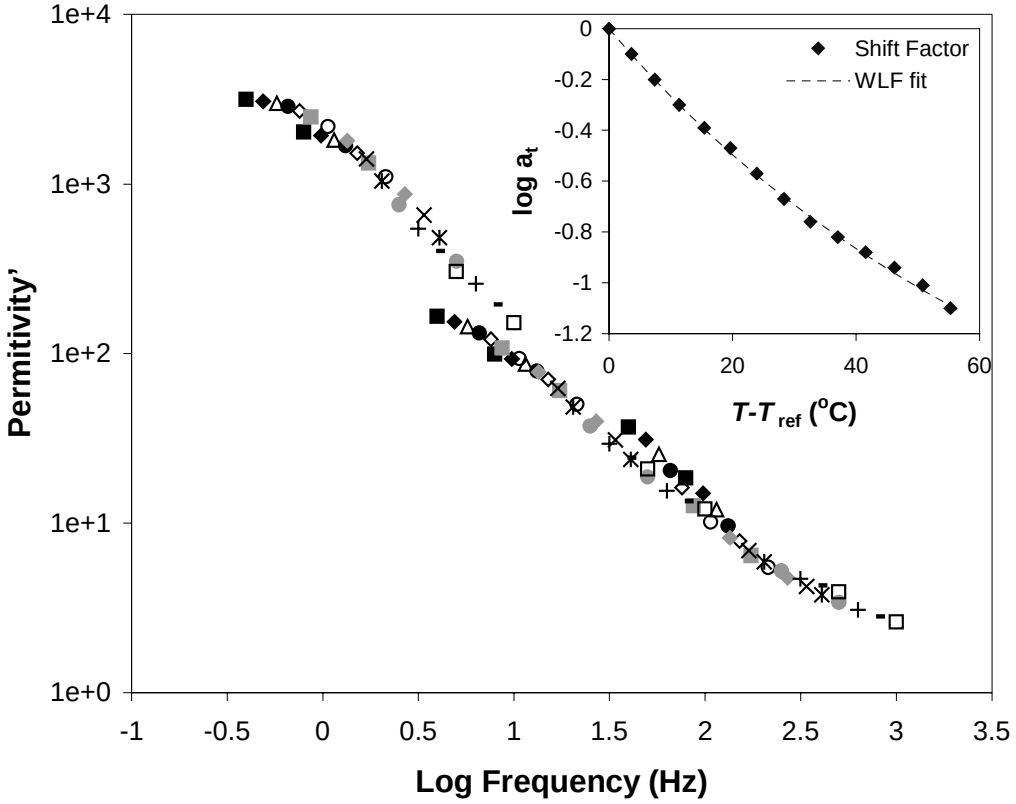

Figure AII.11. Master curve of dielectric permitivity versus log frequency for yellow-poplar mature wood at 12% moisture content. The reference temperature used was 43 °C.

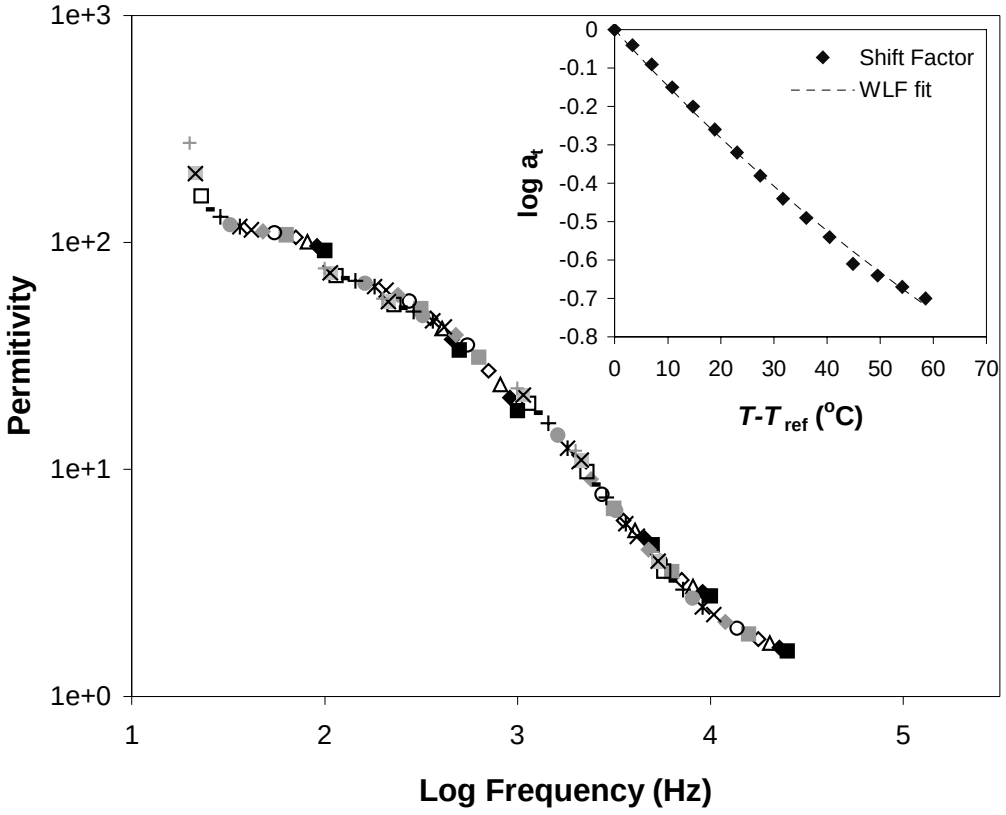

Figure AII.12. Master curve of dielectric permitivity versus log frequency for yellow-poplar mature wood at 0% moisture content. The reference temperature used was 42 °C.

VITA

Christopher Allen Lenth was born in Postville, Iowa, on 28 November, 1967. He graduated from Central Community High School in Elkader, Iowa, in May of 1986.

In May of 1991 he received his Bachelor of Science in Forestry with a specialization in Wood Science from Iowa State University, in Ames, Iowa. He enrolled at Virginia Polytechnic Institute and State University in September 1991 for a Master of Science degree in Wood Science and Forest Products, which he completed in October of 1994. Thereafter he continued his enrollment at Virginia Tech, working towards a Doctorate of Philosophy in Wood Science and Forest Products, which he defended in May of 1999. Since that time he has been employed as a materials scientist at the New Zealand Forest Research Institute.